ORGANIC WALLED DINOFLAGELLATE CYSTS FROM THE TARIM BASIN, WESTERN CHINA;

IMPLICATIONS FOR THE TIMING OF THE EARLY PARATETHYS SEA RETREAT

Universiteit Utrecht

Arjen Grothe
(3017346)

August 2011

ORGANIC WALLED DINOFLAGELLATE CYSTS FROM THE TARIM BASIN, WESTERN CHINA;

IMPLICATIONS FOR THE TIMING OF THE EARLY PARATETHYS SEA RETREAT

Arjen Grothe
(3017346)
Utrecht University
Faculty of Geosciences
MSc. thesis Earth Sciences

Supervisors:
Prof. Dr. H. Brinkhuis; Dr. G. Dupont-Nivet; Prof. Dr. H. Middelkoop
R.E. Bosboom MSc. and A.J.P. Houben MSc.

August 2011

Figure on front: Photo of the Bashibulake Formation at the Mine Section, Western China. The Kalatar and Wulagen Formations are visible in the back. In the right corner a specimen of organic-walled dinoflagellate cyst taxon *Cordosphaeridium funiculatum*.

Table of contents

Table of figures

List of tables

Preface

After a 'gap-year', I started my master in Physical Geography in September 2009 with a focus on *Quaternary Geology and Climate Change*. For this master thesis, which is the final project of my master, I've made a side step to the biomarine and paleomagnetic research groups of the University of Utrecht. Although the time scale (Paleogene vs. Quaternary) and the setting (marine vs. terrestrial) were completely different from what I did before, this project was completed successfully. In this context, I have to thank Guillaume Dupont-Nivet and Roderic Bosboom for the risk they took by taking me, a physical geographer who studied the '(f***ing) Quaternary', onto their geological field trip. Further on, I would like to thank Roderic and Guillaume, as well as Huang Wen-Tao (PhD), for the great time we've had in China. We had some great adventures with flashfloods, police officers, missing the world cup final (Netherlands-Spain) and so on. I've to mention our (fighting) drivers annex cooks Mr. Huang and Mr. Su. Although, there were sometimes a bit lazy, they did a good job by preparing a nice traditional diner and driving us from site to site every day.

Moreover, I would like to thank Sander Houben, Peter Bijl, Henk Brinkhuis, Appy Sluijs and Joost Frieling for guiding me with my first steps into the 'dino-world'. Without their help and time, it would have been a far more though job for me to discover this new world. Furthermore I would like express my thanks Natasja Welters and Jan van Tongeren for their laboratory assistance. In addition, I have to thank, Henk Brinkhuis and Appy Sluijs, for providing me the opportunity to join the scientific world by giving me (and some others) the opportunity to present my (preliminary) results on a poster at the CBEP conference in Salzburg, Austria (June, 2011) as well as the upcoming DINO9 conference in Liverpool, UK (August, 2011).

Finally, This research would not have been possible without funding from the Molengraaff Fund and the Netherlands Organization for Scientific Research (NWO).

Arjen Grothe
August 2011

Abstract

Upper Cretaceous and Paleogene sediments in the Tarim Basin (western China) are archive of the easternmost remnants of the early Paratethys Sea, an epicontinental sea that covered a large part of Eurasia and probably extended into the Mediterranean Tethys in the west. Its final retreat out of the Tarim Basin has been suggested to be associated with the Indo-Asia collision and/or with eustatic sea level falls, e.g. like those across the Eocene-Oligocene transition (EOT, ~34 Ma). However, a recent study dated the final retreat at youngest as earliest Priabonian (~37 Ma), so mismatching previously documented major eustatic sea level falls, like the ones associated with the EOT.

In order to better understand the timing of the regional Paratethys Sea retreat and its paleoenvironmental impact, new magneto- and biostratigraphic data were collected from three earlier studied sections, respectively Aertashi, Kezi and Keliyang. Moreover, two new sections, Mine and Kansu, have been studied and sampled. We investigated the organic walled remains of surface dwelling dinoflagellates (dinocysts), that allowed for biostratigraphic correlation with other calibrated sections. Furthermore, dinocyst assemblages sensitively record environmental changes, which provided the opportunity to reconstruct paleoenvironments of the Tarim Basin. The similarity of assemblages to other assemblages at distal locations may indicate surface–ocean connections between these sites.

Using dinocysts and paleomagnetic date, the uppermost marine deposits from the Aertashi section may correspond to Chron C18r (~40 Ma) or C17r (~38 Ma), of which the latter solution is favoured. The paleomagnetic data from the Mine section turned out to be remagnetized. Relying on dinocysts, the uppermost marine strata from the Mine section have been tentatively correlated to Chron C16n.1r (middle Priabonian, ~35.7 Ma). Both results confirm that the youngest marine deposits in the Tarim Basin clearly predated the eustatic sea level fall across the EOT. However, the EOT and its associated sea level fall cannot be excluded as a mechanism for the final retreat. In such a scenario the youngest marine strata would have been eroded. Furthermore, the recognized sea level fluctuations may correlate to eustatic sea level curves, albeit distal tectonic activity cannot be excluded.

Dinoflagellate assemblages indicate shallow marine environments (~50m water depth) for the sections during the early Priabonian, wherein periods of more open marine (less proximal) conditions were alternated with more restricted ‘lagoonal’ circumstances. These changes from ‘lagoonal’ to ‘marine’ influences may signify alternations of sea level and/or evaporation. Moreover the dinoflagellate assemblages show a strong correspondence to the assemblages in the Turgay region and in a lesser extent to some Italian sites, which confirms that surface water connections existed from the Tarim Basin to the Tethyan and the Turgay regions during the Eocene.

1. Introduction

The Tarim Basin in western China (Figure) was flooded during the Upper Cretaceous and Paleogene by a large epicontinental sea that covered large parts of Eurasia, the 'early Paratethys Sea'[1]. In the west it extended into the Mediterranean Tethys (e.g. Lan and Wei, 1995; Rögl 1999) and it was probably connected to the Arctic region via the Turgay Strait, which was certainly flooded during the Late Paleocene-Eocene Thermal Maximum (PETM), ca. 55.5 Ma (Iakovleva et al., 2001). The early Paratethys has retreated westward since it reached its easternmost extent in the early Eocene (Lan and Wei, 1995). The long term transition from marine to continental conditions, which is marked by five transgression and regression cycles, is recorded in the Upper Cretaceous and Paleogene sediments of the Tarim Basin (Lan, 1997).

The underlying mechanism of the final sea retreat from the Tarim Basin is still poorly understood. It has been suggested to be associated with the Indo-Asia collision; also initial uplift of the Pamir Shan, Tien Shan and the western part of the Kunlun Shan, could have led to in sedimentary overfilling of the Tarim Basin separating it from the Paratethys (Hao and Zeng 1984; Tang 1992; Burtman, 1993; 2000; Lan 1997; Coutland 2002). Alternatively, eustatic sea level drops in the mid-Oligocene (Sobel and Dimitru, 1997) or during the Eocene-Oligocene transition (EOT, ~34 Ma) (Dupont-Nivet et al., 2007) have been proposed as an additional mechanism for the sea retreat. The mechanisms causing the sea to retreat may be indentified by accurately dating the youngest marine deposits.

In addition, paleoenvironmental consequences of the sea retreat are still poorly documented. Sedimentary records from the northeastern Tibetan Plateau reveal a strong aridification and climatic cooling of the Asian interior and an intensification of the Asian monsoon system across the EOT (Graham et al., 2005, Dupont-Nivet et al., 2007). The timing of the paleoenvironmental changes, precisely at the EOT, suggests a link with global climate change. Therefore, Dupont-Nivet et al. (2007) proposed the hypothesis that global cooling, rather than tectonic uplift, was a major factor in the aridification of the Asian interior. By cooler ocean temperatures, the moisture supply to the Asian interior should have been reduced. Moreover, these observed environmental changes have suggested to be caused or enhanced by the retreat of the early Paratethys (Dupont-Nivet et al., 2007). Climate modeling studies (Ramstein et al, 1997; Zhang et al., 2007) indicated that Paratethys Sea retreat indeed can be a potentially important factor in explaining the recorded intensification of the Asian Monsoon and aridification at the Asian interior.

[1] Officially, the birth of the Paratethys is stated to have occurred around the EOT, as the Tethys Sea finally vanished and the Paratethys Sea became isolated from the 'Mediterranean Sea' due to strong tectonic activities that changed the Eurasian configuration (Rögl, 1999). Therefore, we refer in this text to the epicontinental sea covering Eurasia as 'the early Paratethys'.

Cause and impact of the final sea retreat remain matter of debate, both due to a lack of (paleoenvironmental) data and accurate age-assignments. To constrain cause and consequences of the sea level changes, an accurate chronostratigraphic framework is of essential importance. In the summer of 2007, a fieldwork was conducted in order to construct such a stratigraphic framework for the region using foraminifers, ostracods, bivalves, calcareous nannofossils and dinoflagellate cysts (Bosboom et al., 2010). These authors showed that the final sea retreat from the western Tarim most likely occurred in the early Priabonian (~37.2-36.3 Ma). Subsequently, this may imply that the sea retreat at their study area did not coincide with the EOT and its associated eustatic sea level drops (e.g. Miller et al. 2005, 2009). Nevertheless, the transgression and regression cycles are likely reflecting third order eustatic sea level changes, although sedimentary infilling by the early uplift of the Tibetan Plateau cannot be excluded. Remarkably, the retreat, dated as early Priabonian, appears to coincide with strong aridification of the Asian interior around 36.6 Ma recorded in the Xining Basin (Fig. 1; Abels et al., 2010), which suggests that a link between the sea retreat and the aridification may exist.
In order to obtain a better understanding of the timing of the regional Paratethys Sea retreat and its paleoenvironmental impact, a new field campaign to the northwestern Tarim Basin was organized in the summer of 2010. Accordingly, the aim of this thesis is to accurately determine the timing and impact of the Paratethys retreat in the western Tarim Basin by studying key sedimentary successions and its palynological assemblages, which may have recorded the sea retreat.

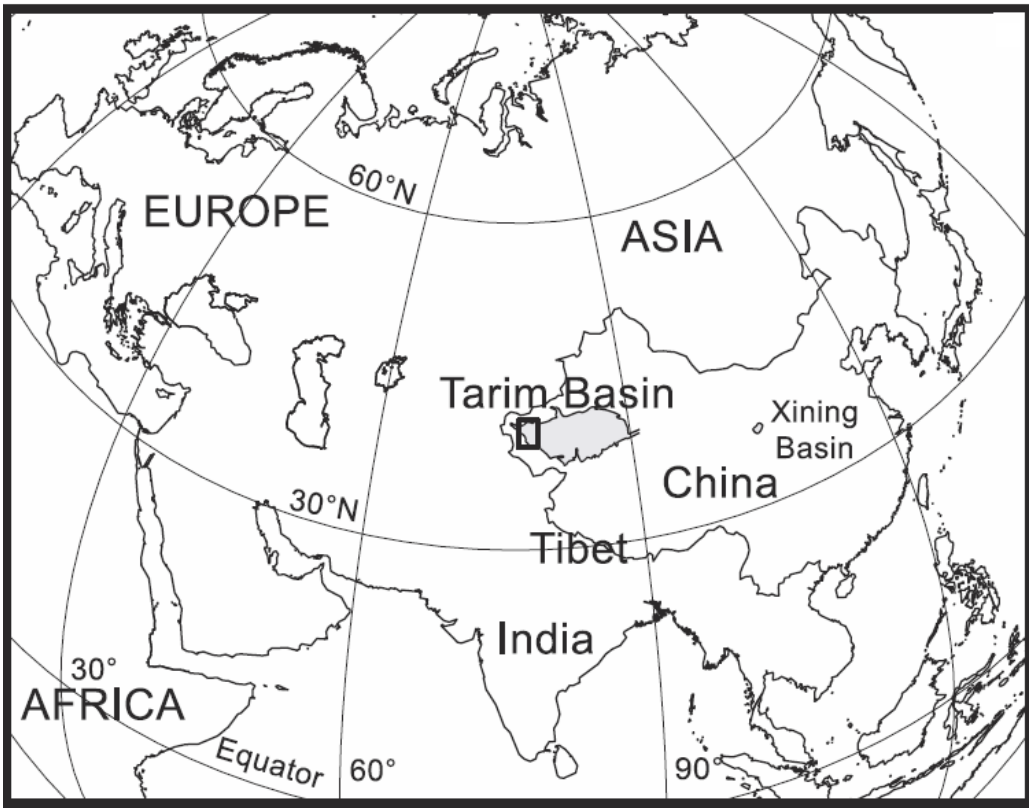

Figure 1 Map showing the location of the Tarim Basin and the Xining Basin. Small box indicates the fieldwork area, see Fig. 3

2 Background information

2.1 Geological Setting

The Tarim Basin is nowadays the world's largest enclosed drainage basin (Bosboom et al., 2010). Quaternary deposits of the Taklamakan Desert dominate the surface in the centre of the basin. It is bordered by Mesozoic and Cenozoic outcrops of the Tien Shan[2] in the north, the Kunlun Shan in the south and the Pamir Shan in the west. The base of the Tarim Basin is formed out of Archean and Proterozoic ocean crustal fragments composed of metamorphic gneisses, which are overlain by carbonates and fine grained clastics of the Paleozoic and coarse grained clastics of the Mesozoic (Tian et al., 1989; Bosboom et al., 2010).

By Upper Cretaceous times, during the Cenomanian approximately 99.6 Ma, the Tarim area became flooded by the Tethys Ocean, resulting in marine deposition (e.g. Mao and Norris, 1988). In total, five marine incursions have been reported from the sedimentary record of the Tarim Basin (Fig. 2), of which the 3rd transgression probably extended most far to the east (Lan and Wei, 1995; Lan, 1997; Bosboom et al., 2010). The 5th transgression was restricted to the western edge of the Tarim Basin (Lan, 1997).

The northward movement of India, which resulted in the onset Indo-Asia collision in the Eocene (Dupont-Nivet et al., 2010), culminated in the uplift of the Pamir Shan, Kunlun Shan and the Tien Shan. Although, thrusting and exhumation of these mountain ranges initiated between the late Eocene and early Miocene, the onset of rapid uplift and topographic expression of the Pamir Shan and Kunlun Shan likely did not occur before late Oligocene–early Miocene times (Cowgill, 2010). Due to these tectonic activities, the Tarim Basin finally developed into a foreland basin. Subsequently, the continental deposits are characterized by high(er) sedimentation rates (Bosboom et al., 2010).

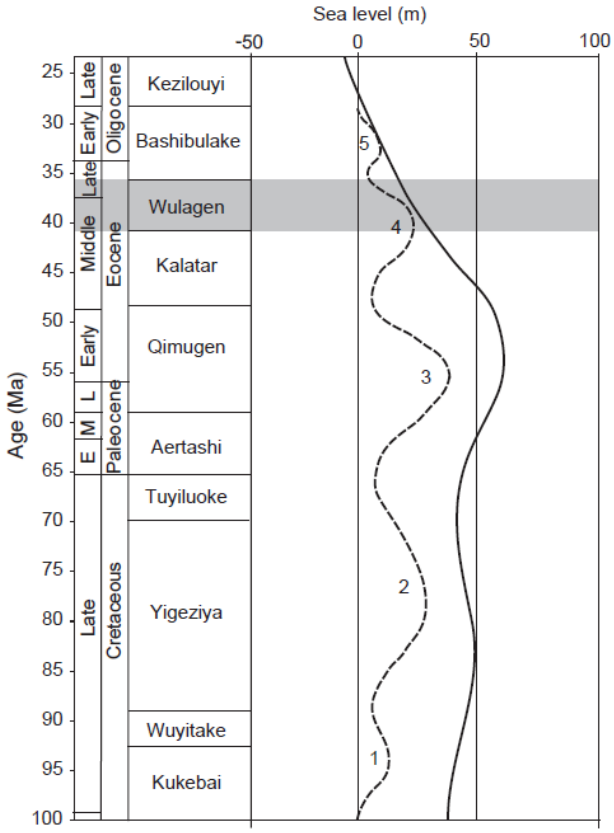

Figure 2 Schematic regional framework of the five marine incursions in the Tarim Basin based on a review of existing Chinese literature (from Bosboom et al., 2010). Dotted line indicates the approximate extent of the marine deposits through time simply based upon the reported easternmost extent of marine deposits (e.g. bivalves). Solid line represents long-term sea-level curve compared to present day sea level (top axis) (Miller et al., 2005; Watts and Steckler, 1979). Ages are based upon earlier literature.

[2] *Shan* is the Chinese word for mountain range

2.2 Stratigraphy of the western Tarim Basin

Upper Cretaceous deposits form the Yingjiesha Group, comprising in chronological order the Kukebai, Wuyitake, Yigeziya and Tuyiluoke Formation. During the Paleogene, the Tarim Basin developed into a unified basin, resulting in rather uniform lithofacies (Mao and Norris, 1988). The Paleogene deposits in the western Tarim Basin are dominated by marine sequences, comprising the Kashi Group. This group consists out of five formations, from base to top respectively: Aertashi, Qimugen, Kalatar, Wulagen and Bashibulake. The continental Wuqia Group, with the Kezilouyi Formation as its lowest unit, is situated on top of the Kashi Group. Usually, the Wuqia Group lies usually unconformable on the Kashi Group, but the geological units are conformable in the Aertashi section (Lan and Wei 1995, Yin et al., 2002). A comprehensive overview of the Paleogene stratigraphy in the area is given in Table 1. The Kashi Group and its formations will be described in more detail in the section below.

2.2.1 Aertashi Formation

The Aertashi Formation (sometimes referred to as Altashi Formation) is composed of massive gypsum beds intercalated with gypsiferous mudstones and dolomitic limestones. Thicknesses vary dramatically from 21 m up to 438 m since parts of the Aertashi Formation lie disconformably on the underlying Cretaceous strata (Mao and Norris, 1988). Fossil assemblages are rare in the Aertashi Formation. Mao and Norris (1988) found only poorly preserved dinoflagellate cysts and some pollen grains in their samples. Their best estimate is an early to middle Paleocene depositional age. Bivalve assemblages indicate an early Paleocene age (Lan, 1997).

2.2.2 Qimugen Formation

The Qimugen Formation lies conformable on the Aertashi Formation. Thicknesses vary from 20 m in the east to 130 m in the west. It comprises mainly grayish-green mudstone intercalated with thin-bedded shelly limestone at the base, whereas brown gypsiferous mudstones and muddy massive gypsum beds dominate the upper part. Abundant dinocyst assemblages are present in this lower member of this formation (Mao and Norris, 1988). Based upon foraminifera, some literature distinguished the upper member as a separate formation: the Gaijietage Formation. Nevertheless, in this study, nomenclature of Yin et al. (2002) will be used, encompassing the upper part to the Qimugen Formation. Mao and Norris (1988) estimated the Qimugen Formation to be deposited most likely during the late Paleocene or middle to late Paleocene, while the overlying Gaijietage Formation was deposited during the early Eocene. He Chengquan (1991) postulates a Paleocene and early Eocene age for the lower and upper member respectively. Also, the bivalve communities signify late Paleocene and early Eocene age (Lan, 1997).

Accordingly the Paleocene Eocene Thermal Maximum (PETM) is likely present within this formation. In the western Tarim Basin, the PETM is characterized by the *Apectodinium homomorphum*-zone, which yields species such as *Apectodinium homomorphum* and *A. quinquelatum* (He Chengquan, 1991).

System	Formation			Thickness	Age	Lithology	Trend
Paleogene	Wuqia Group	Kezilouyi Fm		200-500 m	Oligocene-Miocene	red beds including mudstones, siltstones, sandstones and gypsum interbeds	Continental
	Kashi Group	Bashibulake Fm	5	65 m (east) -380 m (west)	late Eocene-late Oligocene	brownish red-mudstones intercalated by siltstones, thin beds of gypsum and fine-grained sandstones with occasional ripple marks and cross-bedding.	5th regression (final)
			4			brownish-red mudstones with interbeds of siltstones, thinly bedded gypsum and grayish-green sandy shell beds	5th transgression (final)
			3		late Eocene-early Oligocene		
			2				
			1				4th regression
		Wulagen Fm		10-180 m	late middle Eocene	grayish-green mudstones intercalated with thin shell beds, shelly limestones and muddy siltstones, occasionally overlain by massive white gypsum beds interbedded with brownish-red mudstones and siltstones	4th transgression
		Kalatar Fm		25 m (east) -180 m (west)	middle Eocene	grey massive limestones, marls and grayish-green mudstones with interbeds of shelly limestones, oolitic limestones, shell beds and gypsum	
		Qimugen Fm	Upper	20 (east) -130 m (west)	late Paleocene-early Eocene	brown gypsiferous mudstones and muddy massive gypsum beds intercalated with yellowish-green mudstone	3rd regression
			Lower		middle-late Paleocene	grayish-green mudstone intercalated with thin-bedded shelly limestone	3rd transgression
		Aertashi Fm		20-440 m	early Paleocene	massive gypsum beds intercalated with gypsiferous miudstones and dolomitic limestones	

Table 1 Simplified Paleogene lithostratigraphic description for the western Tarim Basin (modified from Bosboom et al., 2010). Note that thicknesses are not scaled.

2.2.3 Kalatar Formation

Grey massive limestones, marls and grayish-green mudstones interbedded with shelly limestones, oolitic limestones, shell beds and gypsum comprise the Kalatar formation. Similar to the Aertashi and Qimugen formations, the formation thickness decreases from west to east. Mao and Norris (1988) have reported only very poorly preserved dinoflagellates (*Thalassiphora bononiensis* and *Thalassiphora petila,* which is known nowadays as *Wilsonisphaera petila*) and some rare pollen grains in this interval. Based upon those two species in combination with the ages of the underlying and overlying formations, they assigned and early to middle Eocene age to the Kalatar

Formation. This is in agreement with the early middle Eocene age assigned by Lan and Wei (1995) based on bivalves.

2.2.4 Wulagen Formation

The Wulagen Formation is situated conformably on top of the Kalatar Formation. It is dominated by grayish green mudstones, intercalated with thin shell beds, shelly limestones and muddy siltstones. Occasionally it is overlain by massive with gypsum beds with intercalations of brownish red mudstones and siltstones. The depositional age of the Wulagen varies from a mid-middle Eocene age (He Chengquan, 1991) to a most likely late Eocene age, postulated by Mao and Norris (1988). Data from Bosboom et al. (2010) indicate an earliest Priabonian deposition. Relying on bivalve assemblages a late middle Eocene age was assigned to this formation (Lan and Wei, 1995). Rich dinocyst assemblages have been described from this formation (Mao and Norris, 1988; He Chengquan, 1991). Material from Bosboom et al. (2010) confirmed those rich and diverse fossil assemblages from the Wulagen Formation.

Mao and Norris (1988) assigned their *Tubiosphaera filosa* Oppel Zone to the Wulagen Formation. Within this zone, more than 50 taxa have their first occurrence (FO), such as *Adnatosphaeridium multispinosum, A. williamsii, Deflandrea phosphoritica, Homotryblium pallidum, H. tenuispinosum, Hystrichokolpoma rigaudiae, Charlesdowniea coleothrypta, Melitasphaeridium pseudorecurvatum, Palaeocystodinium golzowense, Rhombodinium draco, R. longimanum* and *Wetzeliella articulata*.
According to Mao and Norris the following taxa are restricted to the *Tubiosphaere filosa* (Wulagen) zone; *Achilleodinium biformoides, Areosphaeridium diktyoplokum, Charlesdowniea wulagenensis, Distatodinium ellipticum, Thalassiphora pelagica* and *Tubiosphaera filosa*.

He Chengquan (1991) subdivided the *Wetzeliella-Kisselovia* assemblage, which comprises the Wulagen Formation, into three sub-assemblages. The *Microdinium-Cassiculosphaeridia* sub-assemblage from the base of the Wulagen Formation yields abundant *Microdinium granulatum* and *P. golzowense,* while it lacks Wetzellioids. The middle part of the formation, the *Rhombodinium elongatum-Wetzeliella xinjiangenis* sub-assemblage, is known as the most diverse and rich period of dinoflagellate growth in the western Tarim Basin. Common species, includes similar taxa as the *Tubiosphaera filosa* Oppel Zone of Mao and Norris (1988). In addition, the green algae *Pterospermella* is commonly present. The uppermost part of the Wulagen Formation, comprising the *Stomodinium crassum-Rhombodinium wuqiaense* sub-assemblage, is characterized by a low species diversity. Common taxa include *Cyclonephelium* and *Canningia* sp.

2.2.5 Bashibulake Formation

The Bashibulake Formation is subdivided in five members. The first member comprises a massive white gypsum bed at its base (probably the same gypsum layer which is some literature is cited the top of the Wulagen Formation) overlain by brownish red mudstones with muddy silt stones. The second, third and the lower part of the fourth Member comprise brownish-red mudstones with intercalated beds of siltstone, thinly bedded gypsum and grayish green sandy shell beds. Red mudstones with intercalated siltstones, thin gypsum beds and fine-grained sandstones with sedimentary structures like ripple marks and cross-bedding are characteristic for the uppermost fifth Member

of the Bashibulake Formation. Some literature (e.g. Mao and Norris, 1988; Hao et al., 1982) treat the first member of the Bashibulake Formation as a separate formation, the Zhuoyouleigansu Formation. Based upon foraminifera assemblages this part of the Bashibulake shows some strong shared characteristics with the underlying Kalatar and Wulagen Formation.

Thicknesses of the Bashibulake Formation are highly variable and differ from 65m in the east to 380m in the west. The upper members of the Bashibulake have only been described in the westernmost part of the Tarim Basin. Some dinoflagellate cysts have been found in the second and third Member, while in the upper part contained only poorly preserved pollen grains (*Ephedrites* and *Chenopodipollis*). A late middle Eocene (He Chengquan, 1991) or late Eocene age (Hao et al., 1982) has been assigned to Bashibulake's first Member, while the second, third and fourth member are associated with the late Eocene (He Chengquan, 1991; Zhong, 1992) or early Oligocene (Mao and Norris, 1988). Lacking nannofossils and dinoflagellates, the fifth member was estimated to be deposited in the late Eocene or Oligocene (He Chengquan, 1991; Zhong, 1992), whereas foraminifera fauna indicates an Oligocene age (Hao et al., 1982).

Mao and Norris (1988) assigned their *Deflandrea intrasphaerula* Oppel Zone to the Bashibulake Formation. Taxa like *Cordosphaeridium funiculatum, Deflandrea intrasphaerula, D. robusta* and *Wetzeliella gochtii,* are restricted to this interval zone. *Charlesdowniea coleothrypta, Deflandrea phosphoritica, Lentinia serrata, Melitasphaeridium pseudorecurvatum, Palaeocystodinium golzowense, Rhombodinium draco, R. longimanum* and *Wetzeliella articulata*, have their last occurrence (LO) within this interval.

He Chengquan (1991) assigned the *Rhombodinium draco-Dracodinium rhombodinium* assemblage to the Bashibulake Formation. *R. draco* is extremely abundant in this interval, which further comprises species as *Adnatosphaeridium* spp., *C. funiculatum, Cyclonephelium* spp*., D. phosphoritica, Lejeunecysta hyalina* and *Palaeoperidinium*? *sinense*. In contrast to the *Deflandrea intrasphaerula* assemblage (Mao and Norris, 1988), this assemblage yields *Areosphaeridium diktyoplokum*.

2.2.6 Wuqia Group

The Wuqia Group, which lies generally disconformably on the Kashi Group, is composed mostly of continental clastic sediments. Samples from Mao and Norris (1988) were barren, except two dominated by *Chenopodiaceae*. According to foraminifers this group has a Miocene age (Hao et al., 1982 from Mao and Norris, 1988). Yin et al. (2002) dated an 875 m long interval at Aertashi, in which sampling started approximately 200m above the Bashibulake Formation. They assumed the top of the Bashibulake Formation to be deposited ~31 Ma. Using biostratigraphic constraints and a reasonable range of sedimentation rates, the 875m interval can be correlated in two ways to the Geomagnetic Polarity Time Scale (GPTS), resulting in a depositional age of respectively 31-24 Ma or 23-15 Ma.

2.3 Organic-walled dinoflagellate cysts

In order to allow for dating and correlation of the shallow marine sections in the Tarim Basin, a marine palynological approach has been applied, particularly by studying the organic remains of dinoflagellates. Dinoflagellates are a group of single celled, predominately marine, eukaryotic plankton that exhibit high abundances in neritic settings. As part of a complex life cycle, some dinoflagellates produce highly resistant organic-walled hypnozygotic resting cysts (dinocysts), whereas the motile stage is (typically) not preserved (Sluijs et al., 2005). Because of their neritic habitat, dinocysts can provide a tool to determine the relative age of the marine sediments by correlating (indicator) species and assemblages to other well dated records.

Moreover, palynology is a strong tool for reconstructing the environmental conditions (e.g. temperature and salinity) at the time of deposition and the paleogeography by comparison of palynological assemblages to other coeval (marine) records. Based upon the combination of actuo-paleontological, empirical relations and Quaternary distributions, dinocyst groups have been inferred to represent specific ecological niches. An overview of relevant dinocysts for this study and their inferred ecological affinity is given in the paragraph below.

2.3.1 Ecological affinity of dinocysts

In general, fossil dinoflagellate cysts are characterized by two tabulation types, respectively Gonyaulacoid (G-cyst) and Peridinioid (P-cyst). P-cysts are considered to represent predominantly heterotrophic dinoflagellate species that may thrive on diatoms, other phytoplankton or organic detritus (Sluijs et al., 2005), while G-cysts are considered to represent mainly autotrophic dinoflagellates (Powell et al., 1992). Hence the P/G-cyst ratio of dinocyst assemblages has been successfully applied as a tool to reconstruct paleoproductivity (e.g. Brinkhuis et al., 1998). The tabulation type of the grouped dinocysts (P or G) is bracketed behind the group name.

<u>Impagidinium/Corrudinium-group (G)</u>

Impagidinium spp. has been widely accepted to represent open marine conditions (e.g. Brinkhuis, 1994; Powell et al., 1996). Moreover, *Impagidinium* may be used to identify distal, oligotrophic settings (Sluijs et al., 2005). *Corrudinium* has also been thought to represent offshore environments as well (Pross and Brinkhuis, 2005).

<u>*Spiniferites*-group (G)</u>

The *Spiniferites* group is dominated by *Spiniferites* spp. and further comprises *Achomosphaera* spp and *Spiniferites pseudofurcatus. Spiniferites* spp. has a cosmopolitan distribution along oceans and marginal seas. However, the cyst producing stages seems to be restricted to shelf areas (Brinkhuis, 1994; Powell et al., 1996). Brinkhuis (1994) considered this group to represent open marine neritic water masses, or certain influences of the open marine waters. In general, *S. pseudofurcatus* seems to be more common in marginal marine euryhaline environments (Brinkhuis, 1994).

Hystrichokolpoma (G)

Several species of *Hystrichokolpoma* have been claimed to occur in deeper waters, suggesting it to be indicative for outer neritic to more oceanic environments (Van Mourik et al., 2001; Pross and Brinkhuis, 2005). Therefore this group is considered to represent outer neritic conditions in this study.

Adnatosphaeridium-group (G)

This group is represented here by *Adnatosphaeridium multispinosum* and *A. williamsii*. Despite the morphological similarities, in particular the distally connected processes, with the outer neritic to oceanic genera *Nematosphaeropsis* and *Cannosphaeropsis,* this group likely represents inner to outer neritic environments. The abundances of the *Adnatosphaeridium* group match with *Spiniferites*, while oceanic indicators are not abundantly present (Torricelli et al., 2005).

Areosphaeridium/Enneadocysta-group (G)

Areosphaeridium diktyoplokum has been reported from a wide range of environments and is therefore thought be a cosmopolitan (taxa that occupy a wide range of environments). In particular it has been suggested to be a 'relatively offshore' cosmopolitan. In contrast, *Enneadocysta pectiniforme* and representatives have been linked to more restricted and neritic conditions (Brinkhuis, 1994). There are indications that *Enneadocysta* spp. correlates positively to the presence of $CaCO_3$ suggesting slightly more offshore and less eutrophic conditions (Röhl et al., 2004; Sluijs et al., 2005).

Cribroperidiniodeae (G)

Achilleodinium biformoides, *Cordosphaeridium* spp., *Cribroperidinium* spp. and *Thalassiphora* spp. are the representatives of the Cribroperidiniodeae subfamily in this study. In general, *Cordosphaeridium* spp. are cosmopolitans, since they are found in a wide range of ecological niches. They seem to flourish during warm unstable conditions such as during the PETM (Sluijs and Brinkhuis, 2009). *Cordosphaeridium* spp. have been reported to occur abundantly on the shelf during transgressions (Islam, 1984). *Achilleodinium* and *Cribroperidinium* spp. have been suggested to be indicative for inner neritic 'coastal' environments (Van Mourik et al., 2001). Peak abundances of *Thalassiphora pelagica* have been associated with surface water cooling and/or enhanced productivity (Brinkhuis and Biffi, 1993; Vonhof et al., 2000). Moreover, Pross and Schmiedl (2002) associated high abundances of the T. pelagica with periods of enhanced stratification, eutrophication and productivity in the upper part of the water column and/or oxygen depletion in the lower parts of the water column (Sluijs et al., 2005).

Glaphyrocysta/Areoligera-group (G)

Relying on empirical data this group shows a strong relation with relatively coarse glauconite bearing sediments suggesting an affinity to high energy environments. This has led to the suggestion that this group is representative for transgressions (Sluijs and Brinkhuis, 2009). Nevertheless some species, such as *Areoligera gippingensis*, are typical for offshore conditions (Heilmann-Clausen, 1994). Accordingly, some workers retain this group to be represent open marine to inner neritic environments (Jaramillo and Oboh-Ikuenobe, 1999; Torricelli et al., 2005).

Goniodomids (G)

This group includes *Homotryblium* spp. and *Polysphaeridium* spp., *Dinopterygium* sensu Morgenroth 1966, as well as *Heteraulacacysta* spp and *Dapsilidinium*.
The *Homotryblium* cpx. shows great morphological similarities with *Polysphaeridium zoharyi*, which thrives in extreme saline stratified environments. Furthermore, it seems to have a preference for low- to mid-latitude, inner neritic environments (Pross and Brinkhuis, 2005). Accordingly, the same ecological niche as for *P. zoharyi*, has been assigned to the *Homotryblium* cpx. Moreover, *Homotryblium* may have peak abundances comprising almost 100% of the total assemblage. Such dominances are in agreement with taxa that tolerate adverse conditions (Brinkhuis, 1994). *Homotryblium* is not restricted to 'hypersaline' environments, acmes of *Homotryblium tenuispinosum* may co-occur with high loads of the freshwater algae *Pediastrum* spp. implying brackish or euryhaline environments (Pross and Schmiedl, 2002; Sluijs et al., 2005). Besides *Homotryblium* cpx, *Dapsilidinium* is thought to be a restricted marine tolerant taxon (Pross and Brinkhuis, 2005).

Cleistosphaeridium-group (G)

This group includes *Cleistosphaeridium* spp. and representatives of the *Cyclonephelium*/*Canningia* cpx. Most specimens of *Cleistosphaeridium* have a marine origin, probably coastal and neritic (Pross and Brinkhuis, 2005; Sluijs et al., 2005), although there may be also freshwater species (Köhler and Clausing, 2000). *Cyclonephelium* spp. seems to indicate marginal, inner neritic environments (Brinkhuis, 1994). Taxa in this group are primarily of Upper Cretaceous age. Therefore, occurrences of these taxa likely reflect reworking of older deposits (Bosboom et al., 2010).

Wetzelielloideae/Deflandreoideae-group (P)

This group holds Wetzelielloids (*Apectodinium* spp, *Charlesdowniea* spp., *Rhombodinium* spp., *Wetzeliella* spp.), *Deflandrea* spp., *Lentinia serrata* and *Palaeocystodinium golzowense*. *Cerodinium* has not been taken into account since it is thought to be a reworked species in our record. Wetzelielloids and *Deflandrea* are thought to be indicative for enhanced productivity in coastal and neritic settings. Moreover, their elevated occurrences seems to be related to well-mixed rather than stratified waters. The latter suggests that dinocyst assemblages may yield information about the structure of the water column (Pross and Brinkhuis, 2005; Sluijs et al., 2005). There are indications that *Deflandrea* spp. corresponds to $CaCO_3$-depleted sediments, suggesting a relatively more inshore setting (Röhl et al., 2004; Sluijs et al., 2005). Eshet et al. (1994) linked Upper Cretaceous, high P/G-ratios (with *Palaeocystodinium* as an major component of ´P´) to upwelling systems in the Tethys causing increased productivity.

Protoperidinioids (P)

This group involves *Lejeunecysta* spp and *Selenopemphix* spp. As suggested above, P-cysts are thought to be analogous to modern *Protoperidinium*, which represents heterotrophic dinoflagellates. Most brown protoperidinioid cysts have been associated with eutrophic waters and/or upwelling regions (Marret and Zonneveld, 2003; Reichart and Brinkhuis, 2003; Pross and Brinkhuis, 2005; Torricelli et al., 2005).

Phthanoperidinium/Senegalinium-group (P)

Sluijs and Brinkhuis (2009) demonstrated that many 'hexaperidinioids'-taxa (the mid-dorsal anterior intercalary plate is in contact with six adjacent plates), in particular *Senegalinium* and *Phthanoperidinium*, can be positively correlated to magnetic susceptibility of the sediments. The increases in iron (Fe^{2+}) are thought to have been caused by enhanced runoff from the hinterland, supporting the idea that this group was successful in periods of low salinity and increased nutrient supply (Sluijs et al., 2007; Sluijs and Brinkhuis, 2009).

2.3.2 Stratigraphic-important dinoflagellate cysts

LO of *Apectodinium homomorphum*

The LO of *Apectodinium homomorphum* has been correlated to the top of magnetochron C19n in Western Siberia (Iakovleva and Heilmann-Clausen, 2010). In the Kysing-4 borehole, Denmark, *A. homomorphum,* has not been encountered. Since there were no paleomagnetic data available of the Kysing borehole, it has been correlated to a Norwegian–Greenland Sea record, which has been magnetostratigraphically calibrated by Eldrett et al. (2004). After this correlation, the base of Kysing borehole is considered to be within Chron C20r (Heilmann-Clausen and Van Simaeys, 2005). Accordingly, *A. homomorphum* may be present in Kysing in sediments up to the base of Chron C20r.

FO of *Rhombodinium draco*

The FO of *Rhombodinium draco* has been correlated to Chron C19n in western Siberia (Iakovleva and Heilmann-Clausen, 2010). The FO of *R. draco* in the Kysing borehole has been correlated to Chron C18n.2n (Heilmann-Clausen and Van Simaeys, 2005).

FO of *Cordosphaeridium funiculatum*

In SW Siberia, the 'FO' of *C. funiculatum* has been correlated to Chron C22, although it comprehends only two rare specimens (Iakovleva and Heilmann-Clausen, 2010). It occurs more or less consistently from Chron C17n onwards. The FO of this taxon in Italy is within the Mps Interval Zone, of which its base has been tentatively correlated to Chron C17n. In Denmark *C. funiculatum* occurs already at the base of the borehole, which seems to be within Chron C20r. After a long interval without encountered specimens of *C. funiculatum,* a more or less consistent occurrence may be correlated to Chron C18n.2n or C17n.

LO of *Melitasphaeridium pseudorecurvatum*

The presence of *Melitasphaeridum pseudorecurvatum* may correspond to the *Melitasphaeridium pseudorecurvatum* (Mps) Interval Zone in the Western Mediterranean Tethys, Central Italy (Brinkhuis and Biffi, 1993; Brinkhuis 1994; van Mourik and Brinkhuis, 2005). The top of the Mps Interval Zone is defined by the last occurrence (LO) of this *M. pseudorecurvatum* and has been correlated to the top of magnetochron C16n.1n (35.4 Ma). In SW Siberia, the LO of *M. pseudorecurvatum* has been correlated to the top of Chron C17r, while it in Denmark persists till the top of Chron C15n.

FO of *Lentinia serrata*

This species is typical for the Bartonian in NW Europe (Iakovleva and Heilmann-Clausen, 2010). Although, it has not a stratigraphically consistent FO there, it may be useful to consider its FO in relations to other regions. In SW Siberia, the FO has been correlated to the top of Chron C17r, while it appears slightly later for the first time in the Kysing borehole, most likely within C16n. In Italy, *L. serrata* has been encountered for the first time within the MPS Interval Zone (Brinkhuis, 1994), which corresponds to Chron C17n or C16n (Brinkhuis and Biffi, 1993; Brinkhuis, 1994).

FO of *Thalassiphora reticulata*

This distinct specie is typical for the Priabonian in NW Europe (Heilmann-Clausen and Van Simaeys, 2005). The zone wherein *T. reticulata* occurs for the first time in southwestern Siberia, may be correlated to the Chron, C16n.1r, C16n.1n, and C15r or to C15r alone (Iakovleva and Heilmann-Clausen, 2010).

FO of *Charlesdowniea coleothrypta* subsp. *rotundata* sensu De Coninck (1986)

In the Kysing borehole, the recorded FO *C. coleothrypta* subsp. *rotundata* sensu De Coninck (1986) occurs synchronously with the FO of *T. reticulata* (Heilmann-Clausen and van Simaeys, 2005). Interpreting their correlation, the joined FO may be bracketed within the top of C16n.2n and C15r. This subspecies of *C. coleothrypta* has not been encountered in Italy or SW Siberia (Brinkhuis and Biffi, 1993; Brinkhuis 1994; van Mourik and Brinkhuis, 2005; Iakovleva and Heilmann-Clausen, 2010).

LO of *Areosphaeridium diktyoplokum*

The LO of this species has been correlated to Chron C13n in Italy (Van Mourik and Brinkhuis, 2005), whereas it ranges well into C13r in NW Europe (Heilmann-Clausen and Van Simaeys, 2005) and the Norwegian-Greenland Sea (Eldrett et al., 2004). The record in SW Siberia was not long enough to register the LO of *Areosphaeridium diktyoplokum*, nevertheless this species is still present within Chron C15n. The LO of this taxon has been associated with the Oi-1 event (Van Mourik and Brinkhuis, 2005).

2.4 Terrestrial palynomorphs

Whereas dinocysts reveal mainly information about the marine conditions, terrestrial palynomorphs encountered in marine sediments may be interpreted to reconstruct environmental conditions of the hinterland. However, it is important to note that pollen grains can be transported over long distances. Bisaccate pollen may be transported in large numbers to distal (oceanic) locations due to their high buoyancy. Lacking the high buoyancy, spores and other pollen grains, are generally considered to be transported over shorter distances (Brinkhuis, 1994).

Pollen from (sub-)tropical forest, such as *Arecipites, Sabelpollenites* and *Spinozonocolpites*, may imply warm and humid conditions, whereas pollen grains from xerophytic shrubland, such as *Ephedripites* (angiosperm), may interpreted to be representative for relatively arid environments (Dupont-Nivet et al., 2008). Elements produced by conifers, such as *Pinus* and *Picea*, are considered to belong to relatively cold conditions. In addition, present day distribution of the *Picea* is related to high altitudes (Dupont-Nivet et al., 2008). Therefore, Dupont-Nivet et al. (2008) interpreted

the appearance of the ‘cold- indicative’ conifers, initially only *Pinus,* but later on also *Picae* and *Chenopodipollis,* to be indicative for (regional) uplift of the Tibetan Plateau (~38 Ma).

3. Material & methods

3.1 Logging and sampling strategy

During the summer of 2010, five sections in the western Tarim Basin (Fig. 3) have been described and sampled in order to improve the chronological framework established by Bosboom et al. (2010). Two sections were situated in the Southern Tien Shan, respectively Mine (39.848°, 74.538°) and Kansu (39.745°, 74.960°), whereas the other sections, Kezi (38°25.99', 76°24.51'), Aertashi (37°58.15', 76°32.98') and Keliyang (37°16.43', 77°51.47') are located in the foothills of the Western Kunlun Shan. Mine section (Fig. 3) is named after a nearby (inactive) mine, while Kezi refers to a river along the section. All other sections were given names of small villages closeby. In addition to that, 'our' Kezi section is probably situated at the same location as the Qimugen section, cited in some other literature (e.g. Mao and Norris, 1988).

A lithostratigraphic framework was constructed describing sedimentary sequences using measuring tape and a 'Jacob's staff'. Significant layers up to a 10 cm resolution have been described. Magnetostratigraphic samples were taken at a ~1 m resolution at the Mine and Aertashi section.

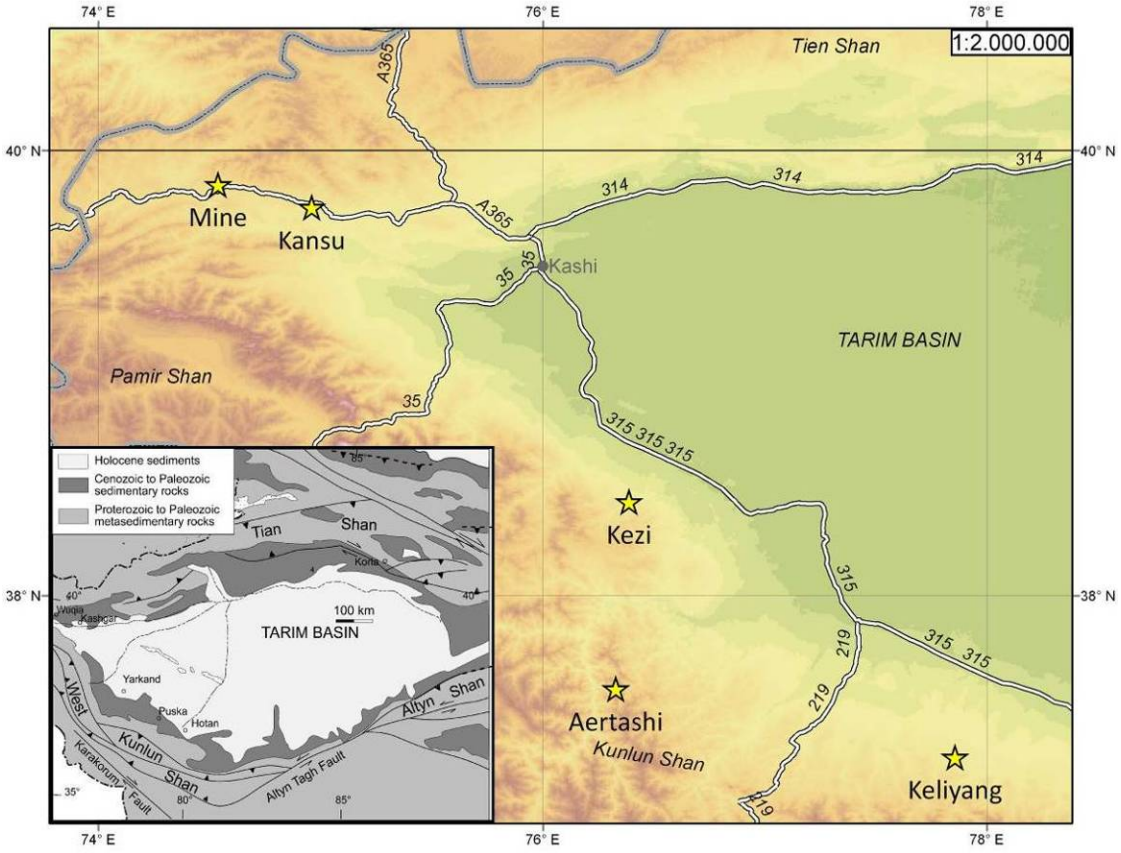

Figure 3 Topographic map showing the study area and its main roads, our sections are marked with a star; inset of geological map shows major lithostratigraphic units and tectonic features (modified from Dupont-Nivet et al., 2002)

3.2 Lithostratigraphy

The lithostratigraphic logs can be found Appendix IV. This paragraph describes the lithology of the Mine Section (Fig. 4). Nomenclature of Yin et al. (2002) was used, comprising the Aertashi, Qimugen, Kalatar, Wulagen and Bashibulake Formation. Formations are assigned to the units based on the lithologic descriptions discussed above. The uppermost shell bed layer has been used to define the zero meter level for all sections.

Lithology of the Mine Section

The upper part of the Kalatar Formation contains some thick resistant limestone beds, which yield some distinctive oyster layers (Fig. 5). Weathered grayish green mudstones form the lower part of the Wulagen Formation and it comprises some interbeds of limestone beds including oysters layers. The upper part comprises a more than 20m thick gypsum bed. On top of the gypsum there is a ~50 m interval of red mudstones with grayish-green silty mud and silt intercalations, which is subsequently covered by a ~40m interval of sand with some (trough) cross-bedding, a small channel fill and ripple marks (Fig. 6). This sequence matches perfectly the description of Bashibulake's first member (Zhuoyouleigansu Formation).

Figure 4 Alternations of heavily weathered continental red beds with grayish-green marine beds of the Bashibulake Formation at the Mine section. In the back: resistant limestones of the Kalatar Formation.

Figure 5 An oyster layer from the Kalatar Formation (hammer for scale)

An 110 m interval of red colored mud alternated by some grayish-green silty mud yielding some shells is situated on top of the sandstone interval. The grayish-green intervals contain some shells, which disappear at the top of the Bashibulake Formation while sandy beds become more abundant again. The Keziliyou Formation lies unconformably on top of the Bashibulake Formation. Its lower part is dominated by sand deposits with some mud intercalations.

Lithological interpretation of the Mine Section (Appendix IV)
Limestone and gypsum beds indicate a shallow, lagoonal conditions (Zhong, 1992). Accordingly, the top of the Kalatar Formation is characterized by a lagoonal environment that likely changed to more open marine conditions during the deposition of the muds from the Wulagen Formation. Its grayish green color indicates non-oxidized conditions during the deposition of the sediments. Previous studies reported rich dinocysts (Mao and Norris, 1988; He Chengquan, 1991; Bosboom et al., 2010) and nannofossil assemblages (Zhong 1989; Zhong, 1992; Bosboom et al., 2010) from such grayish green muddy layers, which is in agreement with an increased water depth. Towards the top of the Wulagen Formation water depths decreased again, as manifest by thick gypsum deposits. Brownish red mudstones and fine grained sand stones with ripple marks cover this gypsum layer. The increase in siliciclastic material may indicate a further decrease in water depth or an increase of sediment supply (Reading, 2006). Nevertheless, the sediments are characterized by a dark red color, which reveals well oxidized conditions during the time of depositional. Hence, the setting was likely very proximal and shallow. Then, the dark red sandy deposits are succeeded by muddy deposits, which may indicate an abrupt increase of the water depth again. Towards the top of the Bashibulake Formation, there is a shallowing trend, since the non-oxidized grayish green beds disappear and become replaced by well oxidized sand and mud alternations.

Ultimately, the marine conditions disappeared completely from the Mine section resulting in the continental deposition of the Keziliyou Formation.
Inferring the lithology to represent sea level variability, we have tentatively recorded two major transgression-regression cycles at the Mine section. Respectively, a first transgression that would have resulted in the muddy deposits of the Wulagen Formation and a second transgression represented by the muddy deposits of the Bashibulake Formation.

Figure 6 The Bashibulake Formation at the Mine section. Top figure shows ripple marks; bottom figure shows a channel fill (hammer for scale).

3.3 Paleomagnetic data of the Tarim Basin

Bosboom et al. (2010) present biostratigraphic data for the Kezi and Aertashi sections using foraminifers, ostracods, bivalves, calcareous nannofossils and dinoflagellates. The use of magnetostratigraphy as a means of dating was hampered because the marine sediments turned out to be remagnetized (Bosboom, pers. comm.).
In the summer of 2010, new paleomagnetic data were collected at the Mine section and Aertashi sections. At the sections of Kansu, Kezi and Keliyang no (new) paleomagnetic data were collected.

However, paleomagnetic data from the Mine Section also turned out to be unsuitable. The marine deposits of the Wulagen and Bashibulake Formation are also characterized by an overprint, which means that the original polarity signal has been altered. Hence, the construction of a reliable magnetostratigraphic framework for the Mine section is hampered.

Paleomagnetic sampling at Aertashi has been extended over more than 560m after the uppermost shell bed, which provided a non-remagnetized signal of the overlying continental sequence of the Kezilouyi Formation (Fig. 7) allowing for a magnetostratigraphic interpretation (see discussion). The lower part, comprising the Wulagen Formation is characterized by a normal polarity. A long reversed signal of approximately 240m starts within the base of the Bashibulake Formation and lasts within in the Kezilouyi Formation. Subsequently, four zones of normal polarity are alternated by three small zones of reversed polarity. The top of the Aertashi section is characterized by a normal polarity.

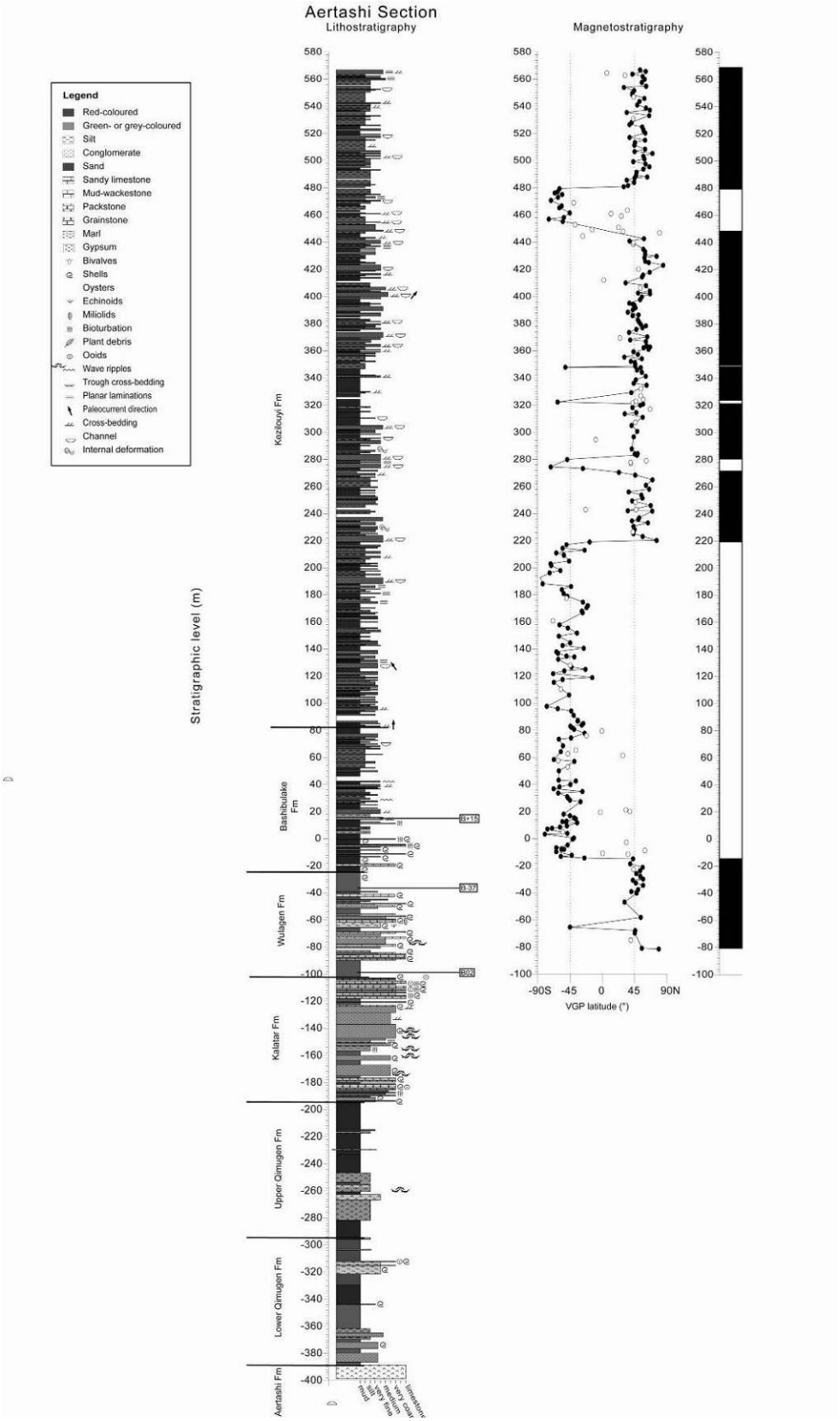

Figure 7 Magnetic polarity and lithology at the Aertashi section. Black and white magnetozones are characterized by a normal polarity and reversed polarity, respectively.

3.4 Palynological preparation & methods

In order to allow for dating and correlation of the shallow marine sections in the Tarim Basin, a marine palynological approach has been applied, particularly by studying the organic remains of dinoflagellates. Samples for palynology have been collected throughout all sections (see lithologic logs in Appendix IV). Sampling was favored from layers that were characterized by the best potential preservation state based upon criteria such 'non-oxidized' or fine grained sediments.

32 of these samples have been palynologically processed. Preparation of all samples was performed using standard methods described in Sluijs et al. (2003). Briefly, material was crushed and ~15 g of the material is freeze-dried sample (60 °C). Additionally, one tablet with exotic *Lycopodium* spores (10679; ± 5%) was added. Then the subtract was treated with 30% HCl and 38% HF in order to remove the carbonates and silicates, respectively. In order to remove most of the HCl and HF, the solution was decanted and centrifuged. Then the samples were sieved with 250 μm mesh, followed by a 15 μm mesh, of which the remaining fraction was mounted on a slide with a glycerine gelly.

If preservation state allowed, quantitative analysis was performed using an optical microscope by counting at least 200 dinoflagellate cysts following nomenclature cited by Fensome and Williams (2004). During this counting process, encountered pollen, spores and acritarchs were also taken into account. After the palynological count, slides were screened for the presence of dinocyst species that were not observed before. If the resolution of an optical microscope was not sufficient to determine on dinoflagellates on a species level, scans were made using an electron microscope (SEM). A list of encountered species can be found in Appendix I.

4. Palynological results

In total, 32 samples have been processed for palynology, of which 13 yield enough dinoflagellate cysts for quantitative interpretation (Table 2). Some rich and diverse assemblages have been recovered from the sediments, although other samples were completely barren (-230.6 to -112.3m) or contained only poorly preserved palynomorphs. The most diverse assemblage from the Bashibulake Formation included 49 species belonging to 33 genera. No samples have been processed yet from the Kansu section.

	Section											
	Mine			Kezi			Aertashi			Keliyang		
Formation	#T	#BI	#AS	#T	#BI	#AS	#T	#BI	#AS	#T	#BI	#AS
Kezilouyi	**1**	**1**	**0**	**0**	**0**	**0**	**0**	**0**	**0**	**0**	**0**	**0**
Bashibulake	**14**	**6**	**8**	**1**	**1**	**0**	**1**	**1**	**0**	**3**	**3**	**0**
Wulagen	**3**	**1**	**2**	**0**	**0**	**0**	**1**	**0**	**1**	**2**	**0**	**2**
Kalatar	**2**	**1**	**1**	**1**	**1**	**0**	**1**	**1**	**0**	**1**	**1**	**0**
Qimugen	**0**	**0**	**0**	**0**	**0**	**0**	**0**	**0**	**0**	**1**	**1**	**0**

Table 2 Number of samples and fossil abundances in different formations and sections. #T total number of samples processed; #BI number of barren samples or oxidized fossils, insufficient to determine; #AS number of samples with abundant and sufficient fossils

4.1 Major palynological groups

Palynological assemblages of all sections are dominated by marine palynomorphs, predominately dinocysts. The Bashibulake Formation is characterized by more terrestrial palynomorphs than the underlying Wulagen Formation (Fig. 8). Terrestrial palynomorphs have a peak abundance at level -82m and 0m, comprising about 28% and 11% of the total palynomorphs, respectively. Most abundantly encountered specimens comprise cf. *Ephedrites* and reticulate, tricolpate aff. *Tamarix*. Moreover, *Pinuspollenites* have been observed. Green algae, predominately *Tasmanites*, show a small peak just below the barren interval at -230m. After the barren interval their abundance increased, culminating in a peak appearance of 25% at level -49m. Above, abundances decrease again, and in the upper part of the section the green algae are absent. Acritarchs do not show a significant interval with high abundances.

4.2 Distribution of 'ecological' dinocyst-groups

The relative distribution of grouped dinocyst assemblages is depicted in Figure 9. Throughout the entire section there is a relatively consistent, high abundance of the *Spiniferites*-group, in general with percentages above 20%. Only at level -231m, which is characterized by an acme of the *Phthanoperidinium/Senegalinium*-group, this group has not been encountered. Furthermore the assemblages of Goniodomids, the *Glaphyrocysta/Areoligera*-group, Cribroperidiniodeae, the *Areosphaeridium/ Enneadocysta*-group, *Adnatosphaeridum, Cleistosphaeridium* and Deflandreoideae/ Wetzelielloideae-group show some significant peaks. The abundance of the *Impagidinium*/*Corrudinium*-group, indicative for open marine conditions, is relatively low reaching a maximum abundance of only ~6.5%.

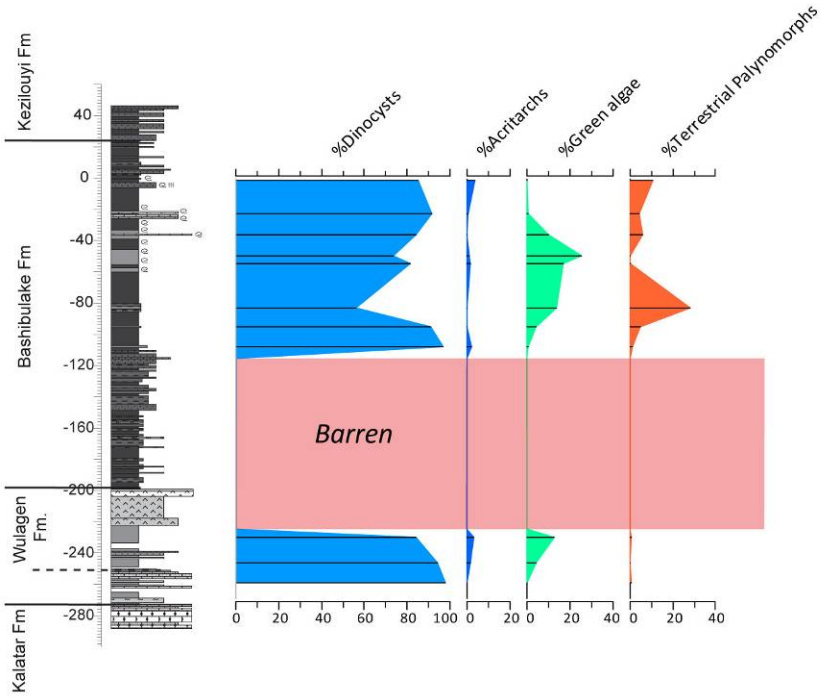

Figure 8 Relative distribution of the recorded palynomorphs through the Mine Section

From base to top, the lowest part of the section is characterized by a peak abundance of the *Spiniferites*-group, which is replaced by a smaller peak in *Homotryblium* at level -247 m. A bloom of the *Senegalinium/Phthanoperidinium*-group, comprising 99% of the total assemblage occurs just below the barren interval.

After the barren interval, the *Spiniferites*-group occurs abundant again, which is subsequently followed by peaks of the Deflandreoideae/Wetzelielloideae-group, Goniodomids and *Adnatosphaeridium.* Also, green algae became more dominant after the barren interval (Fig. 8). Its peak abundance coincides with a strong increase in *Spiniferites*-group and *Enneadocysta pectiniformis*, whereas the dinocyst assemblages of the Goniodomids (here *Polysphaeridium*) and *Adnatosphaeridum* are characterized by a significant decline.

Towards the top of the Mine section there is decline in *Adnatosphaeridium*, while the Cribroperiniodeae and subsequently the *Glaphyrocysta/Areoligera*-group are characterized by a significant increase. At the 0m level there is strong peak abundance of Goniodomids, in particular *Homotryblium* spp.. Moreover, the two uppermost samples, which are dominated by Goniodomids and the *Glaphyrocysta/Areoligera*-group, lack green algae (Fig. 8).

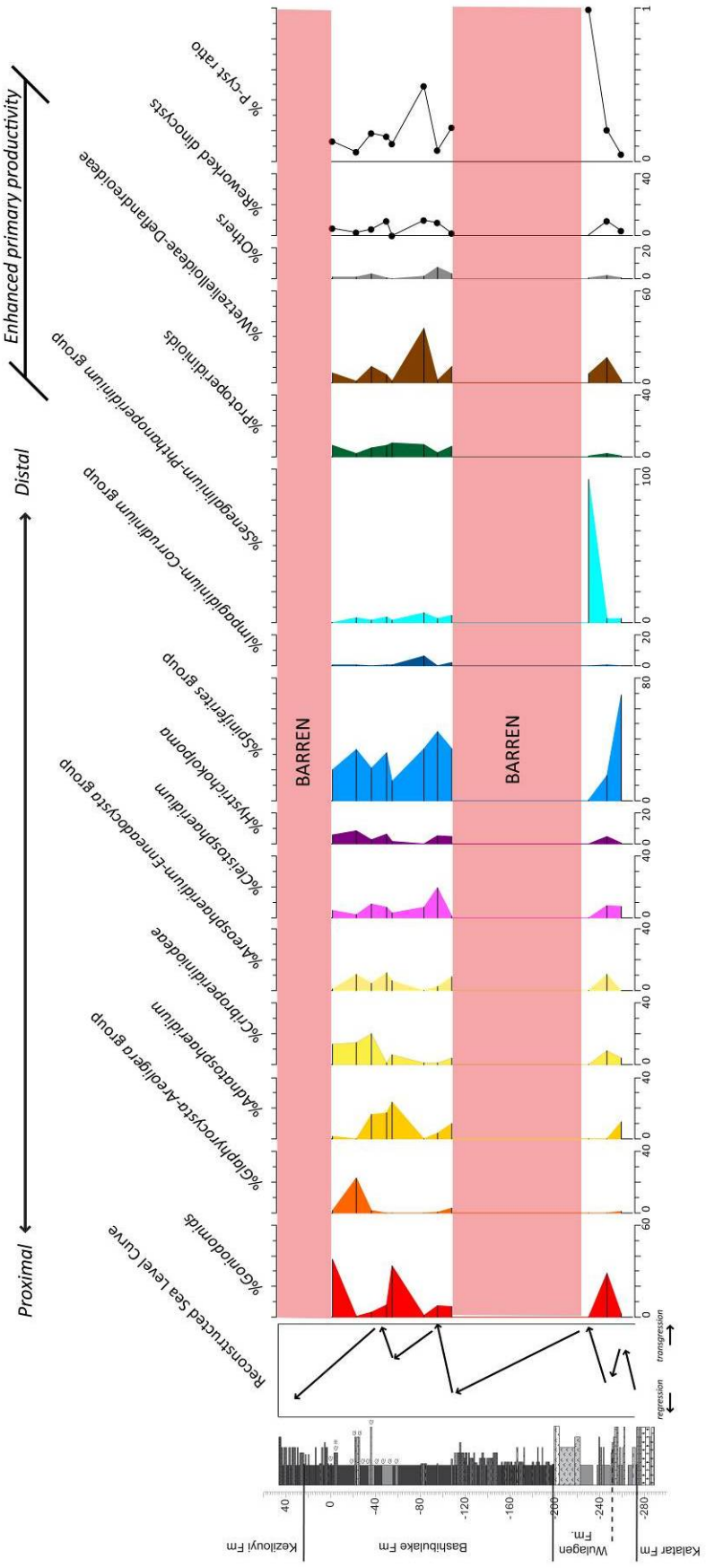

Figure 9 Relative distribution of grouped dinocyst assemblages in percentages of the total dinocysts at Mine Section. Species are grouped after their inferred shared characteristics.

4.3 Stratigraphic distribution of dinocyst taxa

The stratigraphic distribution of organic walled dinoflagellate cysts for the Mine section is depicted in Figure 10. Some species (e.g. *Areosphaeridium diktyoplokum* and *Enneadocysta pectiniformis*) occur (almost) consistently through the entire section, whereas other species lack a consistent occurrence. For instance, *Apectodinium* cf. *homomorphum* has been encountered only until level -247m, while *Thalassiphora reticulata* appears for the first time at level -0.4m.

A clear progression of new incoming species is visible at level -108m after the barren interval of approximately 110m. *Paleocystodinium golzowense*, *Lentinia serrata* and the 'typical Bashibulake'-taxon *Cordosphaeridium funiculatum* (Mao and Norris, 1988; He Chengquan, 1991), have their first occurrence (FO) here. The latter species confirms that the interval belongs to the Bashibulake Formation. The top of the section includes some important age indicative species, such as *Thalassiphora reticulata* and *Charlesdowniea coleothrypta* subsp. *rotundata* sensu De Coninck (1986). Remarkably, *A. diktyoplokum* is not present here. A first biostratigraphic correlation chart for the Tarim Basin has been made using biostratigraphic distributions of taxa throughout the studied sections (Fig 11). These correlations were based upon the FO of dinoflagellate taxa *R. draco* and *C. funiculatum*. Also the FO of the pollen *Pinuspollenites* has been used for correlation.

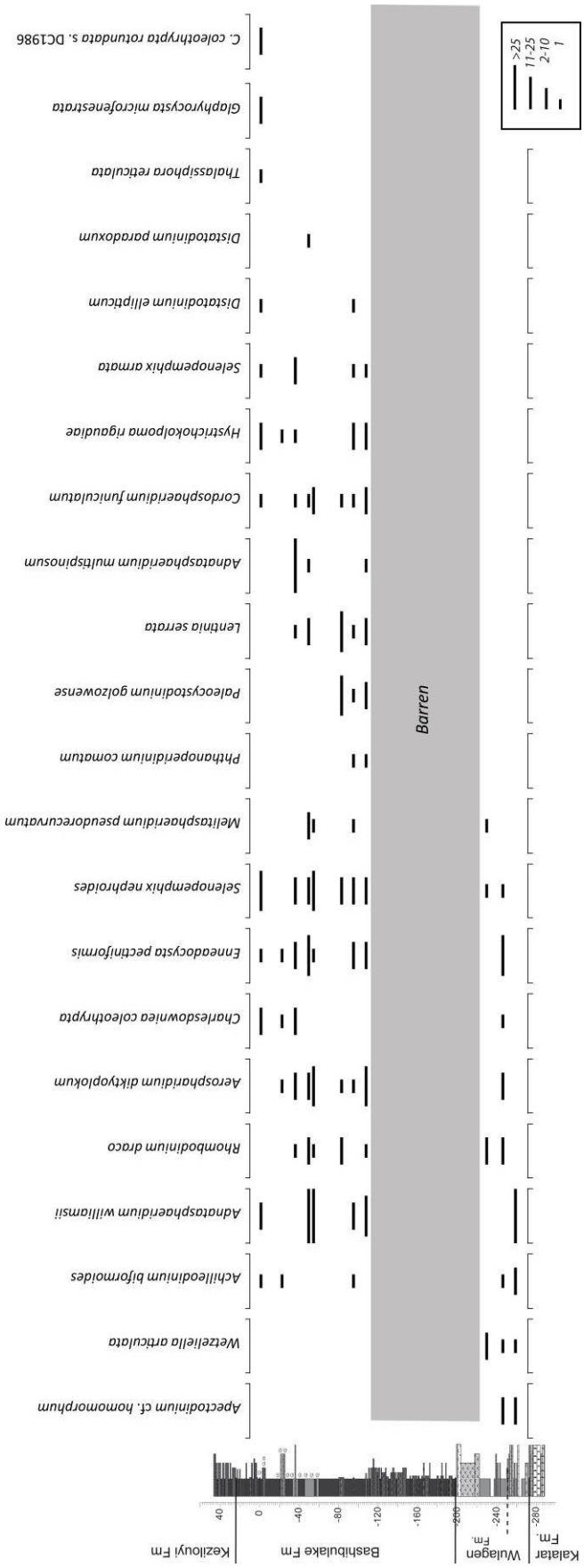

Figure 10 Stratigraphic distribution chart of age diagnostic dinoflagellate cyst at the Mine Section. Thickness of bar gives an indication about relative abundances.

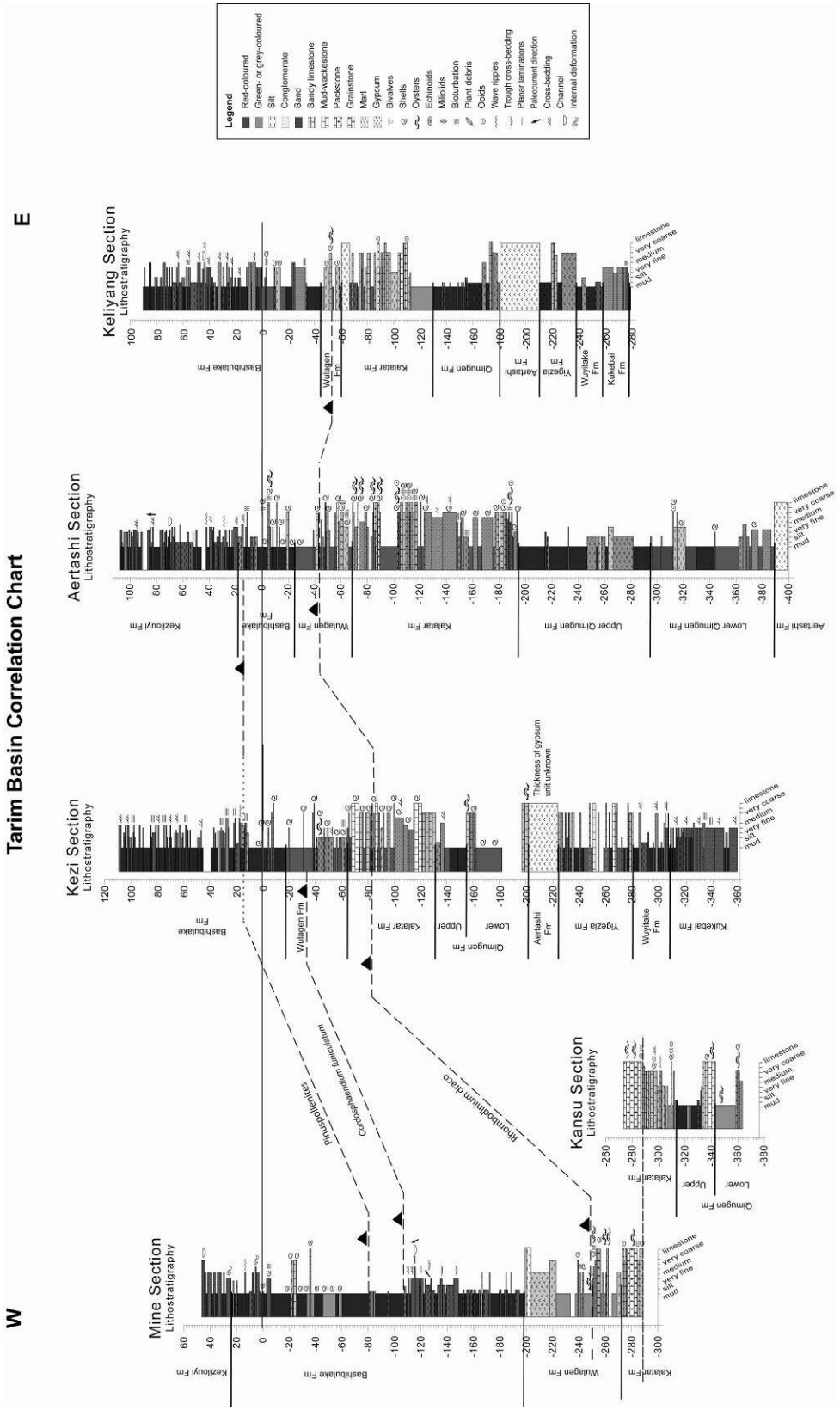

Figure 11 Stratigraphic correlation chart for the studied sites of the Tarim Basin. Correlations were made on the FO of stratigraphical important dinoflagellate taxa, *C.funiculatum* and *R.draco*, as well as pollen *Pinuspollenites*.

4.4 Comparison of dinocyst assemblages with other studies in Tarim Basin

Originally, the boundary between the Kalatar and Wulagen Formation based upon lithology was drawn at ~-250m. This means that our lowermost sample at level -260m belongs to the Kalatar Formation. There have been no earlier reports of dinoflagellate assemblages form the Kalatar Formation, so this inferred that we have described the first dinoflagellate assemblage from the Kalatar Formation ever. However, palynological analysis turned out that the sample from the 'Kalatar Formation' yields abundant dinoflagellate cysts, including typical Wulagen taxa such as *Adnatosphaeridium williamsii*. So, the sampled interval likely belongs to the Wulagen Formation instead of the Kalatar Formation. Alternatively, the observed taxa are not restricted to the Wulagen Formation. Relying on previous lithostratigraphic descriptions (Mao and Norris, 1988), the Wulagen Formation may comprise intercalations of shelly limestones and shelly marls. Therefore, the boundary between the Kalatar and Wulagen Formation should likely be drawn at the top of the limestone bed at -274m. Since Wetzelielloid-taxa is not abundantly present, while *R. draco* and *A. diktyoplokum* have not been encountered, this interval may correspond to the *Microdinium-Cassiculosphaeridia* sub-assemblage of the Wulagen Formation (He Chengquan, 1991).

The other samples belonging to the Wulagen Formation yield typical Wulagen taxa, such as *Adnatosphaeridium williamsii, A. diktyoplokum* and *Charlesdowniea Wulagenensis*. The FO of *Rhombodinium draco* and *Melitasphaeridium pseudorecurvatum* within the Wulagen Formation is in agreement with previous studies (Mao and Norris, 1988; He Chengquan, 1991). Moreover, there is a small peak of the green algae *Pterospermella*. Most likely this interval corresponds to the *Rhombodinium elongatum-Wetzeliella xinjiangenis* sub-assemblage of He Chengquan (1991).

The samples from the Bashibulake Formation include typical Bashibulake taxon *C. funiculatum*. Furthermore, *A. diktyoplokum* has been encountered, which is restricted to the Wulagen Formation according to Mao and Norris (1988). Nevertheless the record of *A. diktyoplokum* within the Bashibulake Formation is in agreement with He Chengquan (1991). Specimens of *W. gochtii* have not been encountered within the studied interval. The stratigraphically important dinocyst taxa *Thalassiphora reticulata* and *C. coleothrypta rotundata* sensu DC1986 have not been reported in the available literature from the Tarim Basin. Likely, *C. coleothrypta rotundata* sensu DC1986, was not distinguished from *C. coleothrypta*.

5. Discussion

5.1 Paleoenvironmental conditions of the Tarim Basin

Dinocysts indicative for open marine conditions, such as *Impagidinium* spp*.,* have relatively low abundances throughout the Mine section, indicating that truly open marine 'oceanic' conditions not occurred within the studied interval. Most assemblages are dominated by outer neritic species, e.g. *Spiniferites* spp. and *Areosphaeridium diktyoplokum* (Brinkhuis, 1994; Powell et al., 1996). Three periods with increased abundance of the restricted marine 'lagoonal' conditions have been recorded, marked by elevated abundance of Goniodomid taxa, in particular *Homotryblium* spp. Moreover, an acme of the *Phthanoperidinium/Senegalinium*-group, likely a reflection of high river input (Sluijs et al., 2005), has been recorded at level -231m. Conspicuously, such a fresh water peak has also been observed at the Kezi section, particularly marked by *Tytthodiscus* (Bosboom et al., 2010). However, the timing of those events seems to differ, inferring it is a more local phenomena than an regional event. Since both sites have a very proximal setting, influence of river input can be significant. Even shifts in a river mouth may have large influences on the fresh water distribution. Therefore, directly linking of such 'fresh water'-pulses to other sites, e.g. Italy, is hard to justify.

In general, the dinocyst assemblages are in agreement with the lithological interpretations. The dinocysts confirm an increase in water depth from the near coastal limestone deposits of the Kalatar Formation towards the grayish green mud deposits of the Wulagen Formation. This increase in water depths is marked by the relatively high abundance of *Spiniferites.* Then, water levels decrease relatively towards the end of the Wulagen Formation, which culminated in the deposition of a thick gypsum layer and well oxidized sandy deposits of the Bashibulake Formation. The gypsum layer and the sandy deposits are barren (lacking preserved palynomorphs), suggesting that the oxygen conditions were not favorable for preservation of the palynomorphs or the environmental conditions were not favorable for the presence of dinoflagellates. After the barren interval the marine deposits recover. The small peak of the *Impagidinium*-group at level -82 m may represent the most open marine conditions throughout the studied interval. This peak is followed by a trend of declining water depths. Outer neritic species, such as *Adnatosphaeridium*, are succeeded by inner neritic species like *Glaphyrocysta.* Finally, the top of the Bashibulake Formation is characterized by more restricted marine 'lagoonal' taxa, in particular *Homotryblium*. These relative fluctuations of water depths may represent trans- and regression cycles. Accordingly two sea level cycles have been recorded. Superimposed on these two sea level cycles, there may be some sea level variations on a shorter time scale, which are marked by the peaks in Goniodomids (Fig. 9)

According to the low amounts of terrestrial pollen, the vegetation was sparse during the deposition of the Wulagen Formation at the Mine section. The *Ephedripites* pollen likely indicate a xerophytic shrubland, because this taxon nowadays occurs on arid mountain slopes (Dupont-Nivet et al., 2008). Even during the peak abundance of the *Phthanoperidinium/Senegalinium*-group no high amounts of terrestrial palynomorphs have been encountered. Despite the presumed fresh water source, likely

a river for the generation of fresh water input, there was only sparse vegetation on the hinterland. Low abundances of terrestrial higher plants in combination with peak abundances of *Senegalinium* have been reported from New Jersey shelf during the PETM. This phenomena was speculative explained by the fact that an extreme hydrological or temperature regime, prevented the establishment of stable vegetation (Sluijs and Brinkhuis, 2009). A climate modeling study showed that subtropical high pressure areas, which are associated with strong descending air, may explain the desert-steppe vegetation pattern of China during the middle Eocene. This pattern could be reduced by a monsoonal increase, although this likely did not play a major role since the paleogeography and warm background conditions in the Eocene epoch favored a relatively weak land-sea thermal contrast (Zhang et al. 2011).

The more consistent occurrence of terrestrial palynomorphs within the Bashibulake Formation of the Mine section, suggests a relatively more humid climate in the hinterland compared to the Wulagen Formation. At 'level -82m', there are no Goniodomid taxa, whereas relative abundance of pollen increased significantly, comprising almost 30% of the palynomorphs. This suggests a more humid hinterland with more stable vegetation.

Furthermore, the recorded dinocyst assemblages show a strong correspondence to the SW Siberian dinocyst assemblages and to a lesser extent the ones from Italy. This confirms the presence of well developed surface connections between the Tarim Basin with respectively the Tethyan realm and SW Siberian Turgay region.

5.2 Biostratigraphic correlation

5.2.1 Age assignment of the Mine section

Considering the FOs and LOs, we tentatively correlate the marine mud bed at level -247m, which is marked by the LO of *Apectodinium* cf *homomorphum* and the FO of *Rhombodinium draco*, to Chron C19n. Note that the resolution in this interval relatively low, therefore the 'real FO' of *R. draco* may be somewhat lower in the record.

The first sample of the Bashibulake Formation at -108m, after the barren interval, holds many new species, such as *Cordosphaeridium funiculatum*. The presence of *Melitasphaeridium pseudorecurvatum* on top of this sample, suggest that this interval may be correlated to the *M. pseudorecurvatum* (Mps) Interval Zone in the Western Mediterranean Tethys, Central Italy (Brinkhuis and Biffi, 1993; Brinkhuis 1994; van Mourik and Brinkhuis, 2005). *C. funiculatum* occurs rather consistent in this interval. Hence, we tentatively correlate the FO of *C. funiculatum* to the consistent occurrence of *C. funiculatum* in SW Siberia in Chron C17n (Fig. 12; Iakovleva and Heilmann-Clausen, 2010). Moreover, the FO of *Lentinia serrata* immediately after the barren interval is in agreement with the almost synchronous FO of *L. serrata* and *C. funiculatum* in SW Siberia.

Following the FOs of *Charlesdowniea coleothrypta* subsp. *rotundata* sensu De Coninck (1986), *Glaphyrocysta microfenestrata* and *Thalassiphora reticulata,* the uppermost marine sample at level -0.4m may be bracketed between the top of Chron C16n.2n and C15r. The observed FO of *G. microfenestrata* at the same level as *T. reticulata* is in agreement with the SW Siberian data and amplifies the correlation with

our record, as well as the synchronous FO of *T. reticulata* and *C. coleothrypta* subsp. *rotundata* sensu De Coninck (1986) is in agreement with the Kysing borehole, Denmark (Heilmann-Clausen and van Simaeys, 2005).

The absence of *M. pseudorecurvatum,* from level -36m to 0m, suggests that these samples uppermost marine interval are younger than the top of the Mediterranean Mps interval zone (C16n.1n). However, due to the fact that of *Schematophora speciosa* (Ssp) and *Stoveracysta ornata* have not been encountered throughout the entire Mine section, there is no clear evidence that these samples indeed correspond to the younger Ssp Interval Zone. Remarkably, these taxa have also not been encountered in SW Siberia (Iakovleva and Heilmann-Clausen, 2010) and Denmark (Heilmann-Clausen and van Simaeys, 2005). Hence, due to the presence *C. funiculatum* and the FO of *T. reticulata* and *C. coleothrypta* subsp. *rotundata* sensu De Coninck (1986), while *S. speciosa* and *S. ornata* have not been encountered, we tentatively correlate the top of the uppermost marine deposits at the Mine Section to Chron C16n.1r, approximately 35.7 Ma (Fig. 12). However, considering the possibility of a minor unconformity in the SW Siberian borehole, the interval may also correspond to Chron C15r (~35.3 Ma).

A. diktyoplokum has not been encountered in the upper part of the Bashibulake Formation. Since, other markers for a Late Priabonian age have not been observed, the absence of here seems to be *A. diktyoplokum* seems to be environmentally controlled. The absence of *A. diktyoplokum* in the early Priabonian was is similar to some Italian sites (Brinkhuis and Biffi, 1993; Brinkhuis, 1994).

The middle Priabonian age assignment (~35.7 Ma) to the final marine deposits at the Mine section, implies that the marine conditions lasted longer at the Mine section than at the Kezi section of which the final marine deposits have likely an early Priabonian age (~37.2-36.3 Ma). This underlines the idea that the epicontinental sea has retreated from east to west.

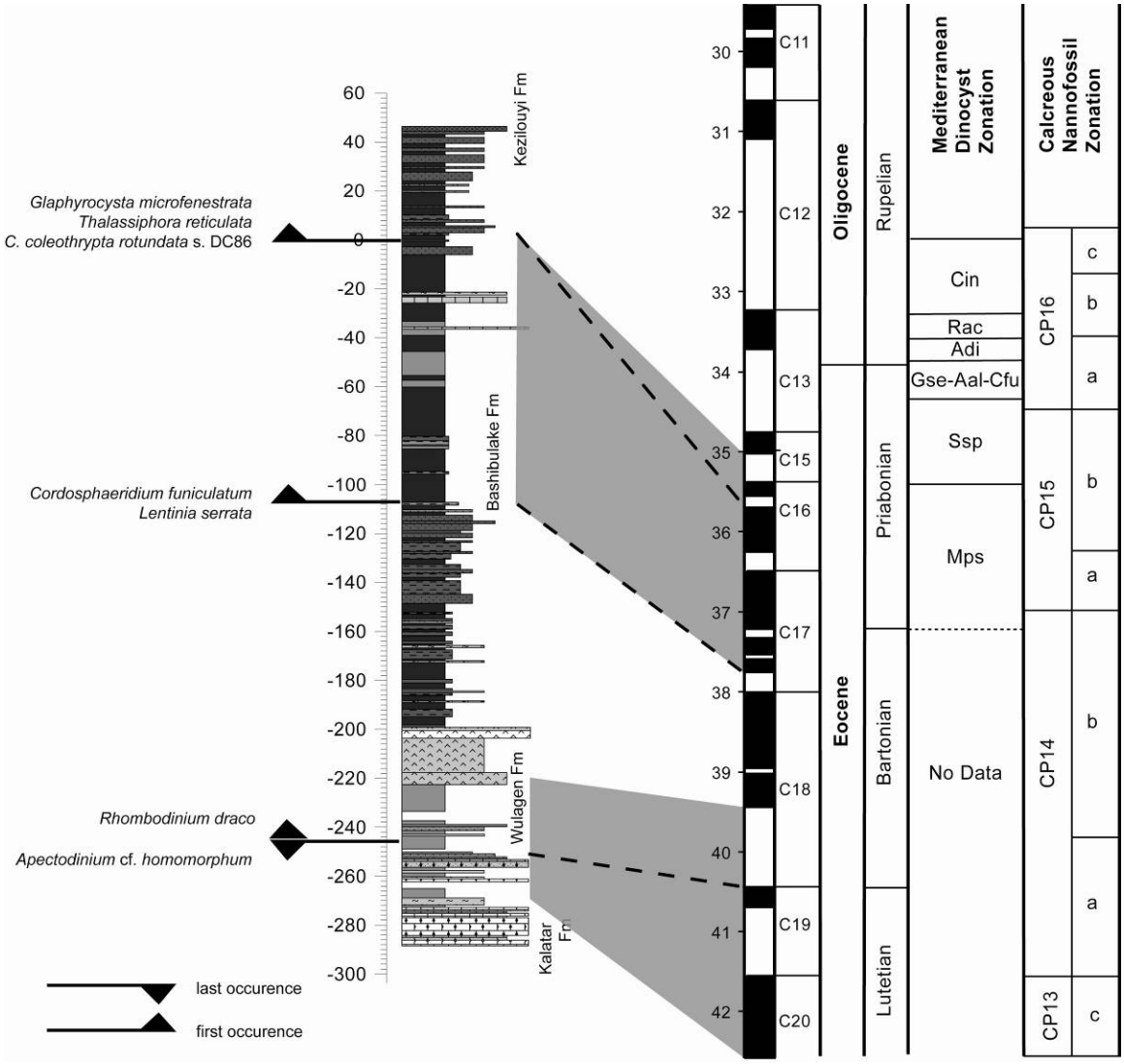

Figure 12 Suggested chronostratigraphy of the Mine Section. Shaded areas indicate possible solutions, dashed lines suggest tentative correlations (see discussion)

5.2.2 Age assignment of the Aertashi section

The magnetostratigrapic chart from the Aertashi section (Fig. 7) is biased in its marine interval. Therefore the lowest normal polarity interval may not be reliable. Simply based on the alternations of polarity and assuming more or less constant sedimentation rates the large reversed magnetochron around the zero level may be correlated to Chron C18r. Alternatively this zone may be correlated to C17r. According to Yin et al (2002) there is no hiatus between the Bashibulake and Kezeliyou Formation, so the long reversed zone likely represents one reversal (Fig. 13).

One dinocyst assemblage from level -37m (normal polarity) hold abundant dinocysts, such as *Diphyes colligerum, Melitasphaeridium pseudorecurvatum* and *Rhombodinium draco*, while it lacks *Areosphaeridium diktyoplokum* and *Cordosphaeridium funiculatum*. According to Iakovleva and Heilmann-Clausen (2010), *R. draco* and *M. pseudorecurvatum* ranged in SW Siberia respectively from Chron C19n to

C16n and until the top of Chron C17r. Assuming there is no big hiatus, the long reversed polarity above the uppermost shell bed indeed may correspond to Chron C18r or C17r. Moreover, 15m above the uppermost shell bed, *Pinuspollenites*, has been encountered. Dupont-Nivet et al. (2008) showed that formation of a conifer forest at the Tibetan Plateau occurred within the top of Chron C18n.1n till C17n.1r (~38.3–37.3 Ma). Therefore, the presence of the *Pinuspollenites* favours a correlation to Chron C17r for the long reversed period at the bottom of the Aertashi section.

The youngest marine sample from Kezi that yielded dinocyst was situated ~18m below the uppermost shell bed and was dated to be deposited approximately 37.2-36.3 Ma. At Aertashi, there is a reversal, approximately 18m below the uppermost shell bed, which can correspond to the transition from C19n-C18r (~40.4 Ma) or C18n-C17r (~38.0 Ma). If this long reversal corresponds to C18r, the average sedimentation rate was ~0.27m/k.y., whereas an average sedimentation rate of ~1.2m/k.y. is inferred if the reversal belonged to C17r. According to Yin et al. (2002) sedimentation rates above the Bashibulake Formation varied between 0.1–1.0 m/k.y., so the latter solution results in relatively high sedimentation rates. However, an average sedimentation rate of 1.2 m/k.y. is, although one magnitude higher, not unlikely since it is still relatively close to the proposed values.

Assuming that sedimentation rates were approximately equal in similar depositional environments, allows for a comparison between the timing of the sea retreat from Aertashi and Kezi. Considering the reversal at level -18m to represent the transition from C19n to C18r, the minimal age difference with the marine deposits of Kezi at level -18m is 3.2 Ma, whereas the other solution gives a minimal age difference of ~0.8 Ma between the section. This interpretation implies that the early Paratethys retreated earlier at the Aertashi section than the slightly more northern oriented Kezi section. However, an interpretation based upon just one biostratigraphic sample and lacking further bio- and/or magnetostratigrapic constraints, dating of the Aertashi section remains speculation. A fieldwork in the summer of 2011, aiming to provide a longer magnetostratigraphic record may shed a new light on the depositional ages.

Nevertheless, previous age-assignments of formations should be considered with care, especially the lowermost and uppermost ages. There was a tendency in the older literature (e.g. Mao and Norris, 1988) to assign ages to the formations for the entire Tarim Basin. In general this is not incorrect, however, in reality different lithofacies (depositional environments) occur diachronous. Therefore, age-assignments of the formations should be carefully interpreted since there may be significant age differences, which has been illustrated by the time discrepancy between the deposition of the Wulagen Formation in the sections of Aertashi and Kezi.

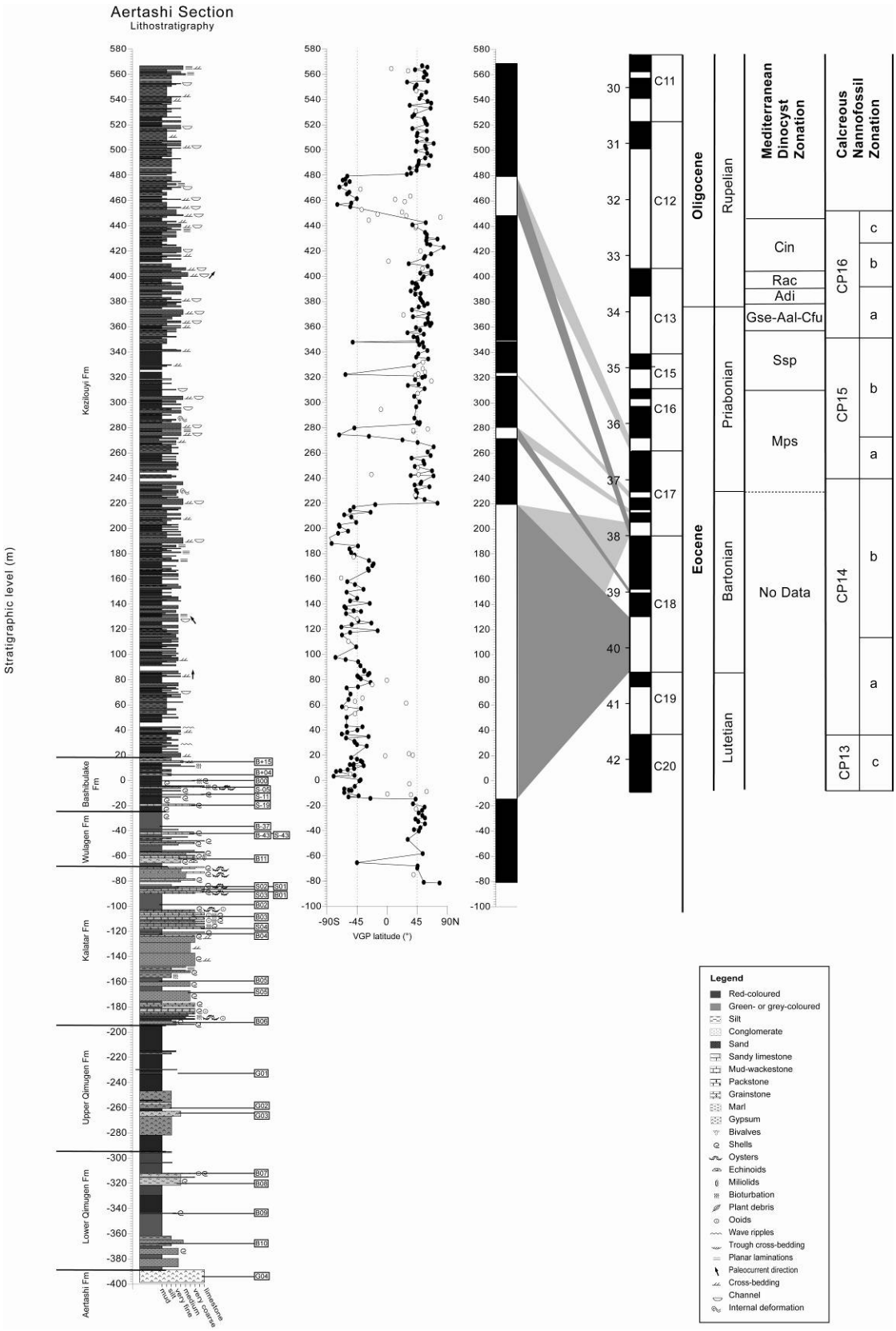

Figure 13 magnetostratigraphic correlation for the Aertashi section; shaded areas indicate possible correlation to the geomagnetic polarity time scale (Gradstein et al., 2004)

5.3 Implications of the age assignments

Ensuing the middle Priabonian age, there may have been a delayed appearance of *S. speciosa* and *S. ornata* in western China, SW Siberia and Denmark in comparison to the Italian sections. An alternative explanation is that these taxa are typical for the low latitudes (Brinkhuis and Biffi, 1993; Brinkhuis, 1994), so the Siberian and Danish section may be situated at too high latitudes. However, a more recent study (Stickley et al., 2004) has encountered both taxa in the higher latitude setting of the Tasmanian Gateway. Finally, there may have been an environmental condition preventing the presence of these species in western China, SW Siberia and Denmark.

The middle Priabonian age assignment to the final marine deposits in the Tarim Basin is in agreement with the late Eocene age proposed by He Chengquan (1991). However, it is in conflict with the early Oligocene age proposed by Mao and Norris (1988). Their age assignment was predominately based on the Oligocene taxa: *Wetzeliella gochtii,* albeit other typical Oligocene taxa have not been observed by them. Furthermore, their correlation was based upon the fact that the typical Eocene taxon, *Areosphaeridium diktyoplokum,* was not encountered in the uppermost marine deposits. However, also in some late Eocene sections in Italy, *A. diktyoplokum* is characterized by a scattered occurrence throughout the Priabonian (Brinkhuis and Biffi, 1993; Brinkhuis, 1994). Thus the absence of *A. diktyoplokum* does not necessary imply an Oligocene age. Moreover, we have observed this typical 'Wulagen'-taxon in the Bashibulake Formation, which is in agreement with He Chengquan (1991). Most likely, the observed *W. gochtii* is a specimen of our 'cf. *gochtii*'. Nevertheless, the Wuluokeqiate section, the westernmost section of Mao and Norris (1988) comprising the Bashibulake Formation, is about 20 km further to the west than our westernmost section Mine section. This implies that marine deposits of a Oligocene age are present in the westernmost Tarim Basin, if their samples indeed contain *W. gochtii*. Consequently, the Paratethys sea had not retreated from a minor part of the Tarim Basin after the EOT. However, in respect of a shallow sea and the invoked eustatic sea level drop of ~70 m across the EOT (Miller et al. 2005), this explanation is not likely.

5.4 Mechanism of the Paratethys sea retreat

Tectonically controlled basin-infilling by the early Tibetan uplift cannot be completely ruled out (Bosboom et al., 2010), since clear indications of tectonic loading, such as conglomerates, may appear significantly later than the onset of the tectonic loading. This is caused by the principle that thrust-belt fronts migrate gradually to the distal foreland, which results in diachronous lithofacies (Yin et al., 2002). In our lithology there are indeed no signs for tectonic loading. Nevertheless, the sea retreated relatively slowly from east to west, according to age differences of the youngest marine deposits from Aertashi, Kezi and the Mine section. This may correspond to some distal uplift due the western Kunlun Shan thrust belt development, which initiated in the east and then diachronously migrated to the west (Yin et al, 2002). However, rather than some distal uplift effects, Yin et al (2002) claim that rapid subsidence occurred after the initiation of

the western Kunlun thrust belt. This subsidence should have started approximately 37 Ma and lasted for more than 10 Ma, at least at Aertashi. Rapid subsidence likely not forces a sea to retreat.

Moreover, basin infilling may have contributed to the final sea retreat from the Tarim Basin. Despite the fact that the water depths were approximately less than 50m, still a vast amount of sediments is necessary the cause a sea retreat due to basin infilling. Because, there are no clear signs for the uplift of the Pamir–Kunlun system earlier than the late Oligocene (Thomas et al., 1994; Sobel and Dumitru, 1997; Sobel, 1999; Burtman, 2000; Yang and Liu, 2002; Sobel et al., 2006; Robinson et al., 2007), there is no likely source for vast amounts of sediments nearby.

The middle Priabonian age (~35.7 Ma) for the final marine deposits of the Tarim Basin (at the Mine section) is in agreement with the conclusion from Bosboom et al. (2010) that final marine deposits of the early Paratethys in Tarim Basin predated the EOT (Bosboom et al., 2010). However, in contrast to their conclusion, the glacioeustatic sea level fall across the EOT (~33.6 Ma; Miller et al., 2009) may still have caused the final sea retreat from the Tarim Basin. In such a scenario, the youngest deposits (latest Eocene) would have been eroded by the sea retreat or afterwards, albeit there is no clear lithological evidence, like an erosional surface. The maximum age difference between the youngest marine deposits of the Tarim Basin and the glacioeustatic sea level fall across the EOT is ~2.1 Ma, while a correlation of the youngest marine deposits to top of Chron C15r, results in an age difference of 1.4 Ma. To cause a hiatus of ~1.4 Ma, likely a vast amounts of sediments should have been eroded, but it is an option that should be kept open with the preliminary data available yet. Accurately dating of the oldest continental deposits, which are situated on the youngest marine deposits, may shed some light on this topic.

Since the observed sea retreat at the Kezi section (~37 Ma) is in close correspondence to the global sea level lowstand around the Bartonian-Priabonian boundary (37.2 Ma; Miller et al., 2005), Bosboom et al., (2010) linked the eustatic sea level lowstand to the final retreat of the early Paratethys Sea out of the Tarim Basin. Moreover, they stated that the transgression and regression cycles in the Tarim Basin as a whole correlate well to the long term global sea level curve (Fig. 2). In the studied interval of the Mine section, two sea level curves can be recognized as discussed above. These sea level curves likely occurred within the time frame of ~40.5 Ma to ~35.7 Ma, which indicates that these are third order sea level cycles. The eustatic sea level curve (Miller et al, 2005), shows within this time interval one major sea level drop, the Bartonian lowstand, as well as two lowstands of a lesser magnitude in the Priabonian. The large Bartonian sea level drop (cycle 4.1; Haq et al., 1987) may be correlated to the first 'regression' in the studied interval at the Mine section, which was marked by the barren interval. The 'final' retreat would than be linked to one of the lowstands within the Priabonian (cycle 4.2; Haq et al, 1987). Since, the amplitude of the Priabonian sea level falls is not as large as the late Bartonian lowstand, the question remains whether these sea level drops solely could have caused the final sea retreat from the Tarim Basin. Most likely, the tectonic activity within the region also contributed to the final sea retreat from the Tarim Basin.

Finally, the final sea retreat from the Tarim Basin may coincide with the potentially impact induced 'Vonhof cooling event', which occurred within Chron C16n and lasted approximately from 35.5 to 35.0 Ma (Vonhof et al.,2000; Bohaty and Zachos, 2003; Abels et al., 2010). Although, the uppermost marine deposits have been tentatively correlated to C16n.1r (~35.7 Ma), correlations to the younger Chrons C16n.1n and C15r, approximately 35.6 - 35 Ma, cannot be excluded. The 'Vonhof cooling event' is characterized by a $\delta^{18}O$ shift of 0.5‰ (Vonhof et al.,2000; Bohaty and Zachos, 2003), which corresponds to a ~2 °C temperature decrease. The relatively long duration of the cooling, in the order of hundred thousand years, has suggested to be the result of feedback mechanisms, such as the build up of ice (Vonhof et al., 2000), which subsequently would have caused a (minor) eustatic sea level fall. So, most likely a part of the $\delta^{18}O$-excursion was caused by the build up of ice volumes. Following calibrations by Miller et al., (2009), a $\delta^{18}O_{seawater}$ excursion of 0.1‰–0.4‰ may be equivalent to a ~10–35 m sea-level fall. Such a sea level fall would have had its impact on the Tarim Basin. In Italy, the 'Vonhof cooling event' is marked by peak abundances of *Thalassiphora pelagica* (Brinkhuis and Coccioni, 1995; Vonhof et al., 2000). Such peaks have not been observed in the western part of the Tarim Basin, possibly because the Italian *Thalassiphora pelagica* peak was a more local phenomenon representing stratified waters (Pross and Schmiedl, 2002) rather than cooling (Vonhof et al., 2000). The lack of direct evidence hampers a correlation with the event. Nevertheless, the magnitude of the hypothesized sea level drop, induced by the possibly impact induced cooling event, may have been too high for the shallow setting, avoiding 'marine' conditions to persist longer in the western Tarim Basin.

5.5 Environmental impact of the Paratethys sea retreat

Modeling studies have emphasized that the Parathethys Sea could have been an important source of moisture for the Asian interior (Ramstein, 1997; Zhang et al., 2007). By a decrease in moisture supply due to the epicontinental sea retreat, aridification of the Asian interior would have been enhanced. Consequently, the Paratethys retreat from the Kezi section (~37 Ma) was tentatively linked to the first aridification step at the top of Chron C17n.1n (~ 36.6 Ma) in the Xining Basin (Abels et al., 2010; Bosboom et al., 2010). Our data indicates that marine conditions persisted at least within Chron C16n.1r (~35.7 Ma) in the '180 km' more westerly situated Mine section. So, the final sea retreat from the Mine section clearly not coincides with this first aridification step of the Xining Basin. However, the 'final' Paratethys sea retreat from the Tarim Basin would likely have enhanced aridification in its hinterland via a decreased moisture supply, albeit there are no high resolution studies available yet in this region to verify this.

The high resolution continental record of the Xining Basin from Abels et al. (2010) is characterized by a second phase of increased sedimentation rates. This second step occurs in the base of Chron C13r, approximately ~34.7 Ma (Abels et al., 2010). Considering the tentatively correlated timing of the 'final' sea retreat from the Tarim Basin (~35.7 Ma), there seems to be a relatively long period, a delay of ~1 Ma, between the sea retreat and the second 'aridification' step. Such a long response time, is thought to be unlikely. Therefore, if we consider the youngest marine deposits in the

westernmost part of the Tarim Basin to be deposited ~35.7 Ma, there is no link with an aridification step in Xining Basin.

However, assuming the correlation of the sea retreat from the westernmost Tarim Basin to the 'Vonhof cooling event', indicates that not only the increased seasonality associated with the 'Vonhof cooling event' (35.5-35 Ma; Abels et al., 2010) may explain the aridification in the Xining Basin. Also, the retreat of the inland Paratethys sea, which was probably still a moisture source for the Asian interior (e.g. the Xining Basin), has then likely contributed to the enhanced aridification. The further decrease in moisture supply may have altered the 'protective' vegetation cover, leading to higher sedimentation rates (Abels et al., 2010).

6. Conclusions

In the summer of 2010 five sections in the Tarim Basin (Mine, Kansu, Kezi, Aertashi and Keliyang) have been lithostratigraphically logged. Magneto- and biostratigraphically samples were taken order to date the final marine deposits. Two sections, 'Mine' and 'Kansu', have not been described in the literature before, of which the Mine section can be confirmed in yielding marine deposits after palynological study.

The final marine deposits at the westerly Mine section are slightly younger than the more eastern oriented Kezi section, ensuing the sea retreated from east to west. The final retreat of the early Paratethys from the Tarim Basin occurred in the middle Priabonian (~35.7 Ma). This date, clearly predates the eustatic sea level drop associated with the Eocene-Oligocene transition (EOT; ~34 Ma) which is in agreement with the conclusion from Bosboom et al. (2010). However, the sea level drop associated with the EOT, cannot be excluded as mechanism for the final sea retreat from the Tarim Basin. In such a scenario the latest Eocene marine deposits would have been eroded. The middle Priabonian age of the final sea retreat may indicate a link with the 'Vonhof cooling event' (~35.5-35.0 Ma). Its associated sea level drop may have induced the final sea retreat from the Tarim Basin. Furthermore the observed sea level cycles within the studied interval may be linked to eustatic sea level variations, such as the late Bartonian lowstand and some minor Priabonian lowstands. Distal tectonic activity cannot be excluded as a mechanism for the final retreat, albeit there is no evidence for tectonic loading in this study and other studies suggest rapid subsidence rather than distal tectonic uplift due to the tectonic activities in the western part of the Tarim Basin.

Dinoflagellate assemblages indicate shallow marine environments (<50m water depth) for the Tarim Basin across the studied intervals, wherein periods of marine (less proximal) conditions were alternated with more restricted 'lagoonal' circumstances. Outer neritic species like *Spiniferites* spp., dominated during the 'less proximal'-environments, whereas Goniodomid taxa like *Homotryblium* spp. mark more restricted environments. The dinocyst assemblages mark, in combination with the lithology, two relative sea level cycles. Moreover, we have recorded a phase of mass occurrence of cysts presumably produced by fresh water tolerant heterotrophic dinoflagellates, indicative for increased supply of freshwater. Finally, dinoflagellate assemblages show a strong correspondence with records from SW Siberia and in a lesser extent Italy, which confirmed that surface water connections existed between these water bodies. According to the (lack of abundant) terrestrial palynomorphs, vegetation was sparse in the middle Eocene. During the early Priabonian vegetation increased, indicating a more humid environment. Subsequent to the sea retreat, the moisture supply from the early Paratethys to the Asian interior likely decreased further. This may have contributed to enhanced regional aridification. There is no firm link between the final sea retreat from the Tarim Basin and increases of aridification in the Xining Basin.

References

Abels, H.A., Dupont-Nivet, G., Xiao, G., Bosboom, R., Krijgsman, W., 2011. Step-wise Asian paleoenvironmental changes preceding the Eocene - Oligocene Transition (EOT) in the terrestrial Xining Basin, China. Palaeogeography, Palaeoclimatology, Palaeoecology 299, 399–412.

Bohaty, S.M., Zachos, J.C., 2003. Significant Southern Ocean warming event in the late middle Eocene. Geology 31, 1017–1020.

Bosboom, R.E., Dupont-Nivet, G., Houben, A.J.P., Brinkhuis, H., Villa, G., Mandic, O., Stoica, M., Zachariasse, W.J., Guo, Z., Li, C., Krijgsman, W., 2010. Late Eocene sea retreat from the Tarim Basin (west China) and concomitant Asian paleoenvironmental change. Palaeogeogr. Palaeoclimatol. Palaeoecol. 299, 385–398.

Brinkhuis, H., 1994. Late Eocene to early Oligocene dinoflagellate cysts from the Priabonian type-area (northeast Italy); biostratigraphy and palaeoenvironmental interpretation. Palaeogeography, Palaeoclimatology, Palaeoecology 107, 121–163.

Brinkhuis, H., Biffi, U., 1993. Dinoflagellate cyst stratigraphy of the Eocene/Oligocene transition in central Italy. Marine Micropaleontology 22, 131– 183.

Brinkhuis, H., and Coccioni, R., 1995, Is there a relation between dinocysts changes and iridium after all? Preliminary results from the Massignano section, in Montanari, A., and Coccioni, R., eds., The effects of impacts on the atmosphere and biosphere with regard to short- and long-term changes: Abstracts and field trips: Ancona, Italy, European Science Foundation, p. 40.

Burtman, V.S., 2000. Cenozoic crustal shortening between the Pamir and Tien Shan and a reconstruction of the Pamir–Tien Shan transition zone for the Cretaceous and Palaeogene. Tectonophysics.

Burtman, V.S., Molnar, P., 1993. Geological and geophysical evidence for deep subduction of continental crust beneath the Pamir. Geological Society of America Special Paper 281, 76p.

Châteauneuf, J.-J., and Gruas-Cavagnetto, C., 1978. Les Zones de Wetzeliellaceae (Dinophyceae) du bassin de Paris. Bulletin du bureau de recherches géologiques et minières, Section IV, 2: 59–93.

Coutand, I., 2002. Late Cenozoic tectonic development of the intramontane Alai Valley, (Pamir-Tien Shan region, central Asia): an example of intracontinental deformation due to the Indo-Eurasia collision. Tectonics 21 (6), 1–19.

Cowgill, E., 2010. Cenozoic right-slip faulting along the eastern margin of the Pamir salient, northwestern China. Geological Society of America Bulletin 122, 145-161.

De Coninck, J., 1986. Organic walled phytoplankton from the Bartonian and Eo-Oligocene transitional deposits of the Woensdrecht Borehole, southern Netherlands. Mededelingen Rijks Geologische Dienst, 40: 1–49.

Dupont-Nivet, G., Guo, Z., Butler, R.F., Jia, C., 2002. Discordant paleomagnetic direction in Miocene rocks from the central Tarim Basin: evidence for local deformation and inclination shallowing. Earth and Planetary Science Letters 199, 473–482.

Dupont-Nivet, G., Krijgsman, W., Langereis, C.G., Abels, H.A., Dai, S. & Fang. X., 2007. Tibetan plateau aridification linked to global cooling at the Eocene-Oligocene transition. *Nature* 445, 635-638

Dupont-Nivet, G., Hoorn, C. & Konert, M., 2008. Tibetan uplift prior to the Eocene-Oligocene climate transition: evidence from pollen analysis of the Xining Basin Geology 36;987-990

Dupont-Nivet, G., Lippert, P.C., van Hinsbergen, D.J.J., Meijers, M.J.M., Kapp, P., 2010 - Palaeolatitude and age of the Indo-Asia collision: palaeomagnetic constraints Geophysical Journal International [Geophys. J. Int.]. Vol. 182, no. 3, pp. 1189-1198.

Eldrett J.S., Harding I.C., Firth J.V., Roberts A.P. 2004. Magnetostratigraphic calibration of Eocene–Oligocene dinoflagellate cyst biostratigraphy from the Norwegian–Greenland Sea. Marine Geology, 204: 91–127.

Eshet, Y., Almogi, L.A., Bein, A., 1994. Dinoflagellate cysts, paleoproductivity and upwelling systems; a late Cretaceous example from Israel. Marine Micropaleontology 23 (2), 231– 240.

Fensome, R.A., Williams, G.L., 2004. The Lentin and Williams index of fossil dinoflagellates. American Association of Stratigraphic Palynologists Foundation Contr. Series. 42, 909 pp.

Gradstein, F.M., Ogg, J.G., Smith, A.G., 2004. The Geomagnetic Polarity Time Scale. A geologic time scale 2004. Cambridge University Press, Cambridge. 589 pp.

Graham, S.A., et al., 2005. Stable isotope records of Cenozoic climate and topography, Tibetan plateau and Tarim basin. American Journal of Science 305 (2), 101–118.

Hao, Y.C., Zeng, X.L., and Li, H. 1982. Late cretaceous and Tertiary strata and foraminifera in Western talimu Basin. Journal of the Wuhan College Geology 7 (2):1-161 (In Chinese)

Hao, Y.C., Zeng, X.L., 1984. On the evolution of the west Tarim gulf from Mesozoic to Cenozoic in terms of characteristics of foraminiferal fauna. Acta Micropalaeontologica Sinica 1 (1), 1–13.

Haq, B.U., Hardenbol, J., and Vail, P.R., 1987, Chronology of fluctuating sea levels since the Triassic (250 million years ago to present): Science, v. 235, p. 1156–1167

He Chengquan, 1991: Late Cretaceous-Early Tertiary microphytoplankton from the western Tarim Basin in southern Xinjiang, China. Nanjing Institute of Geology and Palaeontology, Academia Sinica, p.1-235, pl.1-65. (In Chinese with English summary.)

Heilmann-Clausen C., Van Simaeys S. 2005. Dinoflagellate cysts from the Middle Eocene to ?lowermost Oligocene succession in the Kysing Research borehole, central Danish Basin. Palynology, 29: 143–204.

Iakovleva, A. I., Brinkhuis, H., and Cavagnetto, C.: Late Palaeocene-Early Eocene dinoflagellate cysts from the Turgay Strait, Kazakhstan; correlations across ancient seaways, Palaeogeogr. Palaeocl., 172, 243–268, 2001.

Iakovleva, A., Heilmann-Clausen C. 2010. Eocene Dinoflagellate Cyst Biostratigraphy of Research Borehole 011-BP, Omsk Region, Southwestern Siberia. Palynology, 34(2): 195–232.

Islam, M.A., 1984. A study of Early Eocene palaeoenvironments in the Isle of Sheppey as determined from microplankton assemblages composition. Tertiary Res. 6, 11–21.

Jaramilloa C. A., Oboh-Ikuenobe F. E. 1999. Sequence stratigraphic interpretations from palynofacies, dinocyst and lithological data of Upper Eocene–Lower Oligocene strata in southern Mississippi and Alabama, U.S. Gulf Coast. Palaeogeography, Palaeoclimatology, Palaeoecology, 145, 259–30

Kohler J., Clausing A., 2000. Taxonomy and palaeoecology of dinoflagellate cysts from Upper Oligocene freshwater sediments of Lake Enspel, Westerwald area, Germany, Review of Palaeobotany and Palynology, Volume 112, Issues 1-3, Pages 39-49

Lan, X., 1997. Paleogene bivalve communities in the western Tarim Basin and their paleoenvironmental implications. Paleoworld, 7: 137-157.

Lan, X. and Wei, J. (Editors), 1995. Late Cretaceous-Early Tertiary Marine Bivalve Fauna From the Western Tarim Basin. Chinese Science Publishing House, Beijing, 212 pp.

Mao, S., Norris, G., 1988. Late Cretaceous-early Tertiary dinoflagellates and acritarchs from the Kashi area, Tarim Basin, Xinjiang Province, China. Life Science Contributions, 150. Royal Ontario Museum. 93 pp.

Marret, F., Zonneveld, K.A.F., 2003. Atlas of modern organic walled dinoflagellate cyst distribution. Rev. Palaeobot. Palynol. 125, 1 –200.

Miller, K.G., et al., 2005. The Phanerozoic record of global sea-level change. Science 310 (5752), 1293–1298.

Miller, K.G., Wright, J.D., Katz, M.E., Wade, B.S., Browning, J.V., Cramer, B.S., and Rosenthal, Y., 2009. Climate threshold at the Eocene-Oligocene transition: Antarctic ice sheet influence on ocean circulation, in Koeberl, C., and Montanari, A., eds., The Late Eocene Earth—Hothouse, Icehouse, and Impacts: Geological Society of America Special Paper 452, p. 1–10

Pearson, P.N., Bart, E., van Dongen, B.E., Nicholas, C.J., Pancost, R.D., Schouten, S., Singano, J.M., and Wade, B.S., 2007, Stable warm tropical climate through the Eocene Epoch: Geology, v. 35 pp. 211

Powell, A.J., Lewis, J., Dodge, J.D., 1992. The palynological expressions of post-Paleogene upwelling: a review. In: Summerhayes, C.P., Prell,W.L., Emeis, K.C. (Eds.), Upwelling Systems: Evolution since the Early Miocene. The Geological Society,London, pp. 215– 226.

Powell, A. J., Brinkhuis, H., and Bujak, J. P., 1996. Upper Paleocene - Lower Eocene dinoflagellate cyst sequence biostratigraphy of southeast England, in: Correlation of the Early Paleogene in Northwest Europe, Geological Society Special Publication, 101, edited by: Knox, R. W. O. B., Corfield, R. M., and Dunay, R. S., 145–183.

Pross, J. and Schmiedl, G., 2002. Early Oligocene dinoflagellate cysts from the Upper Rhine Graben (SW Germany): Paleoenvironmental and paleoclimatic implications, Mar. Micropaleontol., 45, 1–24.

Pross, J. and Brinkhuis, H., 2005. Organic-walled dinoflagellate cysts as paleoenvironmental indicators in the Paleogene; a synopsis of concepts, Pal¨aontologische Zeitschrift, 79, 53–59.

Ramstein, G., Fluteau, F., Besse, J., Joussaume, S., 1997. Effect of orogeny, plate motion and land–sea distribution on Eurasian climate change over the past 30 million years. Nature 386, 788–795.

Reichart, G.-J., Brinkhuis, H., 2003. Late Quaternary Protoperidinium cysts as indicators of paleoproductivity in the northern Arabian Sea. Marine Micropaleontology 49 (4), 303– 370.

Reading, H.G. (Ed.), 2006. Sedimentary Environments: Processes, Facies and Stratigraphy. Blackwell Publishing Inc., Oxford. 688 pp.

Rögl, F., 1999. Short note: Mediterranean and Paratethys. Facts and hypotheses of an Oligocene to Miocene paleogeography (short overview). Geologica Carpathica 50 (4), 339–349.

Röhl, U., Brinkhuis, H., Stickley, C.E., Fuller, M., Schellenberg, S.A., Wefer, G., Williams, G.L., 2004. Sea level and astronomically induced environmental changes in middle and late Eocene sediments from the East Tasman Plateau. In: Exon, N.F., Malone, M., Kennett, J.P. (Eds.), Climate evolution of the Southern Ocean and Australia's northward flight from Antarctica; American Geophysical Union Geophysical Research Series.

Sluijs, A., Brinkhuis, H., Stickley, C. E., Warnaar, J., Williams, G. L., and Fuller, M., 2003 Dinoflagellate cysts from the Eocene/Oligocene transition in the Southern Ocean; results from ODP Leg 189., in: Proceedings Ocean Drilling Program, Scientific Results 189, edited by: Exon, N. F., Kennett, J. P., and Malone, M. J., College Station, Texas, 1–42.

Sluijs, A., Pross, J., Brinhuis, H., 2005. From greenhouse to icehouse; organic-walled dinoflagellate cysts as paleoenvironmental indicators in the Paleogene. Earth-Science Reviews Volume 68, Issues 3-4, Pages 281-315

Sluijs, A., Brinkhuis, H., Schouten, S., Bohaty, S. M., John, C. M., Zachos, J. C., Sinninghe Damsté, J. S., Crouch, E. M., and Dickens, G. R., 2007. Environmental precursors to light carbon input at the Paleocene/Eocene boundary, Nature, 450, 1218–1221.

Sluijs, A., Brinkhuis, H., 2009, A dynamic climate and ecosystem state during the Paleocene-Eocene Thermal Maximum: Inferences from dinoflagellate cyst assemblages on the New Jersey Shelf, Biogeosciences, 6(8),1755–1781

Sobel, E.R., 1999. Basin analysis of the Jurassic-Lower Cretaceous southwest Tarim basin, northwest China. Geological Society of America Bulletin 709–724.

Sobel, E.R., Dumitru, T.A., 1997. Thrusting and exhumation around the margins of the western Tarim basin during the India-Asia collision. Journal of Geophysical Research 102 (B3), 5043–5063.

Sobel, E.R., Chen, J., Heermance, R.V., 2006. Late Oligocene-Early Miocene initiation of shortening in the Southwestern Chinese Tian Shan: implications for Neogene shortening rate variations. Earth and Planetary Science Letters 247 (1–2), 70–81.

Stickley, C. E., H. Brinkhuis, S. A. Schellenberg, A. Sluijs, U. Röhl, M. Fuller, M. Grauert, M. Huber, J. Warnaar, and G. L. Williams, 2004. Timing and nature of the deepening of the Tasmanian Gateway, Paleoceanography, 19

Tang, T., Xue, Y., Yu, C., 1992. Characteristics and sedimentary environments of the Late Cretaceous to early Tertiary marine strata in the western Tarim, China. Science Press, Beijing. 138 pp.

Tian, Z., Chai, G., Kang, Y., 1989. Tectonic evolution of the Tarim basin. In: Zhu, X. (Ed.), Chinese Sedimentary Basins. : Sedimentary Basins of the World. Elsevier, Amsterdam, pp. 33–42.

Thomas, J.-C., et al., 1994. Paleomagnetic evidence for Cenozoic block rotations in the Tadjick depression (Central Asia). Journal of Geophysical Research 99.

Torricelli, S., Knezaurek, G., Biffi, U., 2006. Sequence biostratigraphy and paleoenvironmental reconstruction in the Early Eocene Figols Group of the Tremp-Graus Basin (south-central Pyrenees, Spain), Palaeogeography, Palaeoclimatology, Palaeoecology, Volume 232, Issue 1, Pages 1-35

Torsvik, T. H., R. D. Müller, R. Van der Voo, B. Steinberger, and C. Gaina, 2008. Global plate motion frames: Toward a unified model, Rev. Geophys., 46

Yang, Y., Liu, M., 2002. Cenozoic deformation of the Tarim plate and the implications for mountain building in the Tibetan plateau and the Tian Shan. Tectonics 21 (6), 1059.

Yin, A., et al., 2002. Tectonic history of the Altyn Tagh fault systemin northern Tibet inferred from Cenozoic sedimentation. Geological Society of America Bulletin 114 (10), 1257–1295.

Watts, A.B., Steckler, M.S., 1979. Subsidence and eustasy at the continental margin of eastern North America. Deep drilling results in Atlantic Ocean: Continental margins and paleoenvironment. Maurice Ewing Series, 3. American Geological Union, Washington, D. C., pp. 218–234.

van Mourik, C.A., Brinkhuis, H., Williams, G.L., 2001. Middle to late Eocene organic walled dinoflagellate cysts from ODP Leg 171B, offshore Florida. In: Kroon, D., Norris, R.D., Klaus, A. (Eds.), Western North Atlantic Palaeogene and Cretaceous Palaeoceanography. Special Publication - Geological Society of London 183, 225–251

Vonhof, H.B., Smit, J., Brinkhuis, H., Montanari, A., Nederbragt, A.J., 2000. Global cooling accelerated by early late Eocene impacts? Geology 28, 687–690.

Zhang, Z.,Wang, H., Guo, Z., Jiang, D., 2007. What triggers the transition of palaeoenvironmental patterns in China, the Tibetan Plateau uplift or the Paratethys Sea retreat? Palaeogeography, Palaeoclimatology, Palaeoecology 245 (3–4), 317–331.

Zhang, Z., Flatoy, F., Wang, H., Bethke, I., Bentsen, M., Guo, Z., 2011. Early Eocene Asian climate dominated by desert and steppe with limited monsoons, Journal of Asian Earth Sciences, In Press, Corrected Proof

Zhong, S., 1989 Significance of calcareous nannofossils assemblage for Bashibulake Formation (Paleogene) in western Tarim Basin, Xinjiang. Acta Palaeontologica Sinica, 1.

Zhong, S., 1992. Calcareous Nannofossils from the Upper Cretaceous and Lower Tertiary in the Western Tarim Basin, South Xinjiang, China. Chinese Science Publishing House, Beijing. 121 pp

Appendices

Appendix I List of species
Appendix II Plates with palynological specimens
Appendix III Plates with dinocyst (SEM)
Appendix IV Lithologic logs

Appendix I - List of species

Achilleodinium biformoides

Achomosphaera sp

Adnatasphaeridium multispinosum

Adnatasphaeridium williamsii

Aeroligera spp.

Aeroligera spp.

Aerospharidium diktyoplokum

Apectodinium cf. *homomorphum*
Remarks: This species lacks prominent lateral horns; apical and antapical horns are reduced. This species differentiates from *A. homomorphum* in having more prominent, albeit still reduced, apical and antapical horns. It differs from *A. quinquelatum* by its reduced or absent lateral horns. Moreover, *A. paniculatum* is characterized by reduced or absent apical horn, however this species differs in having broad lateral and well developed long antapical horns. Some specimens were folded and poorly preserved hampering identification on species level, however if the horns seemed to be reduced, specimens were assigned to this group.

Cerodinium speciosum

Charlesdowniea clathrata

Charlesdowniea coleothrypta

Charlesdowniea tenuivirgula-crassiramosa

Charlesdowniea coleothrypta subsp. *rotundata* sensu De Coninck (1986)
Remarks: These species is characterized by a rhombic rather than a more pentagonal outline. Moreover it bears numerous fine processes. May be distinguished from *Charlesdowniea clathrata* subsp. *angulosa* (Châteauneuf & Gruas Cavagnetto 1978; Lentin & Vozzhennikova 1989) by its thombic outline (Heilmann-Clausen and van Simaeys, 2005)

Charlesdowniea wulagenensis
Charlesdowniea spp.
Remarks: This group yields specimens of which the preservation state was insufficient to distinguish on a species level, but the cyst was characterized by Wetzelielloid-outline and some united trabeculea have been observed

Charlesdowniea/Wetzeliella
Remarks: transitional form between Charlesdowniea and Wetzeliella

Cleistosphaeridium spp.

Cordosphaeridium cantharellum

Cordosphaeridium funiculatum

Cordosphaeridium inodes

Cordosphaeridium spp.

Corrudinium incompositum

Cribroperidinium tenuitabulatum

Cyclonephelium/Canigia cpx

Dapsilidinium pseudocolligerum

Deflandrea intrasphaerula

Deflandrea oebisfeldensis

Deflandrea phosphoritica

Deflandrea spp.

Dinopterygium sensu Morgenroth 1966

Diphyes colligerum

Diphyes creatum

Diphyes pseudoficusoides

Distatodinium craterum

Distatodinium ellipticum

Distatodinium paradoxum

Enneadocysta arcuata

Enneadocysta fenestrata

Enneadocysta pectiniformis

Enneadocysta spp.

Glaphyrocysta microfenestrata

Glaphyrocysta exuberans

Glaphyrocysta pastielsii

Glaphyrocysta spp.

Gonyaulacacysta spp.

Heteraulacacysta spp.

Homotryblium aculeatum

Homotryblium floripes

Homotryblium pallidum

Homotryblium plecticum

Homotryblium spp.

Hystrichodinium pulchrum

Hystrichokolpoma rigaudiae

Hystrichokolpoma salacium

Hystrichokolpoma truncatum

Hystrichokolpoma? sp.1 sensu Heilmann-Clausen and Van Simaeys 2005

Hystrichokolpoma spp.

Hystrichosphaeridium salpingohorum

Impagidinium brevisulcatum

Impagidinium spp.

Kenleyia spp.

Lejeunecysta spp.

Lentinia serrata

Leptodinium/Impagidinium-group

Lingulodinium machaeophorum

Melitasphaeridium pseudorecurvatum

Oligosphaeridum cpx.

Operculodinium microtriainum

Operculodinium centrocarpum cpx

Paleocystodinium golzowense

Palaeoperidinium sp.B sensu Mao and Norris 1988

Polysphaeridium/Dapsilidinium

Polysphaeridium spp.

Phelodinium pumilum

Phelodinium spp.

Phthanoperidinium spp.

Phthanoperidinium alectrolophum

Phthanoperidinium comatum

Phthanoperidinium geminatum

Phthanoperidinium cf Senegalinium

Rhombodinium draco

Rhombodinium longimanum

Selenopemphix armata

Selenopemphix nephroides

Senegalinium spp.

Spiniferites pseudofurcatus

Spiniferites spp.

Thalassiphora pelagica

Thalassiphora patula

Thalassiphora reticulata

Thalassiphora spp.

Turbiosphaera filosa

Wetzeliella articulata-group

Wetzeliella cf. *gochtii*
Remarks: In contrast to *W.articulata*, the horns are more reduced giving this species a (sub-) pentagonal to rounded ouline, similar to *W. gochtii.* although *W.ovalis* has a more ovaloid shape. The distance between the antapical horns is wider than in *W. gochtii,* causing a slightly more pentagonal outline. As for *W. gochtii*, its continuous and thicker pericoel can be used to distinguish it from *A.homomorphum*. Moreover, processes are more densely distributed and thicker than for *W. gochtii*. The (open) process tip may be characterized by some secae (aculeate-like), similar to e.g. *W. articulate* and *W.gochtii*. Cingulum may be discerned by the processes.

Appendix II – Plates with palynological assemblages

Appendix II
Plate 1

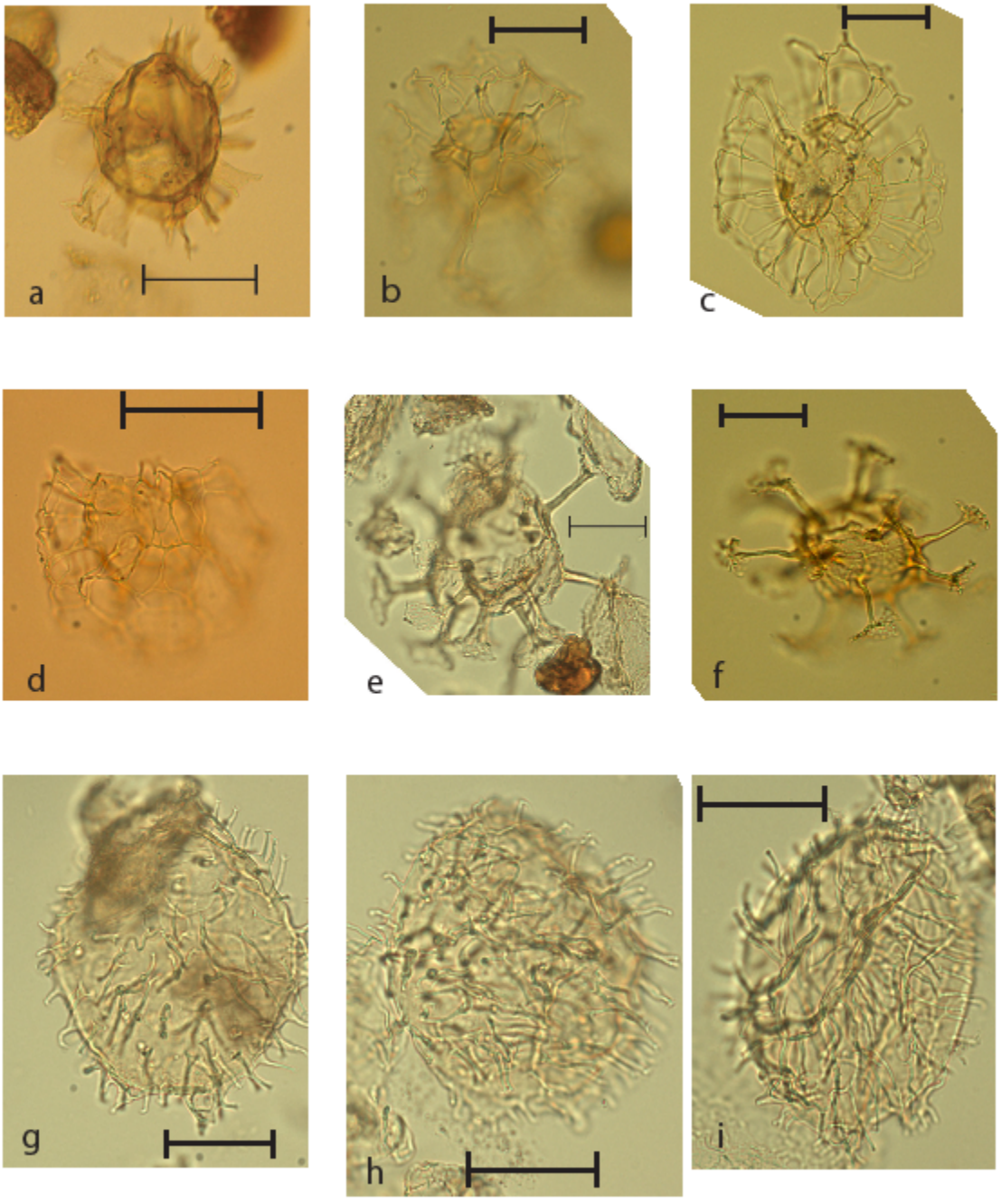

Figure a *Achilleodinium biformoides*, MS-B39
Figure b *Adnatasphaeridium williamsii*, MS-B25
Figure c *Adnatasphaeridium williamsii*, MS-B25
Figure d *Adnatasphaeridium williamsii*, MS-B25
Figure e *Aerospharidium diktyoplokum*, MS-B5
Figure f *Aerospharidium diktyoplokum*, MS-B25
Figure g *Apectodinium* cf. *homomorphum*, MS-B5
Figure h *Apectodinium* cf. *homomorphum*, MS-B5
Figure i *Apectodinium* cf. *homomorphum*, MS-B5

Appendix II
Plate 2

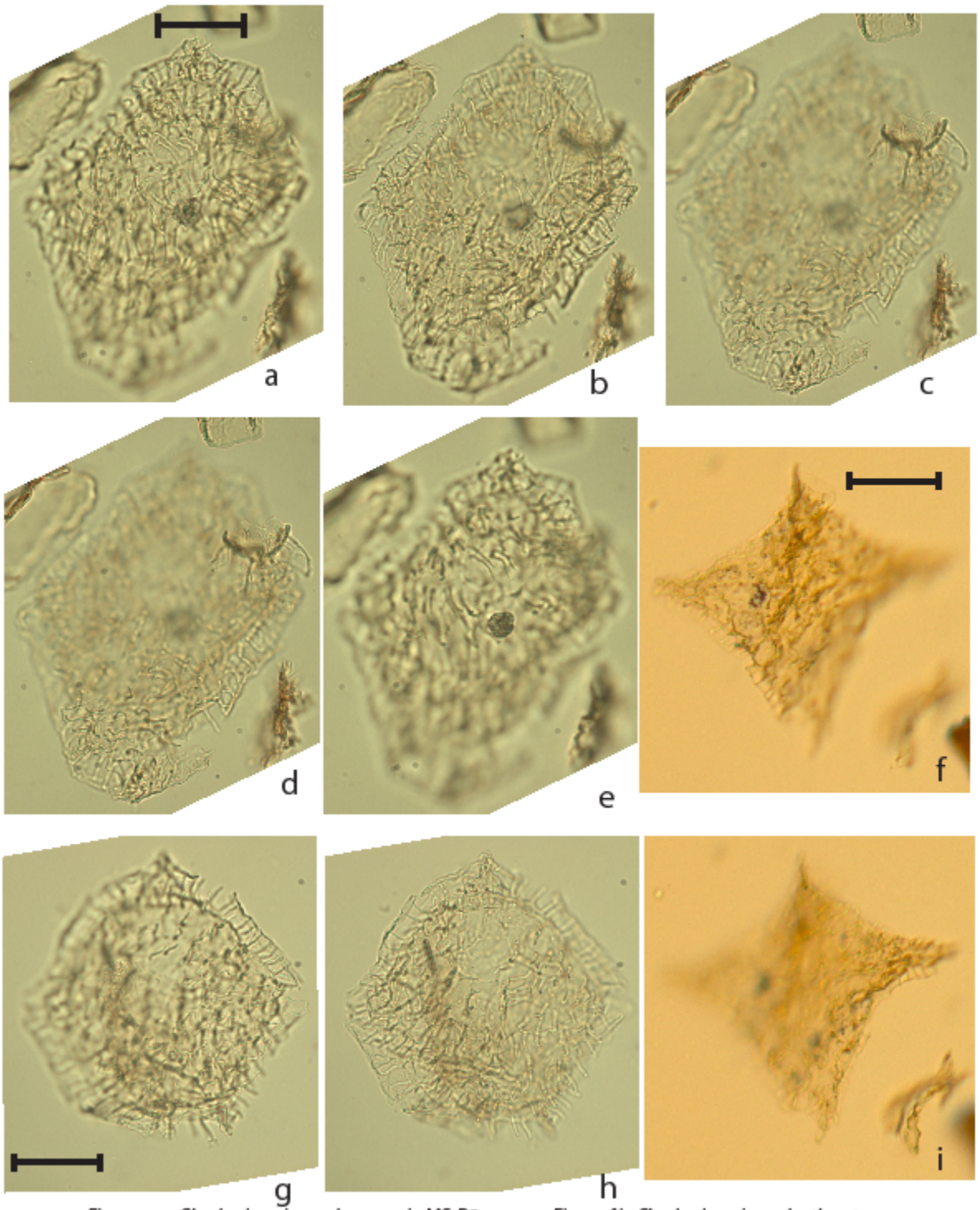

Figure a-e *Charlesdowniea wulagenensis*, MS-B5
Figure g,h *Charlesdowniea wulagenensis*, MS-B5
scale bar = 30 µm

Figure f,i *Charlesdowniea coleothrypta subsp. rotundata sensu De Coninck (1986)*
MS-B39

Appendix II
Plate 3

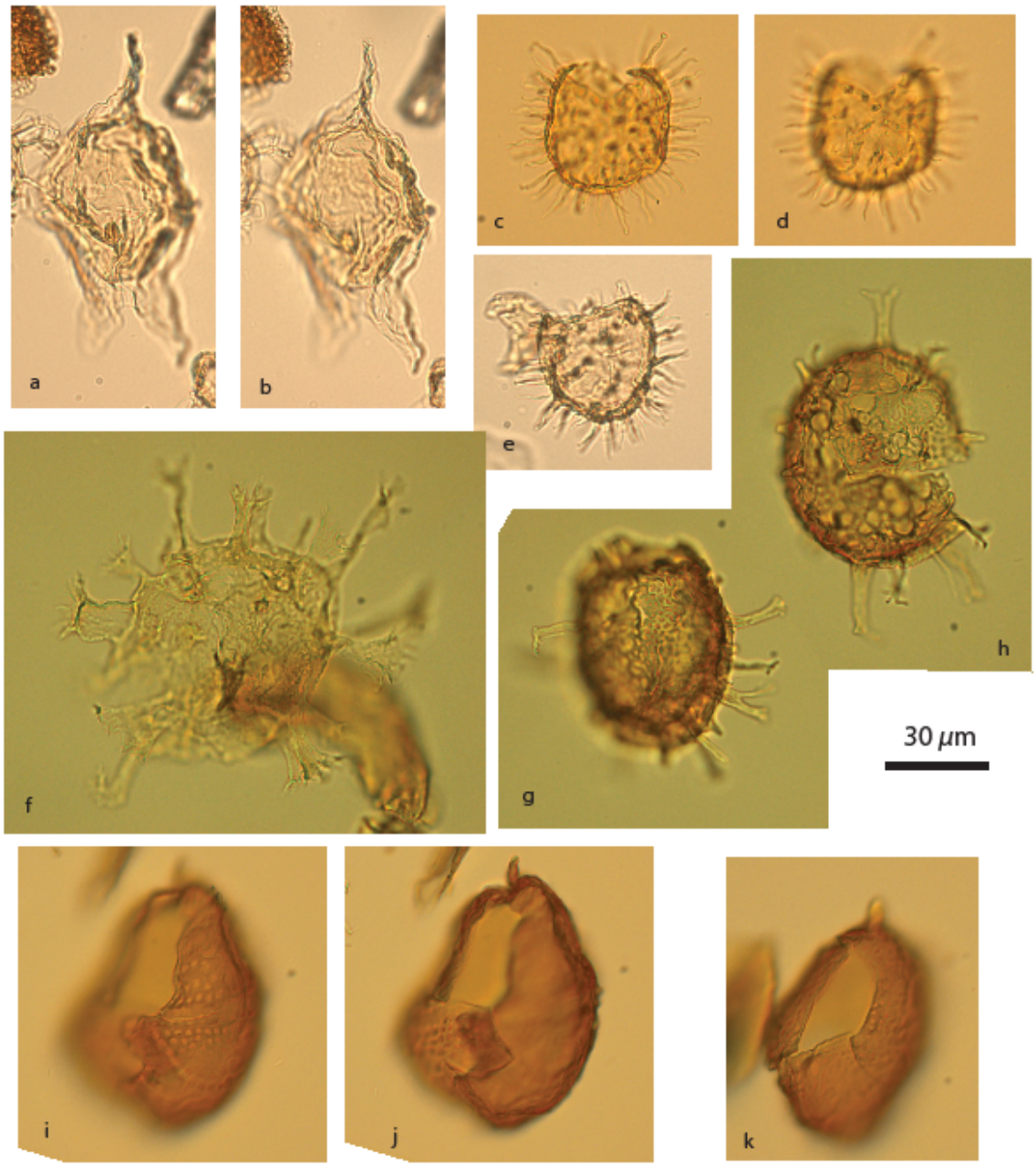

Figure a,b *Cerodinium Speciosum*, MS-B36
Figure c,d *Cleistosphaeridium* spp., MS-B25
Figure e *Cleistosphaeridium* spp., MS-B25
Figure f *Cordosphaeridium* spp., MS-B25
Figure g,h *Cordosphaeridium funiculatum*, MS-B25
Figure i,j,k *Cribroperidinium tenuitabulatum*, MS-B39

Appendix II
Plate 4

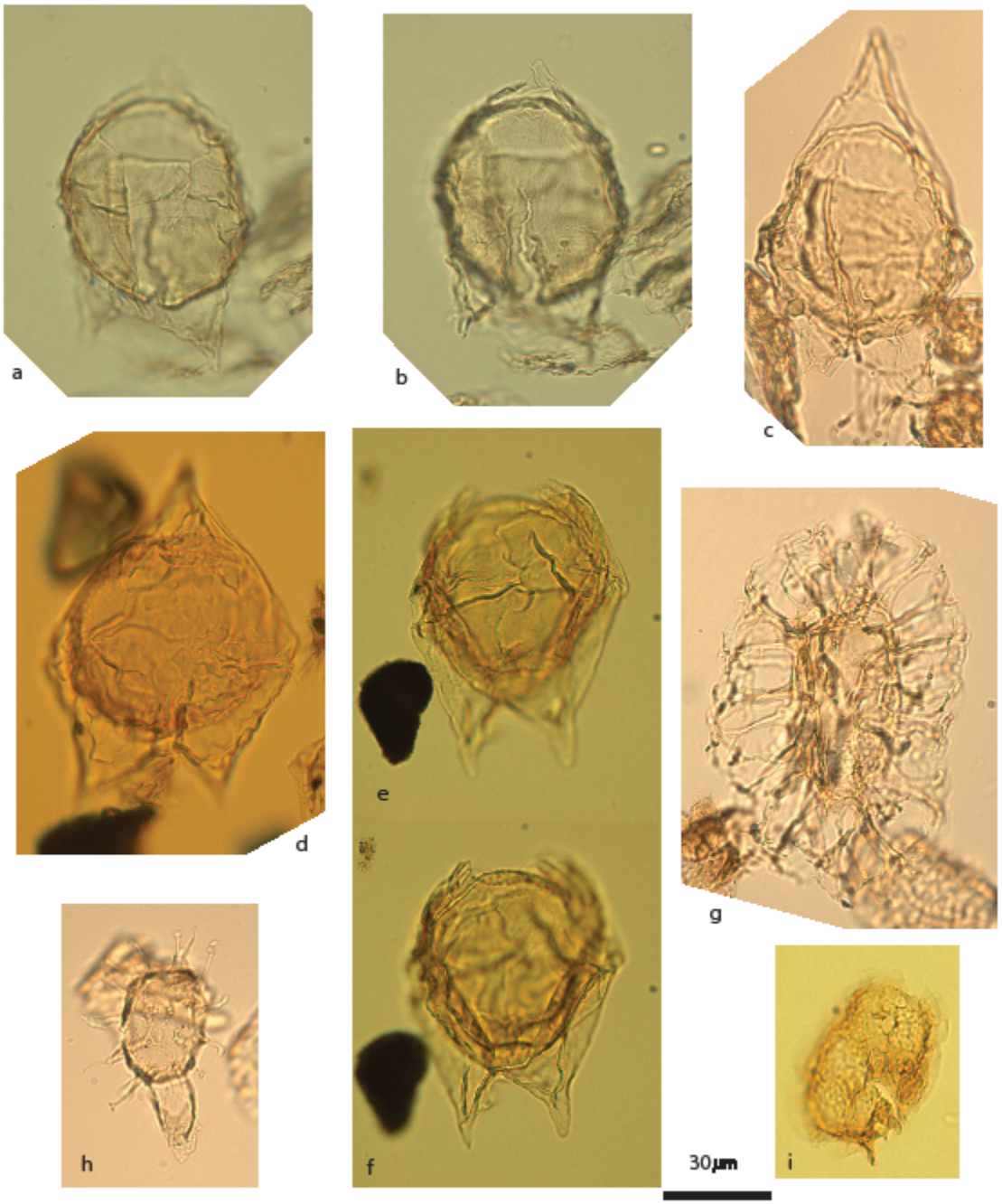

Figure a,b ***Deflandrea phosphoritica***, MS-B5
Figure c ***Deflandrea oebisfeldensis?***, MS-B36
Figure d ***Deflandrea phosphoritica***., MS-B16
Figure e,f ***Deflandrea phosphoritica***., MS-B16
Figure g *Distatodinium ellipticum*, MS-B17
Figure h ***Diphyes pseudoficusoides***, MS-B17
Figure i *Dinopterigium* sp. sensu Morgenroth, MS-B25

Appendix II

Plate 5

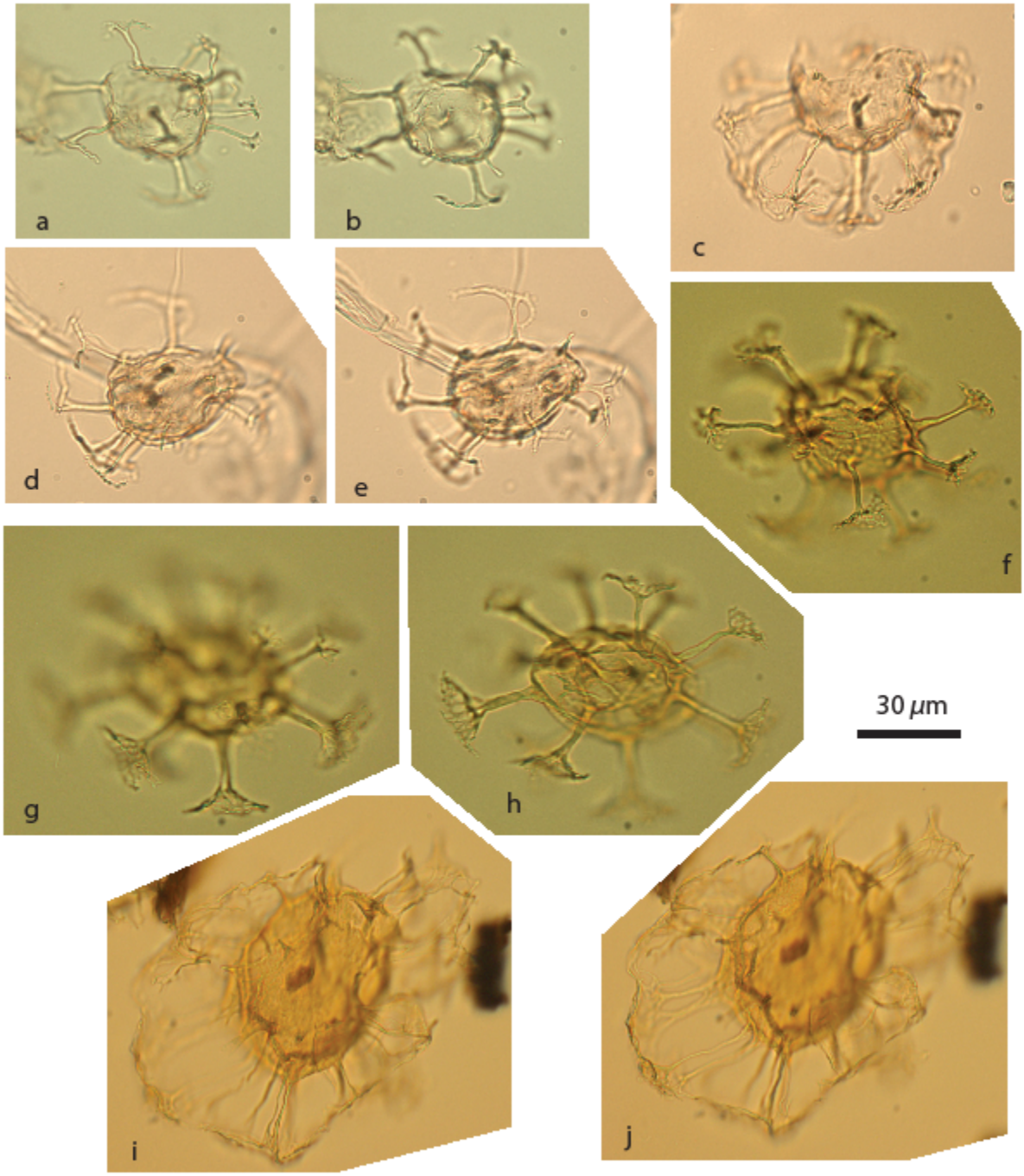

Figure a,b. *Enneadocysta pectiniformis*, MS-B5
Figure d,e. *Enneadocysta pectiniformis*, MS-B17
Figure g,h. *Areosphaeridium diktyoplokum*, MS-B25

Figure c. *Glaphyrocysta?* sp., MS-B36
Figure f. *Areosphaeridium diktyoplokum* MS-B25
Figure i,j. *Glaphyrocysta microfenestrata*, MS-B39

Appendix II
Plate 6

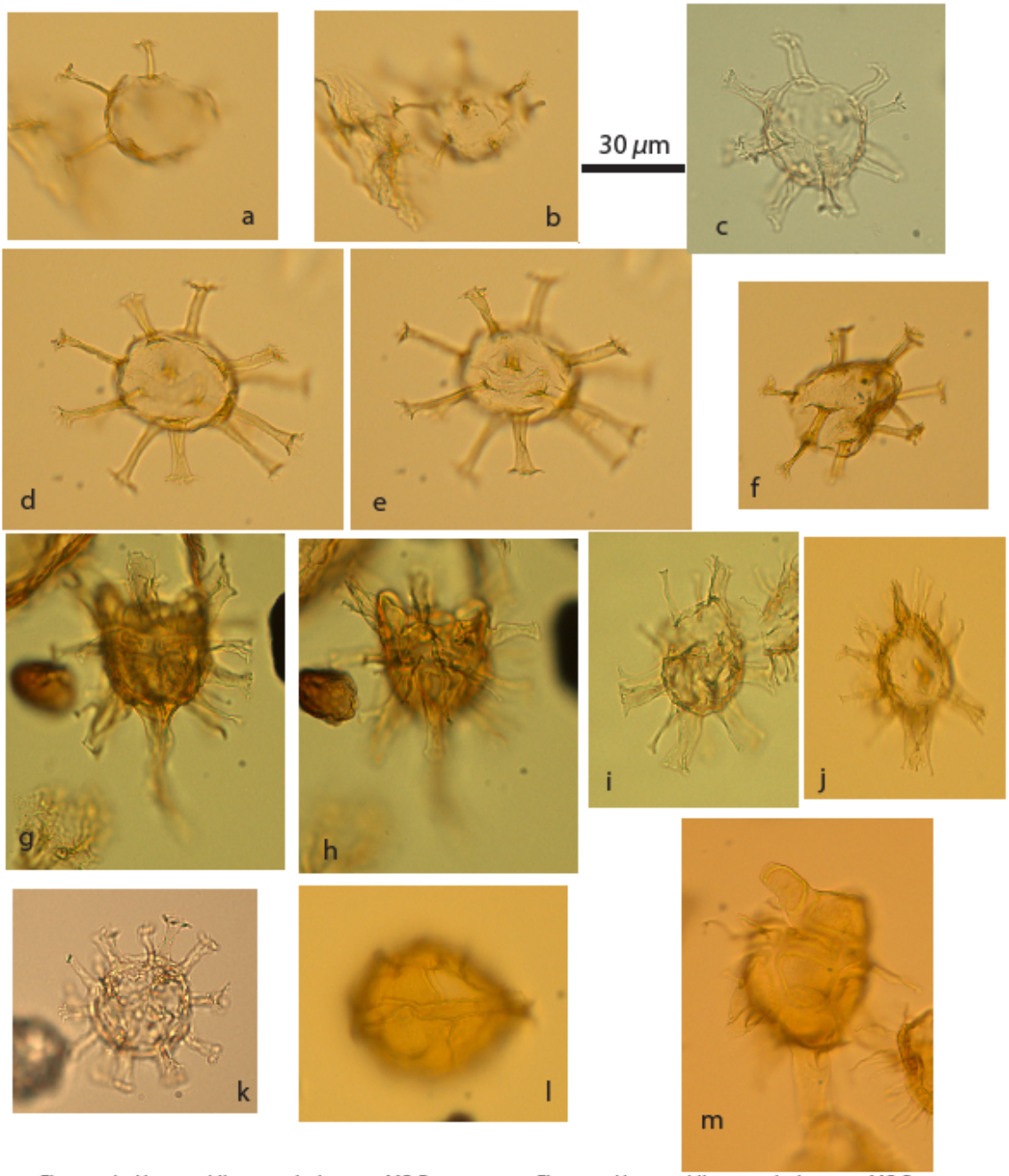

Figure a,b. *Homotryblium tenuispinosum*, MS-B39
Figure c. *Homotryblium tenuispinosum.*, MS-B5
Figure d,e. *Homotryblium tenuispinosum*, MS-B39
Figure f. *Homotryblium tenuispinosum*, MS-B39
Figure g,h. *Hystrichokolpoma rigaudiae*, MS-B16
Figure i. *Hystrichokolpoma rigaudiae*, MS-B25
Figure j. *Hystrichokolpoma rigaudiae*, MS-B16
Figure k. *Hystrichosphaeridium salpingohorum*, AT-B02
Figure l. *Impagidinium brevisulcatum*, MS-B16
Figure m. *Hystrichokolpoma rigaudiae*, MS-B16

Appendix II

Plate 7

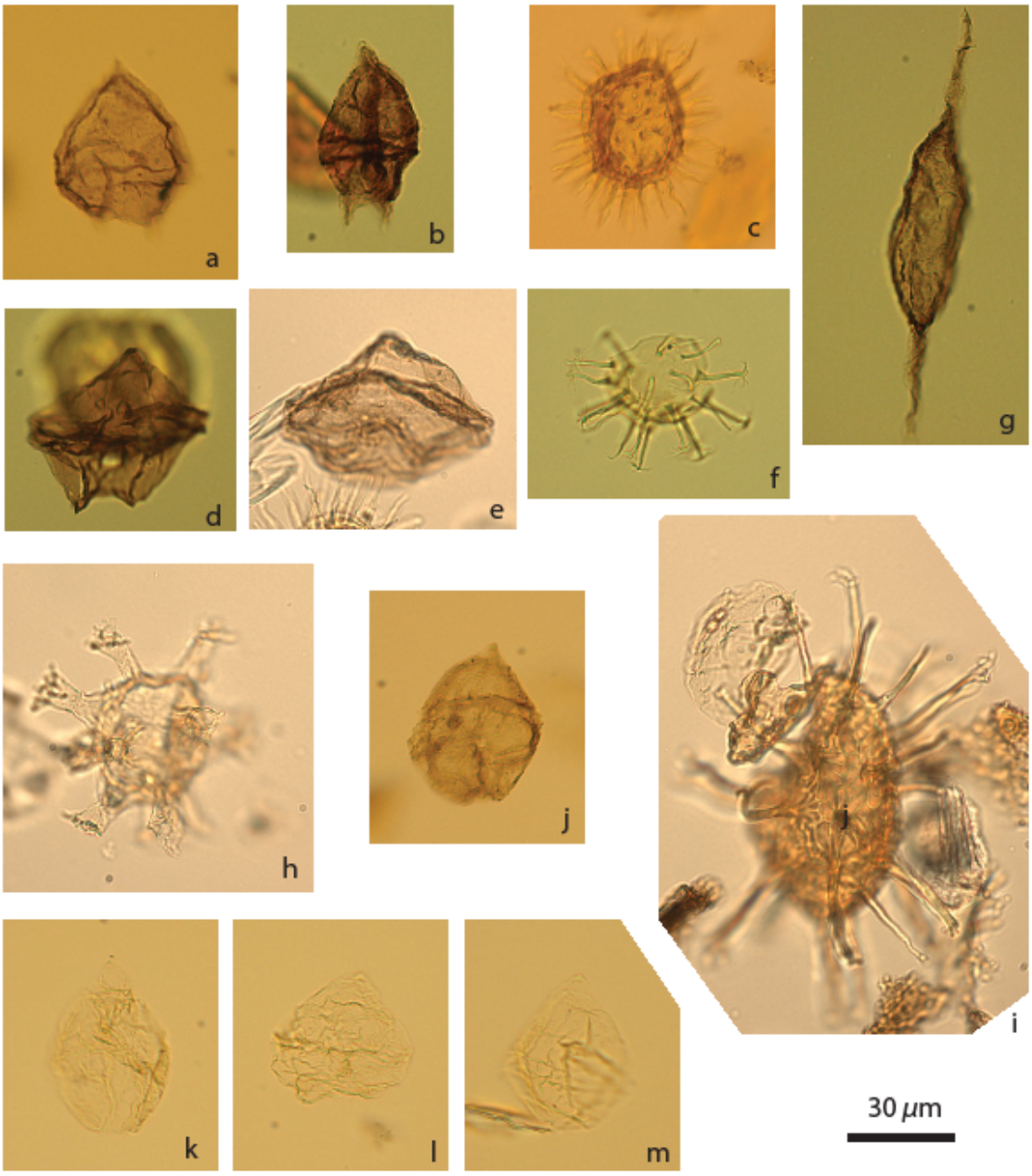

Figure a. *Lentinia serrata*, MS-B16
Figure b. *Lentinia serrata*, MS-B25
Figure c. *Lingulodinium machaerophorum* sp., MS-B16
Figure d. *Lejeunecysta* sp. B25
Figure e. *Lejeunecysta* sp. B17
Figure f. *Melitasphaeridium pseudorecurvatum*, MS-B25
Figure g. *Palaeocystodinium golzowense*, MS-B25
Figure h. *Oligosphaeridium complex*, MS-B17
Figure i. *Operculodinium tiara?*, MS-B17
Figure j. *Phthanoperidinium sp*, MS-B39
Figure k, l, m. *Phthanoperidinium* cf. *Senegalinium*, MS-B7

Appendix II
Plate 8

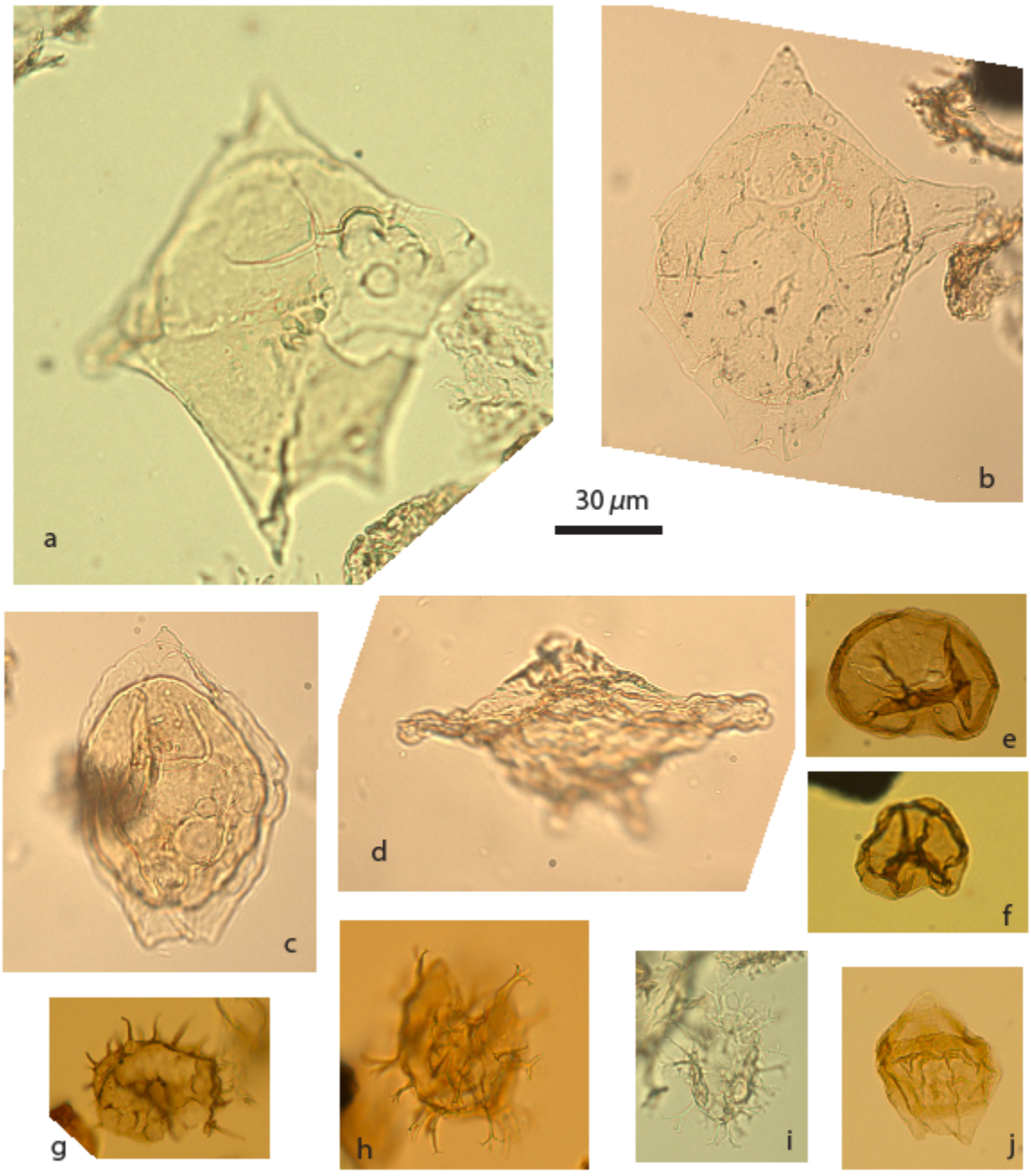

Figure a. *Rhombodinium draco* MS-B5

Figure b. *Rhombodinium draco,* MS-B17
specimen transitional to *R. Longimanum*
Figure c. *Rhombodinium draco.,* MS-B16
Figure d. *Rhombodinium longimanum* AT-B-37
Figure e. *Selenopemphix nephroides,* MS-B16
Figure f. *Selenopemphix nephroides,* MS-B39
Figure g. *Selenopemphix armata,* MS-B16
Figure h. *Spiniferites* spp., MS-B36
Figure h. *Spiniferites* spp., MS-B5
Figure j. *Senegalinium* sp., MS-B7

Appendix II
Plate 9

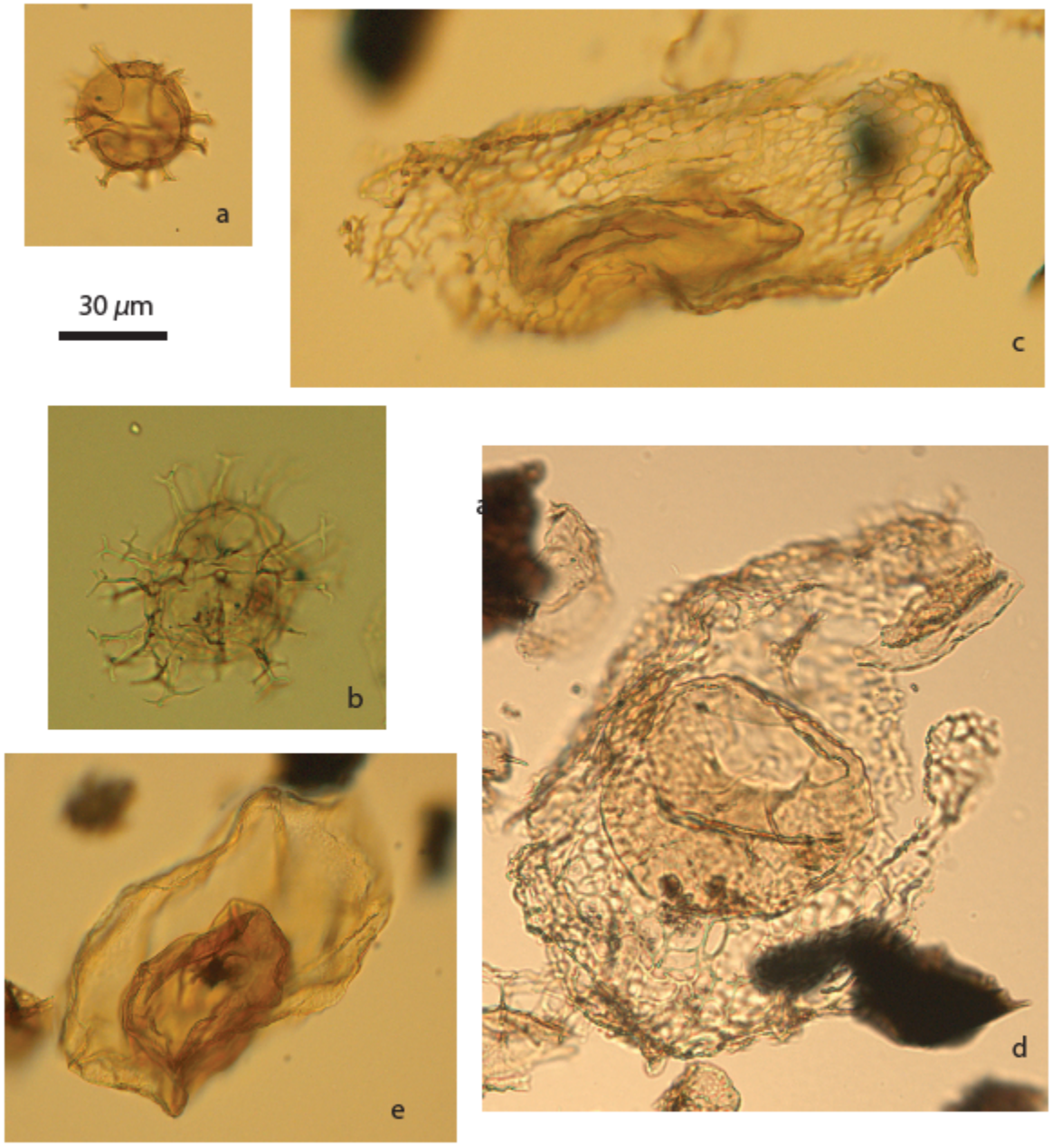

Figure a. *Spiniferites* spp., MS-B39
Figure c. *Thalassiphora reticulata*, MS-B39
Figure e. *Thalassiphora pelagica*, MS-B39

Figure b. *Spiniferites* spp., MS-B16
Figure d. *Thalassiphora reticulata* MS-B39 (2)

Appendix III – Plates with dinocyst (SEM)

Appendix III
Plate 1

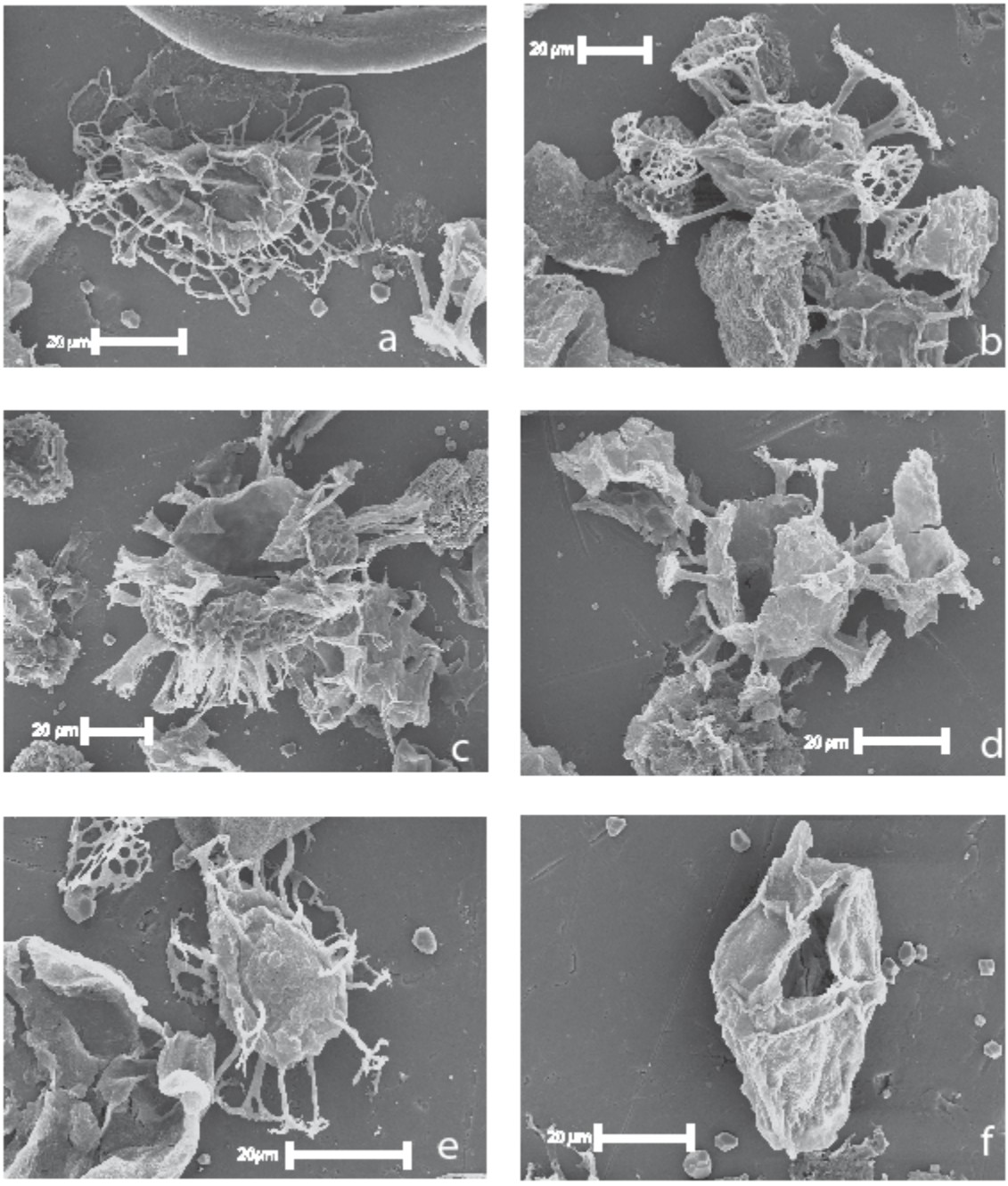

Figure a. *Adnatosphaeridium multispinosum*, MS-B16
Figure b. *Areosphaeridium diktyoplokum*, MS-B5
Figure c. *Cordosphaeridium funiculatum*, MS-B16
Figure d. *Enneadocysta partridgei*, MS-B5
Figure e. *Enneadocysta pectiniformis*, MS-B16
Figure f. *Gonyaulacysta* sp., MS-B5

Appendix III
Plate 2

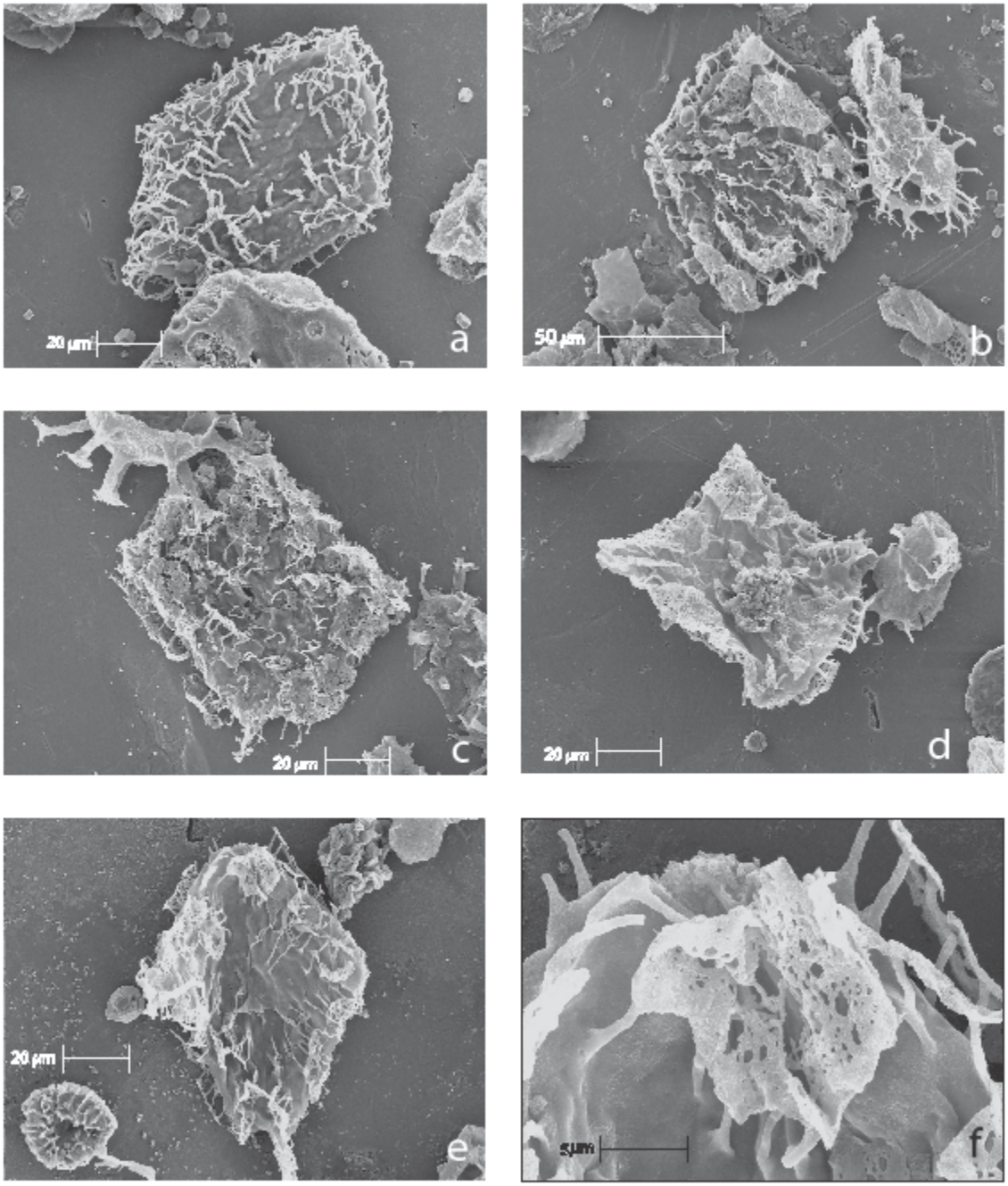

Figure a. *Charlesdowniea clathrata*, MS-B5
Figure c. *Charlesdowniea coleothrypta*, MS-B5

Figure e. *Charlesdowniea coleothrypta*, MS-B39

Figure b. *Charlesdowniea coleothrypta*, MS-B5
Figure d. *harlesdowniea coleothrypta* subsp. *rotundata* MS-B39

Figure f. same specimen as figure e: close up of membranous ectophragm, MS-B39

Appendix III
Plate 3

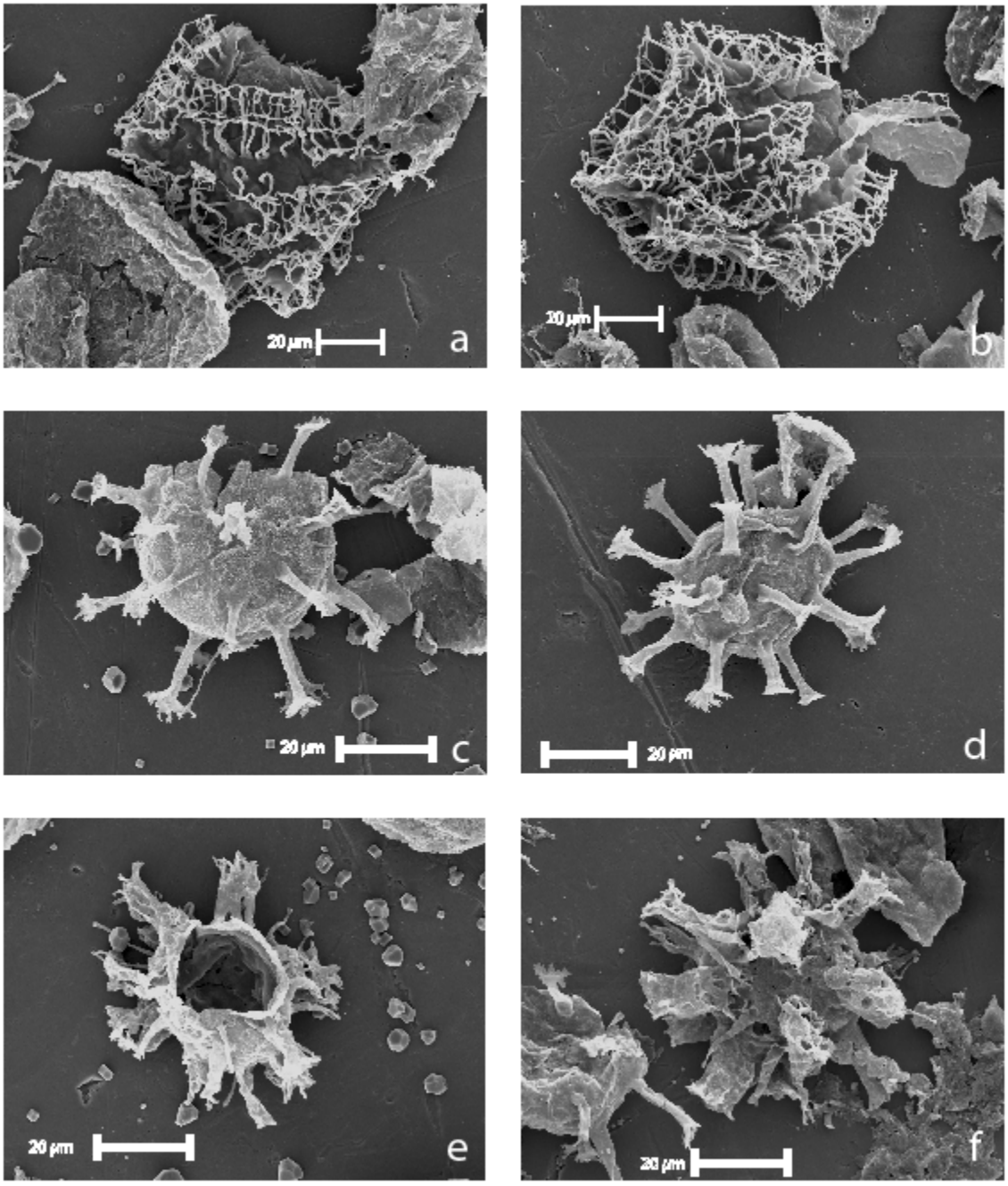

Figure a. *Charlesdowniea tenuivirgula-crassiramosa*, MS-B5
Figure b. *Charlesdowniea tenuivirgula-crassiramosa*, MS-B5
Figure c. *Hystrichosphaeridium salpingophorum*, MS-B5
Figure d. *Hystrichosphaeridium salpingophorum* MS-B5
Figure e. *Hystrichokolpoma rigaudiae*, MS-B5
Figure f. *Hystrichokolpoma rigaudiae*, MS-B5

Appendix III
Plate 4

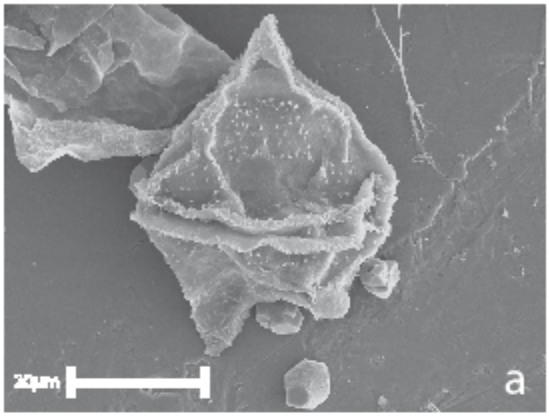

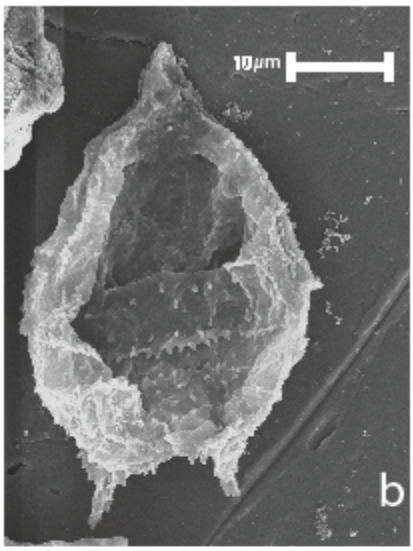

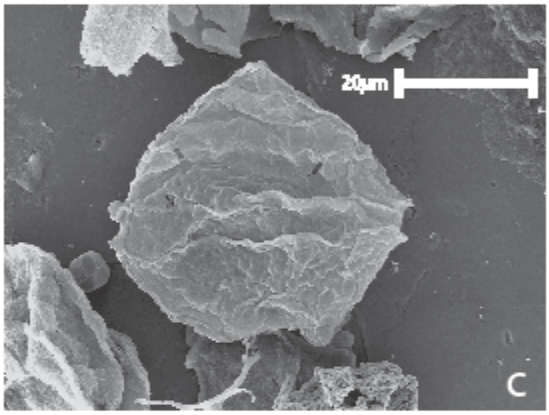

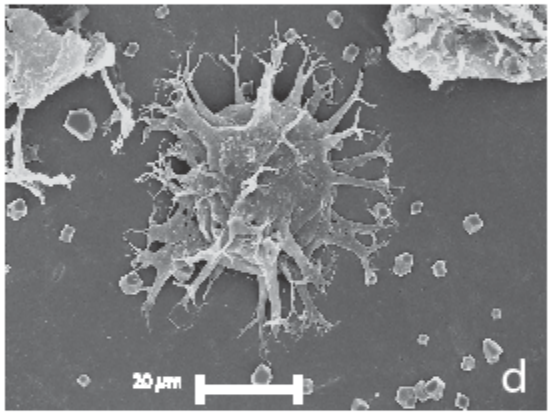

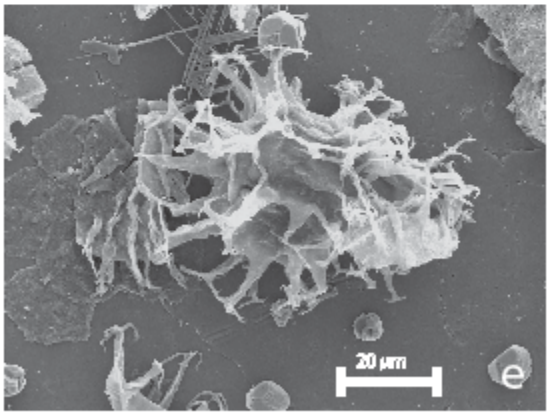

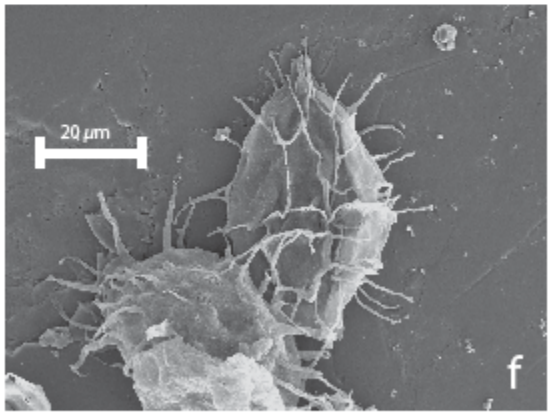

Figure a. *Lentinia serrata*, MS-B16
Figure b. *Phthanoperidinium* sp?, MS-B516
Figure c. *Phelodinium pumilum?*, MS-B16
Figure d. *Spiniferites* spp., MS-B5
Figure e. *Spiniferites* spp, MS-B16
Figure f. *Phthanoperidinium comatum*, MS-B16

Appendix III

Plate 5

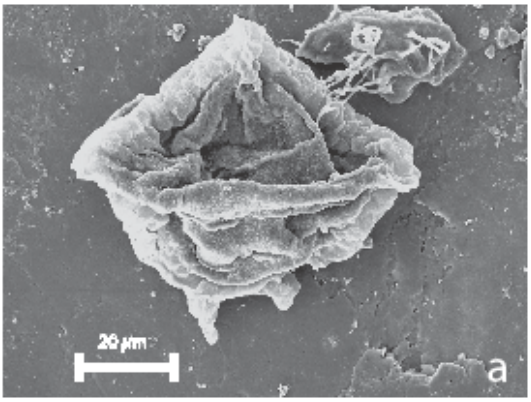

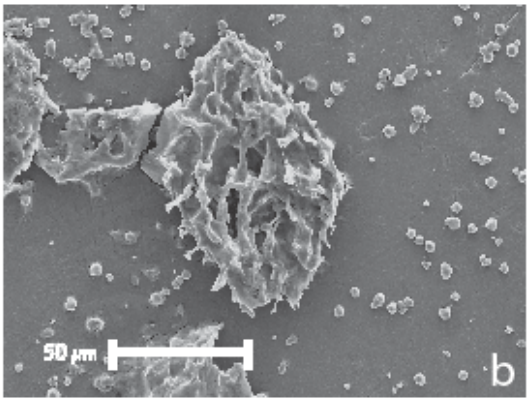

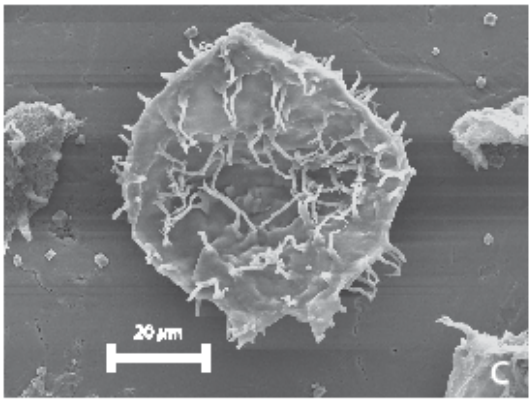

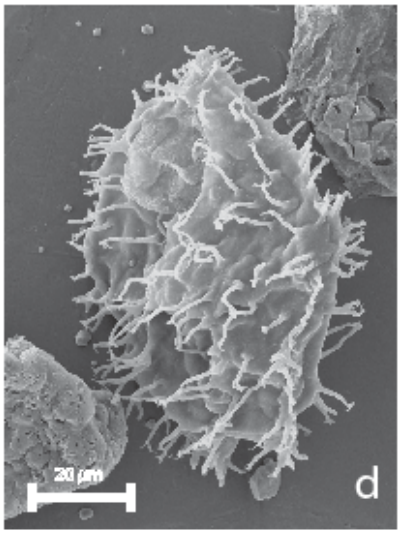

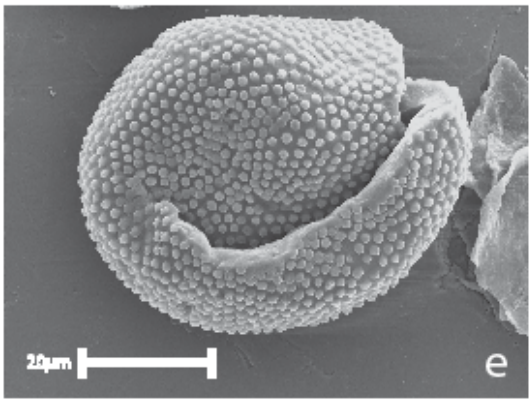

Figure a. *Phelodinium?* sp. , MS-B16
Figure c. *Wetzeliella* cf. *gochtii*, MS-B16
Figure e. *Tasmanites* spp., MS-B16

Figure b. poorly preserved *Wetzellieloid*, MS-B5
Figure d. *Wetzeliella* aff. *articulata*-group, MS-B5

Appendix IV – Lithologic logs

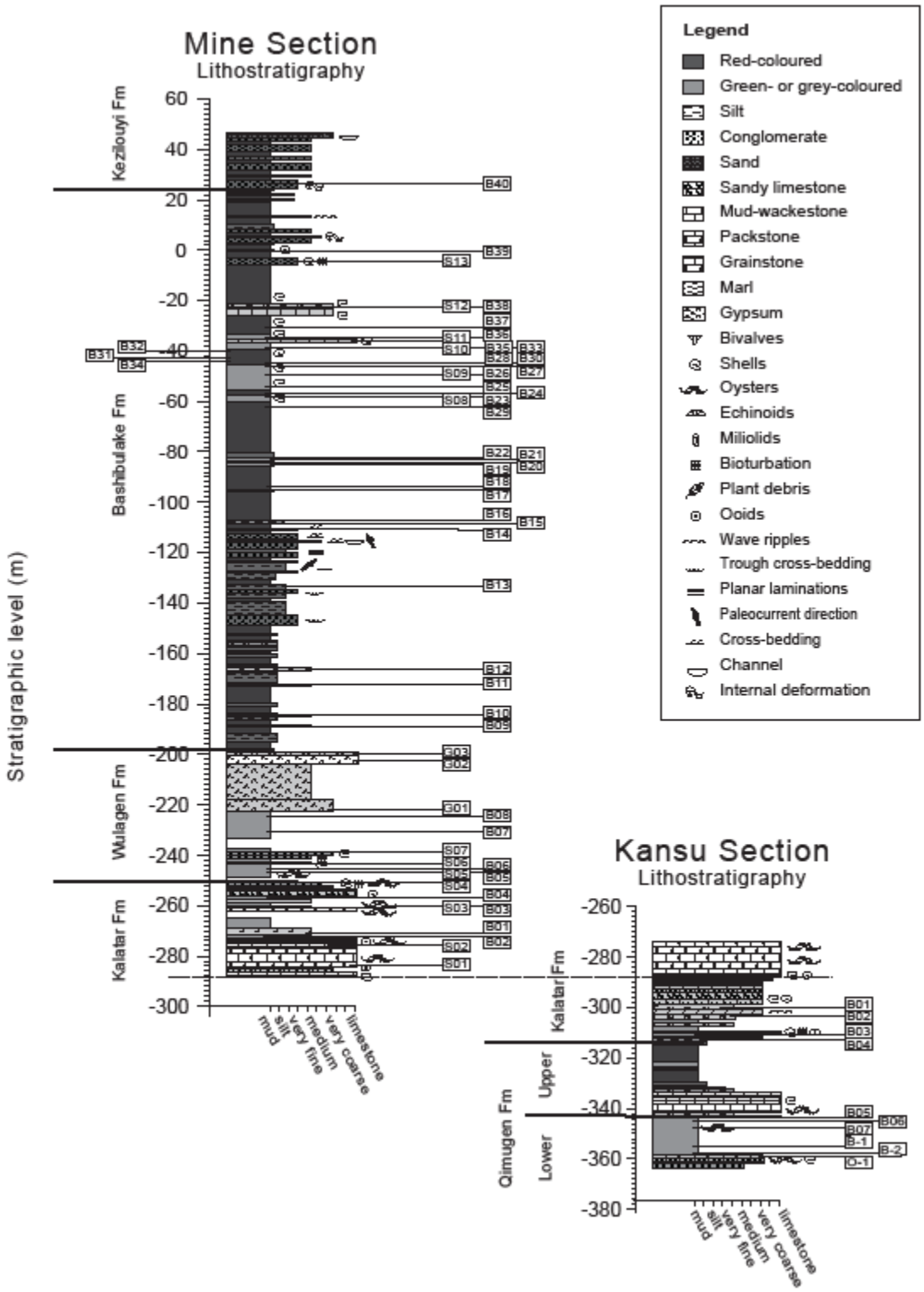
Mine Section
Lithostratigraphy
Stratigraphic level (m)
Kezilouyi Fm
Bashibulake Fm
Wulagen Fm
Kalatar Fm
mud
silt
very fine
medium
very coarse
limestone
Legend
Red-coloured
Green- or grey-coloured
Silt
Conglomerate
Sand
Sandy limestone
Mud-wackestone
Packstone
Grainstone
Marl
Gypsum
Bivalves
Shells
Oysters
Echinoids
Miliolids
Bioturbation
Plant debris
Ooids
Wave ripples
Trough cross-bedding
Planar laminations
Paleocurrent direction
Cross-bedding
Channel
Internal deformation
Kansu Section
Lithostratigraphy
Kalatar Fm
Qimugen Fm
Upper
Lower

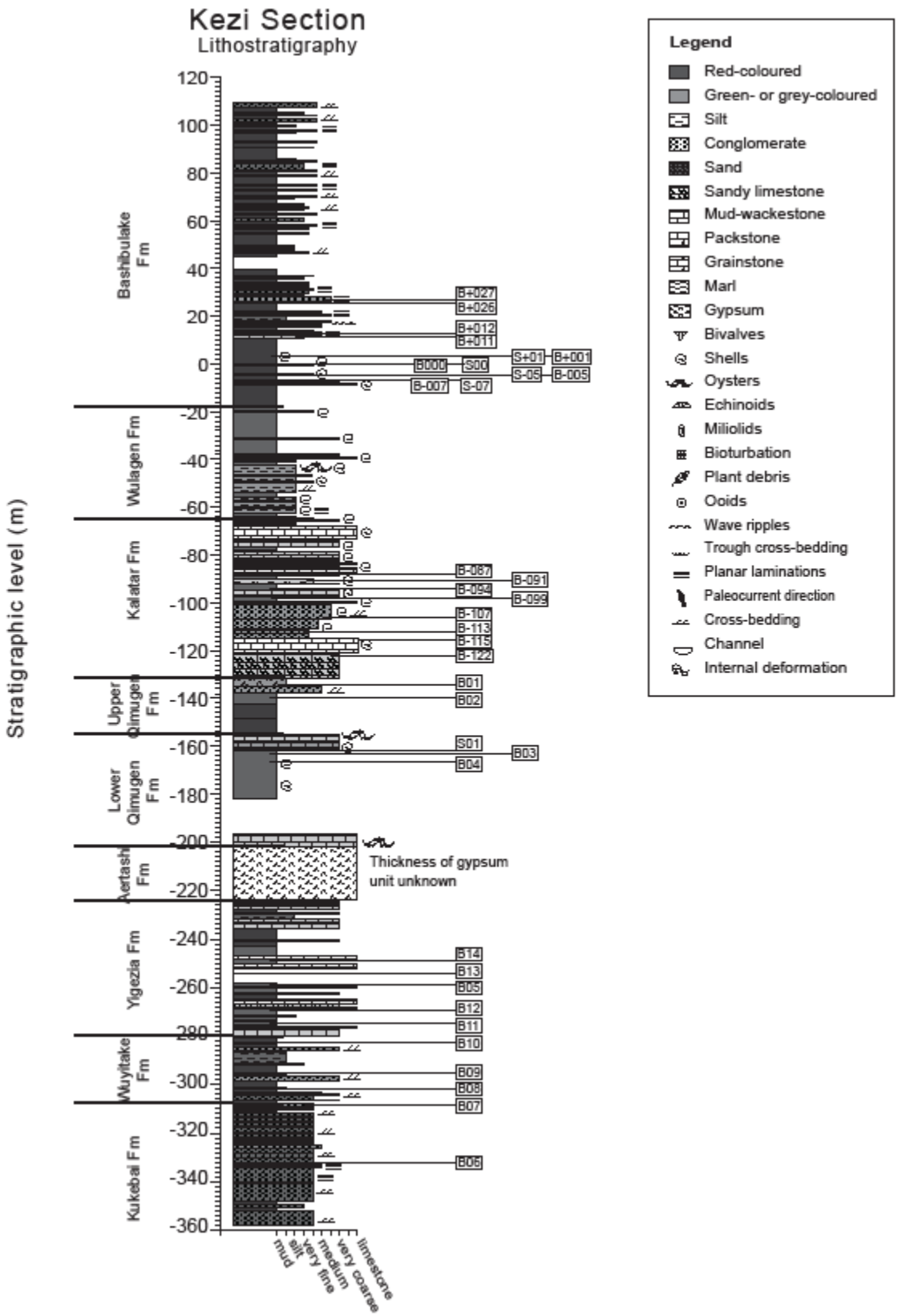
Kezi Section
Lithostratigraphy
Stratigraphic level (m)
Bashibulake Fm
Wulagen Fm
Kalatar Fm
Upper Qimugen Fm
Lower Qimugen Fm
Aertashi Fm
Yigezia Fm
Muyitake Fm
Kukebai Fm
Thickness of gypsum unit unknown
mud
silt
very fine
medium
very coarse
limestone
Legend
Red-coloured
Green- or grey-coloured
Silt
Conglomerate
Sand
Sandy limestone
Mud-wackestone
Packstone
Grainstone
Marl
Gypsum
Bivalves
Shells
Oysters
Echinoids
Miliolids
Bioturbation
Plant debris
Ooids
Wave ripples
Trough cross-bedding
Planar laminations
Paleocurrent direction
Cross-bedding
Channel
Internal deformation

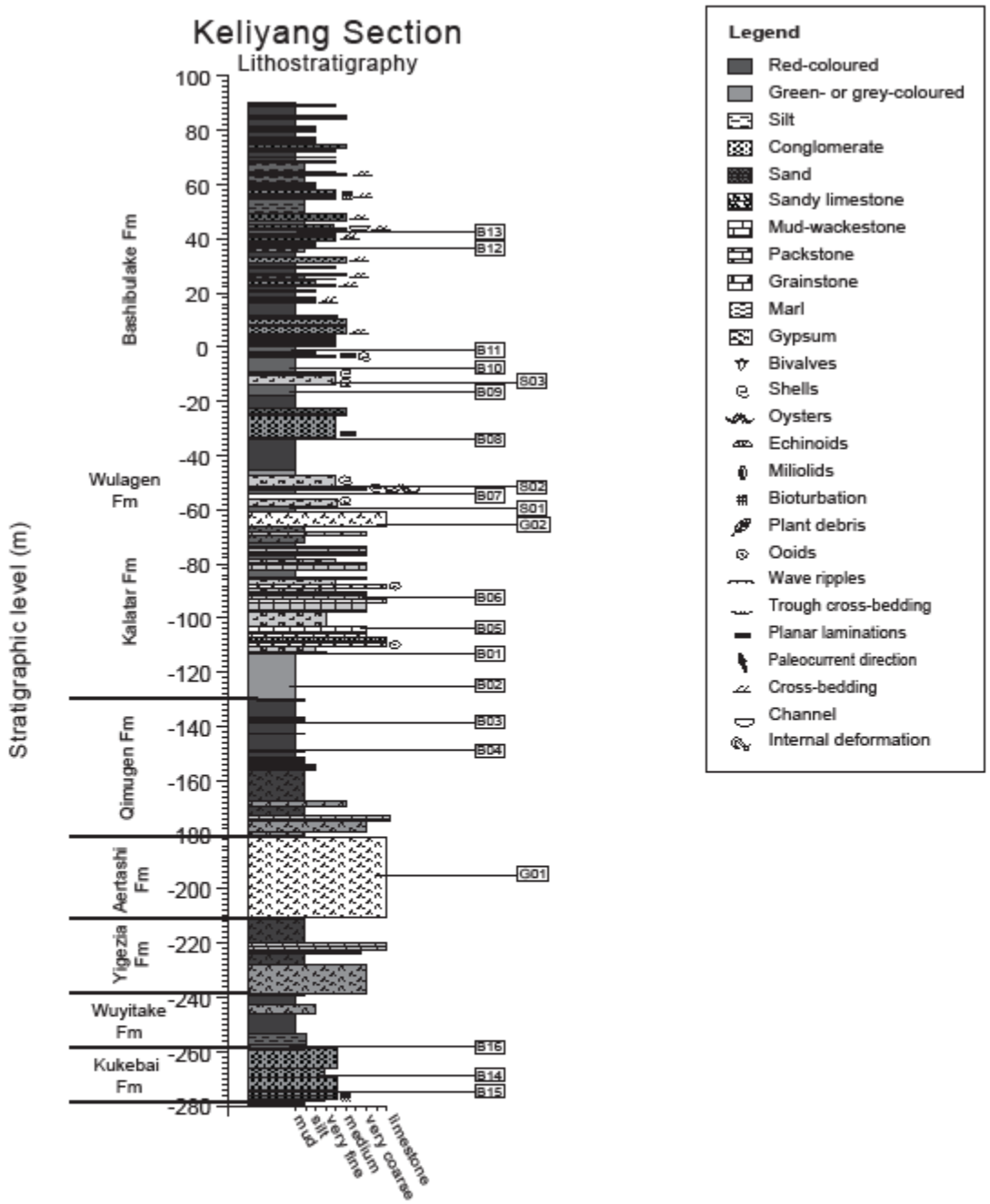
Keliyang Section
Lithostratigraphy
Stratigraphic level (m)
100
80
60
40
20
0
-20
-40
-60
-80
-100
-120
-140
-160
-180
-200
-220
-240
-260
-280
Bashibulake Fm
Wulagen Fm
Kalatar Fm
Qimugen Fm
Aertashi Fm
Yigezha Fm
Wuyitake Fm
Kukebai Fm
B13
B12
B11
B10
S03
B09
B08
S02
B07
S01
G02
B06
B05
B01
B02
B03
B04
G01
B16
B14
B15
mud
silt
very fine
medium
very coarse
limestone
Legend
Red-coloured
Green- or grey-coloured
Silt
Conglomerate
Sand
Sandy limestone
Mud-wackestone
Packstone
Grainstone
Marl
Gypsum
Bivalves
Shells
Oysters
Echinoids
Miliolids
Bioturbation
Plant debris
Ooids
Wave ripples
Trough cross-bedding
Planar laminations
Paleocurrent direction
Cross-bedding
Channel
Internal deformation

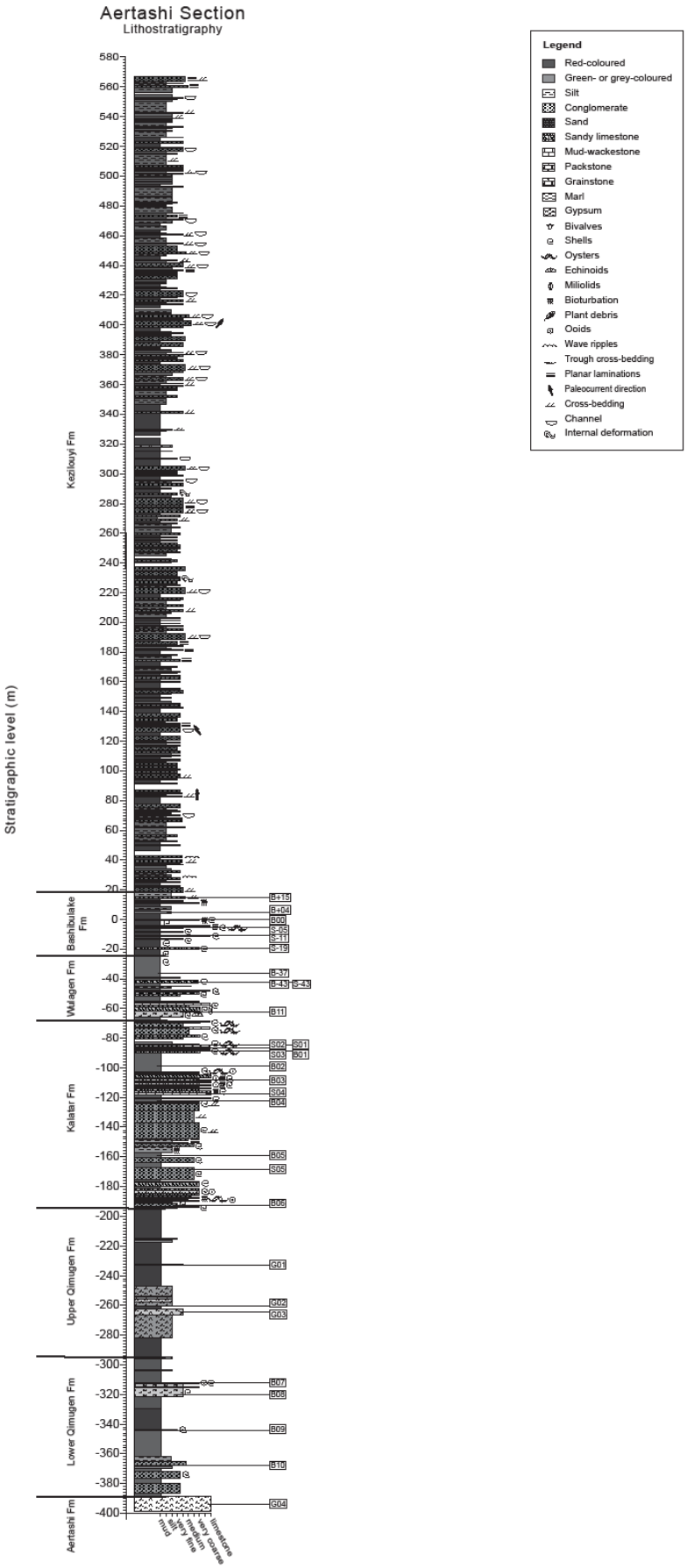
Aertashi Section
Lithostratigraphy
Stratigraphic level (m)
Legend
Red-coloured
Green- or grey-coloured
Silt
Conglomerate
Sand
Sandy limestone
Mud-wackestone
Packstone
Grainstone
Marl
Gypsum
Bivalves
Shells
Oysters
Echinoids
Miliolids
Bioturbation
Plant debris
Ooids
Wave ripples
Trough cross-bedding
Planar laminations
Paleocurrent direction
Cross-bedding
Channel
Internal deformation
Kezilouyi Fm
Bashibulake Fm
Wulagen Fm
Kalatar Fm
Upper Qimugen Fm
Lower Qimugen Fm
Aertashi Fm
mud
silty mud
silty fine
medium
very coarse
limestone

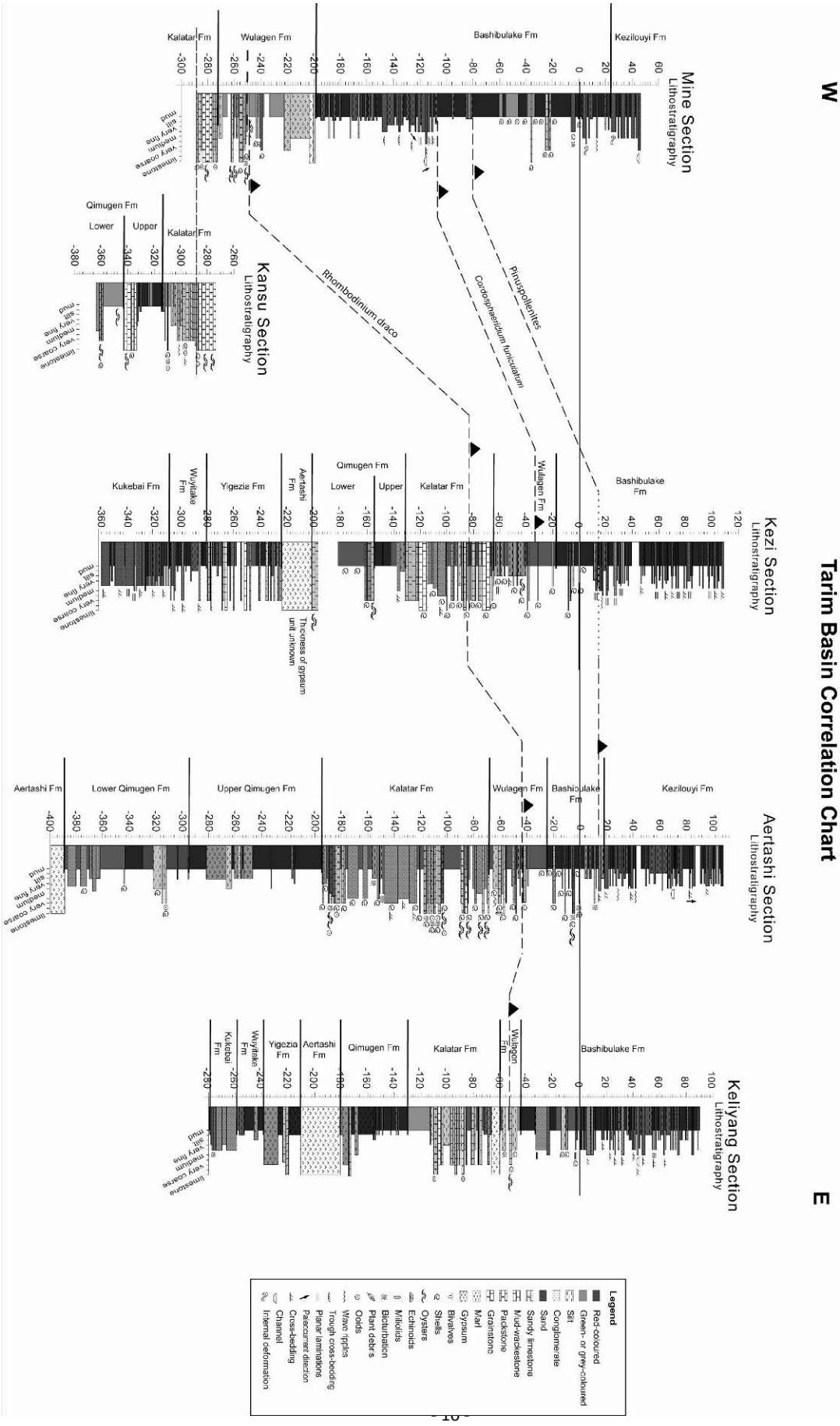
W
E
Tarim Basin Correlation Chart
Mine Section
Lithostratigraphy
Kansu Section
Lithostratigraphy
Kezi Section
Lithostratigraphy
Aertashi Section
Lithostratigraphy
Keliyang Section
Lithostratigraphy
Kalatar Fm
Wulagen Fm
Bashibulake Fm
Kezilouyi Fm
Qimugen Fm
Lower
Upper
Kukebai Fm
Wuyitake Fm
Yigezia Fm
Aertashi Fm
Lower Qimugen Fm
Upper Qimugen Fm
Thickness of gypsum unit unknown
Rhombodinium draco
Pinuspollenites
Cordosphaeridium funiculatum
Legend
Red-coloured
Green- or grey-coloured
Silt
Conglomerate
Sand
Sandy limestone
Mud-wackestone
Packstone
Grainstone
Marl
Gypsum
Bivalves
Shells
Oysters
Echinoids
Miliolids
Bioturbation
Plant debris
Oolds
Wave ripples
Trough cross-bedding
Planar laminations
Palaeocurrent direction
Cross-bedding
Channel
Internal deformation